

PYROLYSIS OF OIL SHALE IN A SPOUTED BED PYROLYSER

by

TINA SUI-MAN TAM

B.A.Sc., The University of Toronto, 1978

A THESIS SUBMITTED IN PARTIAL FULFILMENT OF
THE REQUIREMENTS FOR THE DEGREE OF
MASTER OF APPLIED SCIENCE

in

THE FACULTY OF GRADUATE STUDIES
DEPARTMENT OF CHEMICAL ENGINEERING

We accept this thesis as conforming
to the required standard

THE UNIVERSITY OF BRITISH COLUMBIA

July 1987

© TINA SUI-MAN TAM, 1987

In presenting this thesis in partial fulfilment of the requirements for an advanced degree at the University of British Columbia, I agree that the Library shall make it freely available for reference and study. I further agree that permission for extensive copying of this thesis for scholarly purposes may be granted by the head of my department or by his or her representatives. It is understood that copying or publication of this thesis for financial gain shall not be allowed without my written permission.

Department of Chemical engineering

The University of British Columbia
1956 Main Mall
Vancouver, Canada
V6T 1Y3

Date July, 1987

ABSTRACT

Pyrolysis of a New Brunswick oil shale has been studied in a 12.8cm diameter spouted bed reactor. The aim of the project was to study the effect of pyrolysis temperature, shale particle size, feed rate and bed material on oil yield. Gas and spent shale yields were also determined. Shale of different particle size ranging from 0.5mm to 4mm was studied using an electrically heated reactor containing sand or spent shale which was spouted with nitrogen or nitrogen/carbon dioxide mixtures.

For a given particle size and feed rate, there is a maximum in oil yield with temperature. For particles of 1-2mm at a feed rate of about 1.4kg/hr, the optimum temperature is at 475°C with an oil yield of 7.1% which represents 89.3% of the modified Fischer Assay yield. For the 2-4mm and the same feed rate, the optimum temperature is 505°C with an oil yield equal to 7.4% which is 94.3% of the modified Fischer Assay value. At a fixed temperature of about 500°C, the oil yield increases with increasing particle size. This trend is in agreement with the Fischer Assay values which showed oil yields increasing from 5.2% to about 8% as the particle size was increased. In the spouted bed, the oil yield decreases as the oil shale feed rate increases at a given temperature. The use of spent shales as the spouting solids in the bed also has a negative effect on oil yield. The gas yields which were low (less than 2.1%) and difficult to measure do not seem to be affected by

particle sizes, feed rate and bed material. Hydrogen, methane and other hydrocarbons are produced in very small amounts. CO_2 and CO are not released in measurable yield in the experiments. The trend of the spent shale yield has not been successfully understood due to the unreliability of the particle collection results. Attrition of the spent shale appears to be a serious problem.

Results of the experiments are rationalized with the aid of a kinetic model in which the kerogen in the oil shale decomposes to yield a bitumen and other by products and the bitumen undergoes further decomposition into oil. The spouted bed is treated as a backmixed reactor with respect to the solids. A heat transfer model is used to predict the temperature rise of the shale entering the pyrolyzer.

TABLE OF CONTENTS

ABSTRACT	ii
LIST OF TABLES	vii
LIST OF FIGURES	ix
ACKNOWLEDGEMENT	x
1. INTRODUCTION	1
1.1 Objective of the Thesis	2
2. BACKGROUND	3
2.1 The Properties of Oil Shale	3
2.2 The Basic Principle of Oil Shale Pyrolysis	8
2.3 Oil Shale Pyrolysis Processes	8
2.4 Parameters Affecting Oil Shale Pyrolysis	15
2.5 Heat Transfer in Spouted Beds	23
3. KINETICS OF OIL SHALE PYROLYSIS	32
3.1 Literature Review of the Kinetics of Oil Shale Pyrolysis	32
3.2 Kinetic Model	38
4. EXPERIMENTAL EQUIPMENT AND PROCEDURE	47
4.1 Pyrolysis Apparatus	47
4.2 Properties of Oil Shale	54

4.3	General Procedure	54
4.4	Detailed Operating Procedure	58
4.5	Oil Collection	60
4.6	Gas Analysis	61
4.7	Spent Shale Determination and Analysis	62
5.	RESULTS AND DISCUSSION	63
5.1	General Considerations	63
5.2	Effect of Temperature on Oil Yield and Composition	65
5.3	Effect of Oil Shale Particle Size on Oil Yield and Composition	73
5.4	Effect of Oil Shale Feed Rate on Oil Yield and Composition	78
5.5	Effect of Bed Material on Oil Yield	83
5.6	Effect of Pyrolyzing Gas on Oil Yield	90
5.7	Gas Yields	90
5.8	Spent Shale Yields	95
6.	KINETIC MODEL	100
6.1	General Discussion	100
6.2	The Effect of Rate Constant on Oil Yield	104
6.3	The Effect of Oil Shale Feed Rate on Oil Yield	107
7.	CONCLUSIONS	109

8. RECOMMENDATIONS FOR FUTURE WORK	111
NOMENCLATURE	113
REFERENCES	116
APPENDIX A) Temperature History Model	121
APPENDIX B) Sample Calculations	
B.1 Isokinetic Gas Sampling Calculation	129
B.2 Product Yield Calculations	130
APPENDIX C) Computer Programs	
C.1 Profile	132
C.2 Entrance	149
C.3 Calculate	154
C.4 Model	158
C.5 Jac	162
C.6 Jac (Printout)	166

LIST OF TABLES

Table 1	Inorganic Minerals Present in Typical Medium Grade Oil Shale	4
Table 2	Chemical Composition of the Inorganic Portion of Oil Shale	5
Table 3	Modified Fischer Assay for Typical Oil Shale Samples	6
Table 4	Conversion of Kerogen by the Fischer Assay	7
Table 5	Effect of Temperature on Oil Yield	18
Table 6	Effect of Particle Size on Oil Yield	21
Table 7	Particle Temperature History of the Oil Shales (After One Pass)	29
Table 8	Particle Temperature History of the Oil Shales (After Two Passes)	30
Table 9	Design Characteristics of Spouted Bed Pyrolyzer System	48
Table 10	Proximate and Ultimate Analysis of Blend of Oil Shale A	55
Table 11	Analysis of Oil Shale Ash and Carbon	56
Table 12	Modified Fischer Assay of Oil Shales	57
Table 13	Experimental Conditions for Each Run	64
Table 14	Effect of Temperature on Oil Yield	67
Table 15	Effect of Temperature on Oil Yield and Composition	72
Table 16	Effect of Particle Size on Oil Yield	74

Table 17	Effect of Particle Size on Oil Yield and Composition	77
Table 18	Effect of Feedrate on Oil Yield (Unsteady Height Expt.)	79
Table 19	Effect of Feedrate on Oil Yield (Unsteady Height Expt.)	80
Table 20	Effect of Feedrate on Oil Yield (Steady Height Expt.)	84
Table 21	Effect of Feedrate on Oil Yield and Composition	86
Table 22	Effect of Bed Material on Oil Yield	88
Table 23	Effect of Pyrolyzing Gas Composition	91
Table 24	Gas Yields	93
Table 25	Spent Shale Properties and Yield	96
Table 26	Spent Shale Yields	98
Table 27	Effect of Temperature on Oil Yield (Predicted vs Experimental Values)	102
Table 28	Effect of Feed Rate on Oil Yield (Predicted vs Experimental Values)	108
Table 29	Coordinates of the Tridiagonal Matrix	126
Table 30	Correlations used for estimation of the Hydrodynamic Properties for the Spouted Bed	127

LIST OF FIGURES

Figure 1	Effect of Pressure on Oil Yield	16
Figure 2	Effect of Retorting Temperature on Oil Yield	20
Figure 3	Effect of Particle Size on Tar Yield	22
Figure 4	Schematic Diagram for Spouted Bed	25
Figure 5	A Schematic Diagram for the Experimental Apparatus	50
Figure 6	Oil Yield Versus Temperature Plot ($d_p=1-2\text{mm}$)	68
Figure 7	Oil Yield Versus Temperature Plot ($d_p=2-4\text{mm}$)	69
Figure 8	% Fischer Assay Vs Temperature Plot	71
Figure 9	Oil Yield Vs Particle Size Plot	75
Figure 10	Oil Yield Vs Feedrate Plot ($d_p=1-2\text{mm}$)	81
Figure 11	Oil Yield Vs Feedrate Plot ($d_p=2-4\text{mm}$)	82
Figure 12	Oil Yield Vs Feedrate Plot (Steady Height Expt.)	85
Figure 13	Oil Yield Vs Spent Shale in Bed	89
Figure 14	Hydrogen Gas Yield Vs Temperature	94
Figure 15	Oil Yield vs Temperature Plot (Predicted vs Experimental values)	103
Figure 16	C_K , C_B , C_A and Oil Yield vs Time Plot	105

ACKNOWLEDGEMENT

I wish to thank Dr. A.P. Watkinson and Dr. J. Lim, under whose supervision and guidance this research work was conducted, for their advice and encouragement in all stages of this work.

I am also grateful to Dr. B. Bowen for his advice on the mathematical modelling; to Dr. G.K. Khoe for his assistance in the modifications to the apparatus and the carry out of some of the experimental runs; and to Dr. K.C. Teo for his help in doing the gas samples analysis.

In addition, I wish to thank Mr. Michael Standbrook for his assistance in operating the experimental apparatus.

Finally, my appreciation to the staffs of the Chemical Engineering Department workshop and stores for their continuing assistance through this work.

1. INTRODUCTION

Oil shales are widely distributed throughout the world with known deposits in every continent. The vast majority of known oil shale resources are found in United States (75% of the estimated world recoverable oil reserves), with other major deposits in China (about 11% of the estimated world reserves) and Canada (about 7% of estimated world reserves)(''). After the discovery of crude oil and petroleum, the oil shale industry which had previously become established could not compete. At present, oil shale is exploited in only two countries - the USSR and China.

Synthetic crude oil can be obtained from oil shale. The organic matter in oil shale is composed of about 10% bitumen, and about 90% kerogen. Both are thermally unstable, and with the application of heat (250°C or greater), thermally decompose to form gaseous and liquid products that can be refined to synthetic crude. Therefore, many studies have been made of oil shale retorting. For the Western US shales, a high level of conversion can be achieved by a simple thermal retorting procedure, whereas for the Eastern US shales, rapid retorting or the use of hydrogen as a retorting gas is employed to achieve comparable organic matter recovery.

By contrast, little attention has been paid to oil shales in Canada. Only a few research studies have been done on the shales from New Brunswick, Ontario, Quebec, Newfoundland and Nova Scotia. Since oil shale is one of the

promising alternate energy resources in parts of Canada, given the level of reserves, it is essential to investigate those parameters that will influence the overall yield of products derived from oil shale retorting, and which affect the distribution of products among gases, light oils and heavy oils. In this research, a spouted bed reactor that was constructed for coal pyrolysis⁽²⁾ was used to study the pyrolysis of New Brunswick oil shale.

1.1 Objective of the Thesis

The object of the study is to investigate the effect of pyrolysis temperature, shale particle size, shale feed rate and bed composition on oil, gas and spent shale yield from Albert Formation New Brunswick oil shale in a spouted bed pyrolyser. The shale is pyrolysed in either N_2 - CO_2 mixtures or N_2 , and in beds of either inert silica (Ottawa sand) or spent shale. Results are compared with predictions of the Fischer Assay, which is a standardized test for potential oil yield. *

* The Fischer Assay method is used for determining the quantity of recoverable liquid oil and other products from oil shale. A 100 gm sample of finely crushed oil shale is heated at a rate of $12^\circ C$. per min to a final temperature of $500^\circ C$ and held for an additional 70 minutes at $500^\circ C$ in a sealed aluminum retort under controlled conditions. As kerogen is pyrolysed, the gaseous and liquid products evolved are collected and measured using standardized equipment.

2. BACKGROUND

2.1 The Properties of Oil Shale

Oil shales are geologically classified as marlstones because of their large percentage of carbonates. Average shales are composed of about 86% mineral and 14% organic matter. Table 1 shows the inorganic minerals present in a typical medium grade oil shale and Table 2 shows the chemical composition of the inorganic portions of oil shale.

The organic matter is present in the oil shale as a resinous solid, not as an oily liquid. It is composed of about 10% bitumen and 90% kerogen. The bitumen is a heteroatomic polymer soluble in many organic solvents, whereas the kerogen is a heteroatomic polymer having a molecular weight of greater than 3000 and is insoluble in most organic solvents. To the unaided eye, kerogen appears black in colour. Under the microscope, thin sections of kerogen appear yellow in colour with a minor portion appearing brown or black. It has no well designated structure, appearing as stringers, masses and irregular granules all intermixed with the inorganic materials in the rock. The kerogen subunits are cross-linked to one another by oxygen and sulfur. Upon application of heat, both kerogen and bitumen decompose to form gaseous and liquid products. Table 3 shows a modified Fischer assay for typical oil shale samples. Table 4 shows the conversion of kerogen by Fischer assay.

TABLE 1: Inorganic Minerals Present in Typical Medium Grade Colorado Oil Shale

Mineral	Formula	Wt %
Dolomite	$(\text{CaMg})\text{CO}_3$	33
Calcite	CaCO_3	20
Plagioclase	$\text{NaAlSi}_3\text{O}_8$ and $\text{CaAl}_2\text{Si}_2\text{O}_8$	12
Illite	$\text{K}_2\text{O} \cdot 3\text{Al}_2\text{O}_3 \cdot 6\text{SiO}_2 \cdot 2\text{H}_2\text{O}$	11
Quartz	SiO_2	10
Analcite	$\text{NaAlSi}_2\text{O}_6 \cdot \text{H}_2\text{O}$	7
Orthoclase	KAlSi_3O_8	4
Iron	Fe	2
Pyrite (or marcasite)	FeS_2	1
Total		100

TABLE 2: Chemical Composition of the Inorganic Portion of Colorado Oil Shale

Chemical Constituent	Very Low Grade Shale	Medium Grade Shale	High Grade Shale	Very High Grade Shale
SiO ₂ , percent	40.9	26.1	25.5	26.4
Fe ₂ O ₃	4.3	2.6	2.9	3.1
Al ₂ O ₃	9.4	6.5	6.3	7.0
CaO	11.0	17.5	14.2	8.3
MgO	5.4	5.3	5.6	4.5
SO ₃	0.1	0.6	1.2	1.4
Na ₂ O	1.8	2.6	2.7	1.9
K ₂ O	3.4	1.0	1.9	1.0

TABLE 3: Modified Fischer Assay for Typical Colorado Oil Shale Samples

	For Very Low Grade Shale	For Medium Grade Shale	For High Grade Shale	For Very High Grade Shale
Oil, gal/ton	10.5	26.7	36.3	61.8
Oil, wt %	4.0	10.4	13.8	23.6
Water, wt %	0.5	1.4	1.5	1.1
Spent Shale, wt %	94.4	85.7	82.1	70.4
Gas, wt %	1.1	2.0	2.2	4.2
Loss, wt %	-	0.5	0.4	0.7

TABLE 4: Conversion of Kerogen by the Fischer Assay

Grade of Shale, gal/ton	10.5	26.7	36.3	57.1	61.8	75.0
Conversion of Kerogen by the Fischer Assay to						
Oil, wt %	51	65	69	66	69	71
Gas, wt %	14	12	11	12	12	11
Organic Residue, wt %	35	23	20	22	19	18
Water	(Excluded from calculations)					
	100	100	100	100	100	100

2.2 The Basic Principle of Oil Shale Pyrolysis

Oil shale pyrolysis involves the heating of oil shales in an inert atmosphere to cause decomposition. Over a long period of time, complete devolatilization can be achieved at temperatures of around 400-425°C. The mechanism usually given for oil shale decomposition is as follows:

Kerogen \longrightarrow Bitumen + Gas₁ + Carbon Residue₁

Bitumen \longrightarrow Oil + Gas₂ + Carbon Residue₂

Typically at temperatures below 470°C the decomposition of kerogen into soluble bitumen is a fairly rapid step compared to the decomposition of bitumen to oil. However, at temperatures above 470°C, the decomposition of bitumen appears to be rapid⁽⁴⁾. The kinetics of oil shale pyrolysis will be discussed in Section 3.1.

2.3 The Oil Shale Pyrolysis Process

There are many types of retorting processes described in the literature. Only the most developed ones are discussed in the thesis.

Retorting processes can be classified into two types: the direct-heating processes and the indirect-heating processes. The direct-heating processes rely on internal combustion of fuel with air or oxygen within the bed of shale to provide all necessary process heat requirements.

The indirect-heating processes rely on the heat provided by the injection of heated solid or gaseous heat-carrier media into the retort.

Among the direct-heating processes are the Gas Combustion retorting process and the Union Oil retorting process⁽¹⁾⁽⁵⁾. The Gas Combustion retorting process features the continuous pyrolysis of coarsely crushed oil shale in a vertical kiln retort. The heat is provided by an internal combustion of the process-derived fuel with air within a downward-moving bed of shale. The kerogen in the shale is pyrolyzed or decomposed by heat in the retorting zone. The necessary heat is provided by the hot gases rising from the combustion zone. As the kerogen pyrolyzes, it yields oil (as vapour), gas, and a residual carbonaceous product which adheres to the solid retorted shale. All vapours and gases are swept upward, and the solids descend into the combustion zone where oxidation of the carbon occurs to produce the hot flue gases. The oil recovery of the Gas Combustion process is in the range of 80 to 90 percent of the Fischer Assay.

The Union Oil retorting process features a 'rock pump' shale feeding device which pushes oil shale upward into an inverted-cone-shaped vessel which is open to the atmosphere at the top. The shale solids, after having been pyrolyzed, overflow the vessel walls at the top. Air enters the bed of shale at the top and supports combustion within the bed of shale. The flow of air, combustion product gases and pyrolysis product vapors is downward, countercurrent to the

upward flow of solids.

The TOSCO II, the Petrosix, and the Lurgi-Ruhrgas processes use indirect heating⁽¹⁾⁽⁵⁾. The TOSCO II oil shale retorting process⁽⁶⁾ features the use of a circulating load of heated ceramic balls as a heat carrying medium for transferring the necessary process heat to finely crushed oil shale for pyrolysis of the shale's kerogen in a rotating drum type of vessel. The vessel is kept under an internal pressure of about 135.8kPa to prevent admittance of air. No combustion occurs in the retort. The ceramic balls and the finely ground spent shale are first separated from each other by a trommel. Then the ceramic balls are reheated in a separate gas-fired furnace. Some of the balls break from repeated thermal shock of alternate heating and cooling. The TOSCO II retorting technology is well advanced and has been demonstrated at a semi-works scale.

The Lurgi-Ruhrgas process requires finely crushed oil shale. It features the use of heat carrier solids of small particle size such as sand grains, coke particles, or spent shale solids derived from the shale retorting process. The hot heat-carrier solids are mixed with the oil shale in a sealed screw-type conveyor and pyrolysis occurs during the mixing operation.

In the Petrosix retorting process⁽¹⁾⁽⁵⁾ heated recycle gas rather than combustion air is injected into the bed of shale to provide the necessary heat for pyrolysis. The retort unit is 5.48m in diameter and is capable of

processing about 2500 tons of oil shale feed/day. This scale of operation is much greater than any other modern retorting process. This process utilises a vertical kiln retort very similar in design to the Gas Combustion retort. However, in this case, recycle gas heated in a separate furnace is used instead of combustion gas.

Most of the processes described above are slow retorting processes in which large particles are slowly heated to reaction temperature. In theory, rapid pyrolysis processes tend to produce higher liquid yields than slow retorting processes due to the minimization of secondary cracking of the liquid to solids and gases. Typically, slow retorting processes have a particle heating rate around $12^{\circ}\text{C}/\text{min}$ whereas the rapid retorting processes have a heating rate of upto $33,000^{\circ}\text{C}/\text{min}$.

For liquid yield reasons, fluid bed technology has been suggested as a basis for an oil shale retort. Marshall J. Margolis⁽⁷⁾ investigated the pyrolysis of Eastern U.S. Oil shales in a fluidized bed system. The fluid bed reactor provides a rapid heat-up of the oil shale particle because of its excellent heat transfer characteristics; and its short vapour residence time helps to minimize coking and oil decomposition. The basic unit consisted of a quartz reactor vertically mounted within an electrically heated tube furnace and was capable of operating at temperatures up to 1200°C . The fluid bed capacity was approximately 15 grams of shale. Raw shale was fed into the fluidized bed through a

variable speed screw feeder which was mounted at the top of the reactor. Nitrogen gas was used to maintain fluidization. During operation, the spent shale was continuously displaced as raw shale was added to the reactor bed. Volatile products were swept from the reactor into a series of two cooled traps. The amount of oil produced was determined by weighing the amount of material collected in the traps and correcting for water and particulate matter content. The experimental results showed that there is an improvement over the carbon removal achieved under Fischer Assay conditions. Also, evaluation of spent shale carbon analyses and product collection data suggest that oil yield equivalent to 120-140 % of the Fischer Assay may be achieved.

Salib, Barua and Furimsky⁽⁸⁾ have studied the retorting of New Brunswick oil shales in direct and indirect modes in a pilot scale moving bed retort. The retort had a square cross-sectional area of 0.053m^2 and a height of 2.4m. The crushed shale was fed by gravity through a rotary valve at the top of the reactor. The descending shale was heated by the ascending hot gas (air + recycle retorting gas). Oil was recovered from the off gases by hot cyclone, condenser, packed column and electrostatic precipitator. Spent shale was discharged by an extraction screw. The effect of shale grade, bed height, retort temperature profile, recycle gas and its distribution, and air feed rate on oil recovery were studied. The maximum oil recoveries are 81% and 89% of the Fischer Assay for direct and indirect mode retorting

respectively.

Levy et al⁽⁴³⁾ have investigated the vapour phase thermal behaviour of shale oil samples derived from the Condor, Nagoorin carbonaceous and Stuart deposits of Australia. The oil vapours released during retorting were passed through packed beds of sand, or the spent shale ash corresponding to the particular oil at temperatures between 500 and 600°C over a range of residence times. The results showed that there was minimal oil cracking over the sand. Oil degradation was attributed to thermal cracking. When the oil vapours were passed through the spent shale, their behaviour was quite different from that over the sand. The spent shale ash catalysed oil degradation greatly and resulted in major oil losses due to coking even at 500°C the lower range of the temperature studied.

Dung et al⁽⁴⁴⁾ report the pyrolysis behaviour of Condor and Stuart Shales in a 150mm diameter fluidized bed process development unit. The process used the hot shale ash as a heat carrier. The aim of the project was to determine if the recycle of the shale ash from this oil shale would adversely affect the oil yield. When the ash to shale recycle ratio was two, the results show an oil yield of loss of 28% compared to retorting in the absence of hot shale ash. The loss oils were mainly heavy fractions which adsorbed onto the shale ash. The loss seriously affect the economic feasibility of oil shale processing. Dung⁽⁴⁵⁾ has studied a new concept for retorting oil shales. The principle of the

proposed method was the transfer of heat through walls separating the heat source and the shales. The heat was supplied by combusting spent shale. The oil shale particles were conveyed by gas through heat exchange tubes, the heated shales then being retorted in the absence of ash. Calculations based on data and correlations in the literature demonstrated that shale particles can be heated effectively while being conveyed, in dilute phase, in heat exchanger tubes immersed in a fluidized bed of combusting spent shale. Experimental information about the performance and operation of the reactor is required to confirm the proposed advantages.

One of the main disadvantages of the fluidized bed is the difficulties in handling relatively large particle sizes (>1 mm) which may lead to unstable fluidized bed operation. The employment of a spouted bed reactor could solve this problem. Spouted bed technology was developed in the 1950's in Canada to dry wheat with air prior to storage. The properties and applications of spouted beds are described in a book by Mathur and Epstein⁽⁹⁾ and other literature⁽¹⁰⁾⁻⁽¹⁵⁾.

Leite et al⁽¹⁶⁾ have studied oil shale pyrolysis in a 8cm diameter spouted bed reactor. The oil shale of 1.11mm particle size is pyrolyzed at 600°C at a feed rate of 2.7 to 9.0kg/hr with nitrogen, steam and air mixture as spouting gas.

Jarallah⁽²⁾ has studied coal pyrolysis in a 12.8cm diameter continuous spouted bed reactor. The effects of coal feed rate, particle size, reactor temperature and bed height on yields from two British Columbia bituminous coals and one Alberta sub-bituminous coal were investigated. The spouting gases used were either nitrogen or a nitrogen-carbon dioxide mixture. Coal sizes between 0.6 and 3.36mm were fed at atmospheric pressure to the electrically heated reactor containing sand as spouting media. The tar yield was determined by sampling the outlet gas through a series of cooled impingers. In this thesis, the spouted bed developed by Jarallah⁽²⁾ was used to study the pyrolysis of New Brunswick oil shale.

2.4 Parameters Affecting Oil Shale Pyrolysis

Studies show that the oil shale pyrolysis is affected by many parameters, such as pressure, temperature & heating rate, particle size and shale feed rate.

Bae⁽¹⁷⁾ has investigated the effect of pressure and surrounding atmosphere on the retorting of oil shale. He conducted batch experiments at 510°C using different retort gases such as N₂, CO₂, H₂O, NH₃, and H₂ at pressures ranging from atmospheric to 2500 psig. Test results in Figure 1 indicate that high pressure reduces the oil yield significantly, but produces a larger volume of light hydrocarbon gases. High pressure favours the secondary reaction of the primary volatiles. Oil yields were generally

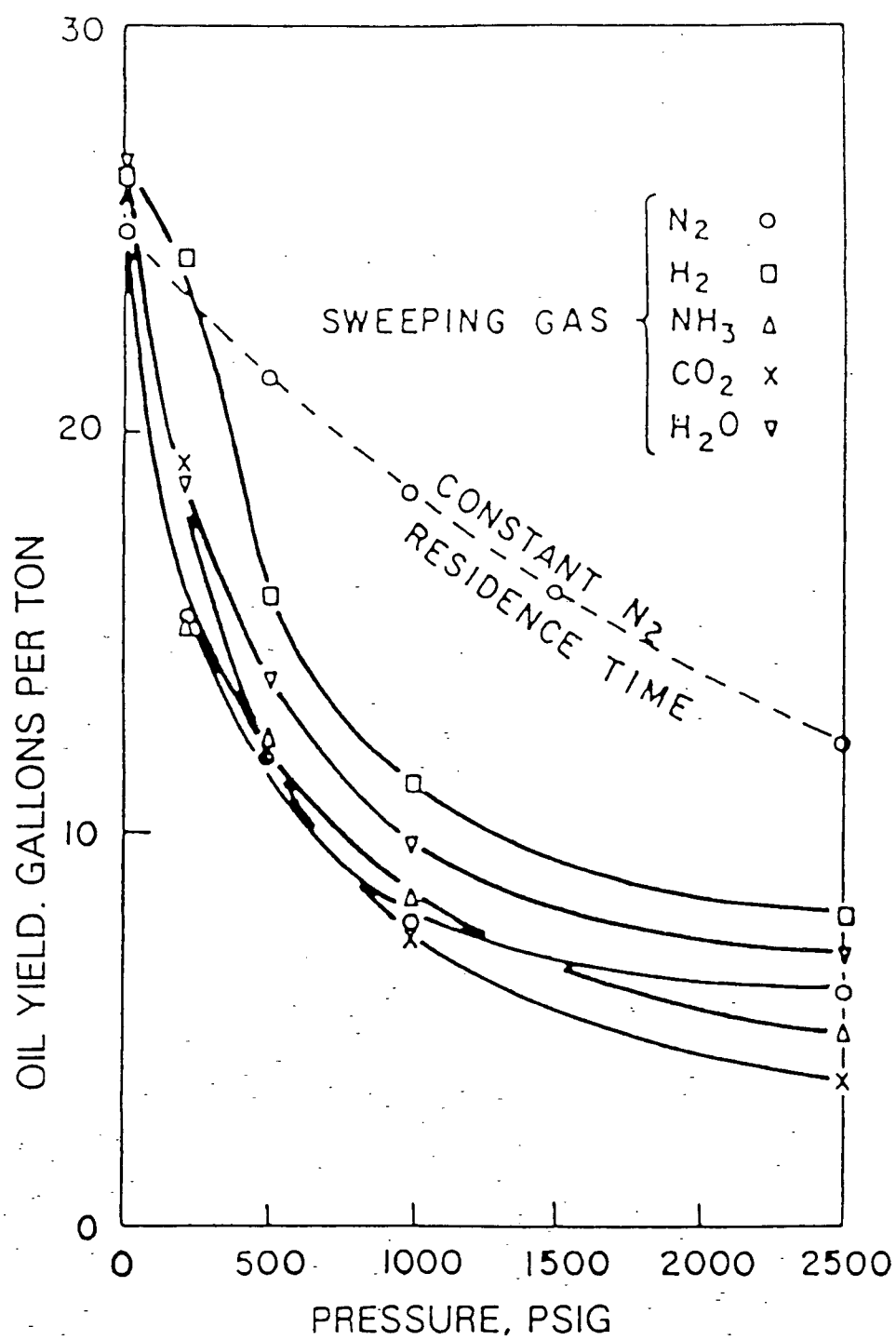


Fig 1: Effect of Pressure on Oil Yield

(Adapted from Reference No. 17)

similar in nitrogen than carbon dioxide atmospheres. As the aim of the present project is to find conditions for high oil yield, experiments have been conducted under atmospheric pressure.

Furimsky et al⁽¹⁸⁾ have studied the retorting of thirty oil shales samples from Eastern Canada by Fischer assay retort and pyrochem retort. The oil yield increased significantly with hydrogen as the retorting gas. This is due to the stabilization of reactive radical intermediates by hydrogen which would otherwise polymerize to higher molecular weight species.

The effect of temperature on oil shale pyrolysis, especially the oil yield, is very significant. Studies show that the kerogen in oil shale will begin to decompose at 250°C. and will even pyrolyse completely at temperatures around 400°C. Table 5 lists the results of a temperature study on Colorado oil shale by Hill⁽¹⁹⁾. It can be seen that for lower temperatures, a longer retorting period is required. From a practical standpoint, therefore a higher temperature is preferred to shorten the retorting period.

The temperature affects both the decomposition of oil shale and the secondary reactions of the primary volatiles. In the absence of secondary reactions, the oil yield will increase gradually with temperature. In the presence of substantial secondary reactions, an increase in temperature will enhance the cracking of the oil into lighter volatiles. Therefore, typically there is a maximum oil yield at an

TABLE 5: Effect of Temperature on Oil Yield

Test	Temperature (°C)	Duration (hr)	Oil Wt%	Yield %Fischer Assay
D-4	331	550	4.0	33.6
D-5	347	425	4.8	40.4
D-19	353	159	4.3	39.1
D-7	364	312	6.0	52.6
D-22	395	71	7.6	71.6
D-16	399	86.5	8.0	72.8
D-17	420	38.0	8.8	80.0
D-10	427	37.5	8.9	78.1
D-1	500	13.5	7.6	92.6

Tests were performed at the University of Utah
All experiments were carried out at atmospheric pressure

optimum temperature. This is in agreement with the findings of Liu et al⁽²⁰⁾. They have studied the pyrolysis of 20-40 mesh Colorado oil shale in a twin fluidized bed reactor. A mixture of nitrogen and steam was used as the fluidizing gas. The feed rate of oil shale was 7.2Kg/hr. Figure 2 shows the test results. It indicates that oil yield increases from 60% Fischer Assay at 427°C to 67% Fischer Assay at 491°C. Beyond 491°C, oil yield decreases to 42% Fischer Assay at 548°C. The optimum retorting temperature for this condition is estimated to be approximately 477°C.

The study of the effect of particle size on oil yield is necessary because the operational requirements of a retorting process frequently require the shale to be of a specific particle size range. For example, the TOSCO II process requires feed shale to be smaller than 1.27cm , so that the spent shale can be separated from the 1.27cm diameter heat-carrier ceramic balls by screening. Gas combustion and Petrosix processes require discrete particle larger than 0.64cm size. A series of Fischer Assays was made on 100 gram of a Colorado oil shale crushed to various sizes range from 2 to 65 mesh and pyrolysed according to the standard retorting rate. The results are listed in Table 6 and it can be seen that the effect seems to be very small. Jarallah⁽²⁾ has also studied the particle size effect on coal pyrolysis and found that there is a higher oil yield with decreasing particle size. Figure 3 shows the plot of coal particle size versus tar yield. His explanation is that

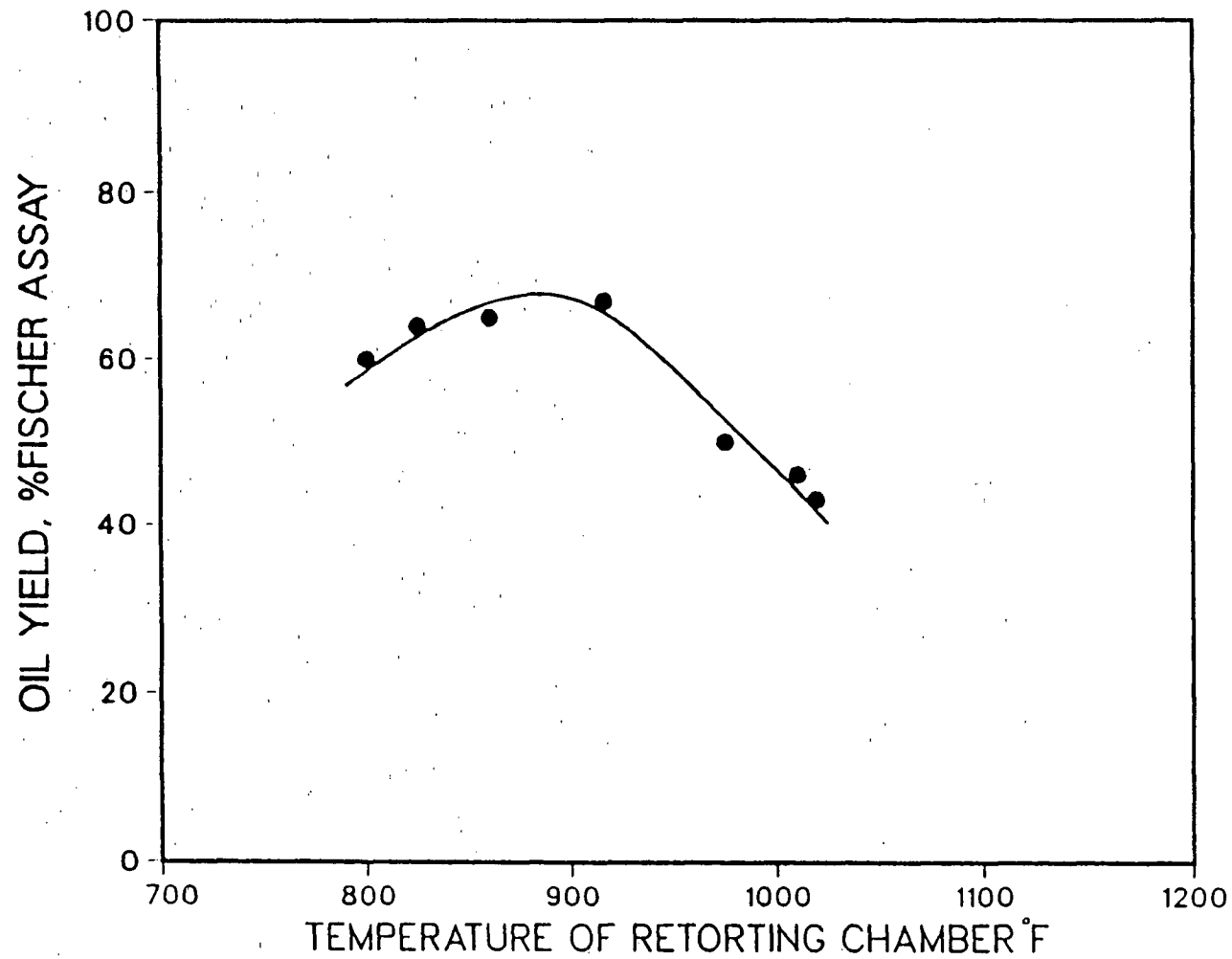


Fig 2: Effect of Retorting Temperature on Oil Yield

(Adapted from Reference No. 20)

TABLE 6: Effect of Particle Size On Oil Yield

Particle Size (mesh)	Number of determinations	Oil Wt%
Minus 2	2	14.22
Minus 4	2	14.78
Minus 8	5	14.37
Minus 20	2	14.45
Minus 65	2	13.47

100.0gm samples of Colorado oil shale No. 44L-69 were heated from room temperature to 500°C in 50 minutes and then maintained at 500°C for an additional 70 minutes.

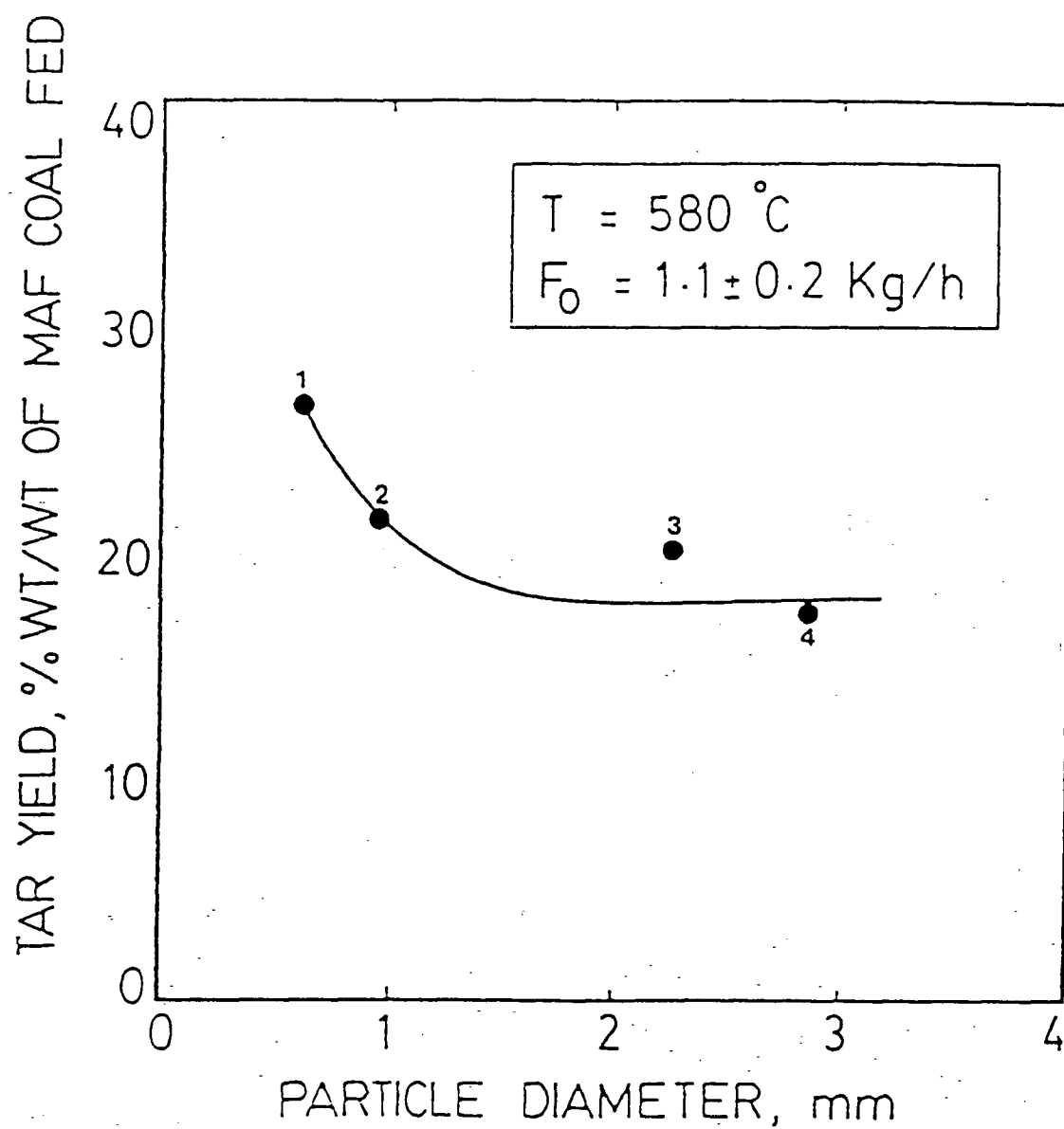


Fig 3: Effect of Particle Size on Tar Yield

(Adapted from Reference No. 2)

for smaller particles, the pyrolysis is more rapid and the opportunity for polymerization and deposition within the particle is reduced. However, the Fischer Assay values for the New Brunswick oil (Table 12) shale A indicate that the smaller oil shales particles have a smaller potential oil yield, and therefore comparisons of particle size effects should not be based on the magnitude of the oil yield alone.

The study of shale feed rate on oil yield is of special interest in this case. Jarallah⁽²⁾ found that increasing coal feed rate has negative effect on oil yield. The char accumulated in the reactor apparently enhanced the secondary cracking of tar to volatiles. Therefore, it is necessary to observe if the spent shale accumulated in the reactor over the time of the experiment would have a similar effect on oil yield.

2.5 Heat Transfer in Spouted Beds

Because retorting is an endothermic process, it is very important to understand the heat transfer in a spouted bed. In our experiment, the oil shale is fed at room temperature to the apex of the spouted bed. It is necessary to find out the time required for the oil shale particle to reach the bed temperature, and whether a significant intraparticle temperature gradient exists. In other words, knowledge of the temperature history of the oil shale particle helps in understanding the pyrolysis kinetics.

Work on spouted beds to 1974 can be found in the book by Mather and Epstein⁽⁹⁾. The spouted bed consists of two distinct regions: the spout and the annulus. Figure 4 shows a schematic diagram of a spouted bed. In the spout, the average gas velocity is often one or two orders of magnitude higher than the annulus, whereas the volume fraction of particles, $(1-\epsilon)$, is at most one-fifth of that in the dense phase annulus. An equation⁽⁹⁾ for estimating the heat transfer coefficient in the spout for the particle Reynolds number higher than 1000 is,

$$Nu = A + BPr^{1/3} + Re^{0.55} \quad (2.1)$$

where $A = 2/[1-(1-\epsilon)^{1/3}]$ and $B = 2/3\epsilon$

For the annulus region, the packed bed correlation⁽⁹⁾ for estimating the heat transfer coefficient where Re for the particle is generally smaller than 100 is,

$$Nu = 0.42 + 0.35 Re^{0.8} \quad (2.2)$$

It should be noted that the above correlation is based on experimental data using air near room temperature. In this research, the reactor temperature is at least 450°C , therefore equation 2.2 may only give an estimate of the heat transfer coefficient.

It can be shown that the heat transfer coefficient in the spout is much higher than in the annulus region.

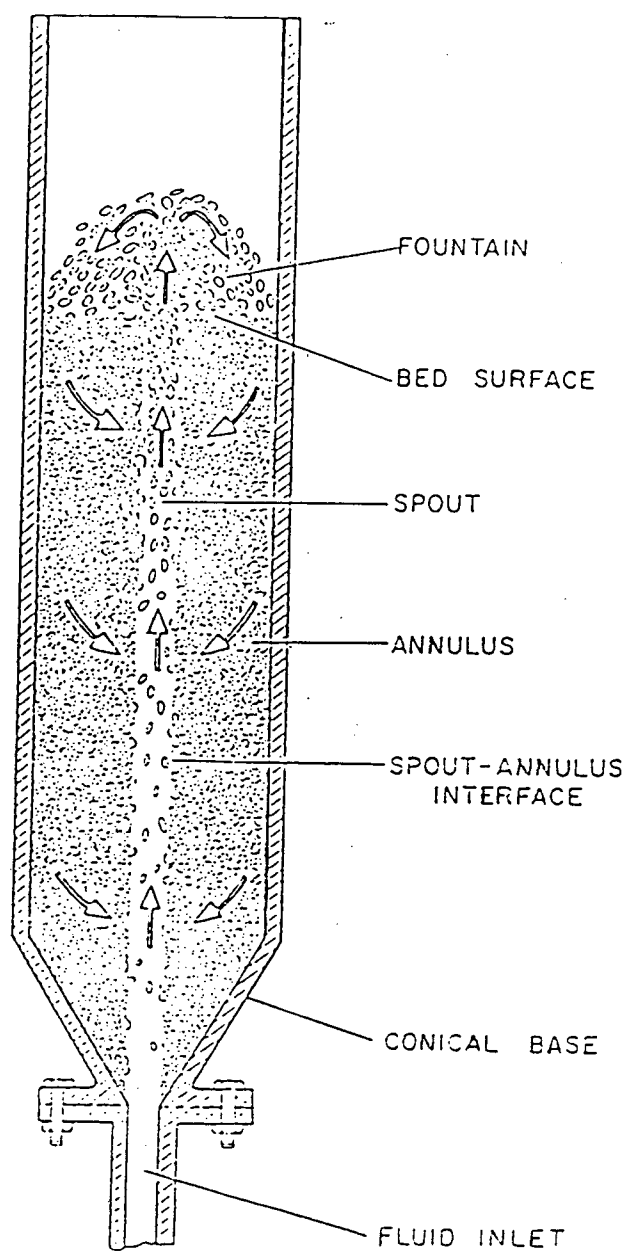


Fig 4: Schematic Diagram for Spouted Bed

However, the time which a particle spends in the spout is very small compared to that in the annulus. Therefore, the total heat transferred in the spout will be less than that in the annulus. The time required to bring a feed particle close to the bulk solids temperature is given by the following unsteady state equation,

$$\frac{T_p - T_{po}}{T_b - T_{po}} = 1 - \exp\left[-\frac{h_p A_p t}{M_p C_{pp}}\right] \quad (2.3)$$

From this equation, the time required to heat up a typical size oil shale particle, say 2 mm diameter from room temperature to a bed temperature of 500°C was estimated to be of the order of 20 seconds. Since the practical mean residence time in the annulus is at least several minutes, the steady state concentration of bed particles reaching the bed temperature is high. Therefore, the overall heat transfer rate would not normally be limited by the external heat transfer. For equation 2.3, the temperature within the particle is assumed uniform. However, in the case of the spouted bed where large sized particles may be used, the intraparticle temperature gradient could not be ignored. The magnitude of the intraparticle temperature difference relative to the temperature difference between the particle surface and fluid is determined by Biot number, $Bi_H = h_p r_p / k_p$, provided that the Fourier number $Fo_H = at / r_p^2$, which is a dimensionless time variable, exceeds a minimum value of 0.2. The relative magnitude of intraparticle temperature

difference decreases with decreasing Bi_H , the maximum value becoming less than 5% of the temperature difference between the fluid and particle surface at $Bi_H=0.1$.

For the oil shale particles used in our experiment, assuming that an intraparticle temperature gradient exists, the particle temperature profile can be predicted by the unsteady state conduction equation,

$$\frac{\partial T}{\partial t} = \frac{a}{r^2} \frac{\partial(r^2 \partial T / \partial r)}{\partial r} \quad (2.4)$$

and can be calculated as a function of time for the variable conditions along the 4 different regions of the spouted bed: spout, fountain (upward), fountain (downward) and annulus region, by a numerical solution of this equation as the longitudinal profiles of gas and particle velocities, gas temperature and spout voidage are known. The boundary condition in this case is,

$$k_p(\partial T / \partial r)_{r=r_p} = h_p(T_b - T_{r=r_p}) \quad (2.5)$$

The details of the computer program are given in Appendix A. Table 7 and 8 list the particle temperature history for oil shale of 3mm, 1.5mm and 0.75mm diameter after one and two passes in the reactor respectively. The temperature history is estimated at a function of time along the spout, fountain (upward), fountain (downward) and annulus regions. The reactor temperatures chosen are 723,

773 and 823K. The velocity of the oil shale particle at the apex of the spout is assumed to be zero.

From the typical results shown in Table 7, it can be seen that for the 3mm particle size oil shale, there is a considerable temperature gradient in the spout, fountain (upward) and fountain (downward) regions. But during the slow travel down in the annulus section, the temperature gradient is effectively relaxed. It should be noted that after the first pass through the four regions, the particle has not yet reached the reactor temperature. In fact, the temperature of the particle is only at 568.0 - 606.2K which is not even high enough for pyrolysis to start. The particle has to travel the cycle the second time in order to effectively reach the reactor temperature, and pyrolysis is expected to take place in the annulus.

For the 1.5mm diameter size oil shale, a temperature gradient still exists in the particle but is less significant than for the 3mm particle size. For reactor temperature 773 and 823K, the particle reaches to 732.1 and 767.6K respectively in the annulus region, which is high enough for pyrolysis to begin. Again, pyrolysis is expected to take place in the annulus.

For the 0.75mm particle size oil shale, intraparticle temperature gradient greater than 10K hardly exist. At the top of the spout, the particle has not reached the reactor temperature but the temperature is sufficient for pyrolysis to take place. As the 0.75mm oil shale is smaller than the

Table 7: Particle Temperature History for 3.0, 1.5 and 0.75mm Oil Shale (After One Pass)

Reactor Temperature (K)	Particle Size (mm)	Particle	Spout (K)	Fountain (Upward) (K)	Fountain (downward) (K)	Annulus (K)
723.0	3.0	centre	361.8	367.4	372.9	567.1
		surface	431.4	422.3	418.1	568.0
	1.5	centre	533.8	543.6	550.0	690.0
		surface	566.2	559.3	557.9	690.1
	0.75	centre	693.2	696.1	696.8	722.2
		surface	697.8	696.8	697.1	722.2
773.0	3.0	centre	359.8	366.7	373.5	591.1
		surface	439.1	428.1	423.4	592.2
	1.5	centre	545.0	557.8	565.6	731.9
		surface	584.3	575.6	574.2	732.1
	0.75	centre	732.3	736.4	737.3	771.9
		surface	738.7	737.3	737.7	771.9
823.0	3.0	centre	347.2	356.4	365.6	604.9
		surface	438.1	423.9	419.0	606.2
	1.5	centre	533.4	552.8	562.7	767.3
		surface	584.4	572.8	572.2	767.6
	0.75	centre	757.5	764.5	766.0	821.0
		surface	767.9	765.8	766.9	821.0

* Inlet temperature of the particle is assumed to be at 298K

* The temperatures are calculated as particle leaving different regions of the spouted bed reactor

Table 8: Particle Temperature History for 3.0, 1.5 and 0.75mm Oil Shale (After Two Passes)

Reactor Temperature (K)	Particle Size (mm)	Particle	Entrance (K)	Spout (K)	Fountain (Upward) (K)	Fountain (downward) (K)	Annulus (K)
723.0	3.0	centre	567.1	590.9	593.0	595.0	666.3
		surface	568.0	616.4	613.1	611.5	666.3
	1.5	centre	690.0	708.3	709.1	709.6	720.4
		surface	690.1	710.9	710.3	710.2	720.5
	0.75	centre	722.2	722.9	722.9	723.0	723.0
		surface	722.2	723.0	723.0	723.0	723.0
773.0	3.0	centre	591.1	615.3	617.9	620.5	703.6
		surface	592.2	645.6	641.4	639.6	704.0
	1.5	centre	731.9	753.3	754.4	755.1	769.5
		surface	732.1	756.7	756.0	755.9	769.5
	0.75	centre	771.9	772.9	772.9	772.9	773.0
		surface	771.9	772.9	772.9	772.9	773.0
823.0	3.0	centre	604.9	625.9	629.8	633.6	732.7
		surface	606.2	663.7	657.8	655.8	733.2
	1.5	centre	767.3	792.4	794.4	795.5	817.1
		surface	767.6	797.8	796.5	796.5	817.1
	0.75	centre	821.0	822.8	822.8	822.8	823.0
		surface	821.0	822.8	822.8	822.8	823.0

* The temperatures are calculated as particle leaving different regions of the spouted bed reactor

spouting sand, 1.11mm , it is expected that some of the oil shale will actually escape from the fountain (upward) region and be entrained to the cyclone. Even in this case, these particles will still undergo pyrolysis.

In the actual experimental case, there is a 17.8cm long section between the feed point and the apex of the spouted bed. A supplementary program (in Appendix A) was written to calculate the particle temperature profile for this section. It was found that the oil shale particles are still essentially at room temperature as they leave this section. This indicated that the above assumption that the particle at the apex of the spouted bed is at room temperature is correct.

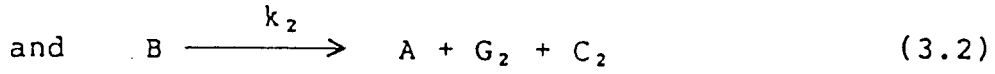
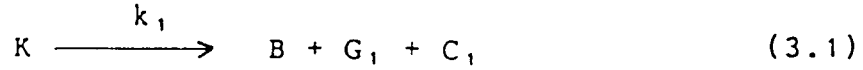
3. KINETICS

3.1 Literature Review of the Kinetics of Oil Shale Pyrolysis

Several investigations⁽²²⁾⁻⁽³⁴⁾⁽³⁹⁾⁻⁽⁴¹⁾ have been carried out on the kinetics of the decomposition of kerogen in oil shale. The first comprehensive experimental study of the process was reported by Hubbard and Robinson⁽²²⁾. They studied the decomposition of kerogen in Colorado oil shale at temperatures from 400 to 525°C by heating the shale sample in the absence of oxygen at atmospheric pressure and measuring the decomposition products. The first decomposition products to form were gas and bitumen. On further heating, the bitumen decomposed to form the final products: gas (the non-condensable vapors), oil (the condensable vapors) and carbonaceous residue. Hubbard and Robinson interpreted their data by assuming that the total amount of kerogen that decomposed was equal to the total amount of gas, oil and bitumen.

Braun and Rothman⁽²⁴⁾ studied the Hubbard and Robinson data and proposed to include a thermal induction period in the data analysis, and represented the kinetics of oil production by a simple mechanism involving two consecutive first order reactions. The thermal induction period was required to account for the non-isothermal heating effects in the Hubbard and Robinson experiments.

The pyrolysis of kerogen can be expressed as:



The rate of kerogen decomposition is given by,

$$\frac{\partial K}{\partial t} = -k_1 K \quad (3.3)$$

The net rate of bitumen formation and decomposition is,

$$\frac{\partial B}{\partial t} = k_1 f_1 K - k_2 B \quad (3.4)$$

The rate of oil production is given by,

$$\frac{\partial A}{\partial t} = k_2 f_2 B \quad (3.5)$$

The rate of gas production is

$$\frac{\partial G}{\partial t} = k_1 f_3 K + k_2 f_4 B \quad (3.6)$$

Integrating equation (3.3) for $K=K_0$ at $t=t_0$ gives:

$$K = K_0 e^{-k_1(t-t_0)} \quad (3.7)$$

By combining (3.4) and (3.7), and integrating for $B=0$ at

$t=t_0$, then the amount of B, bitumen at any time is:

$$B = \frac{k_1 f_1 K_0}{(k_2 - k_1)} [e^{-k_1(t-t_0)} - e^{-k_2(t-t_0)}] \quad (3.8)$$

Combining equations (3.5) and (3.8), and integrating for $A=0$ at $t=t_0$, then the fraction of initial kerogen A/K_0 that is converted to oil at any time t is:

$$\frac{A}{K_0} = \frac{f_A}{(k_2 - k_1)} \{ k_2 [1 - e^{-k_1(t-t_0)}] - k_1 [1 - e^{-k_2(t-t_0)}] \} \quad (3.9)$$

Combining equations (3.6) and (3.8), and integrating for $G=0$ at $t=t_0$, the fraction of initial kerogen G/K_0 that is converted to gas at any time t is:

$$\frac{G}{K_0} = f_3 [1 - e^{-k_1(t-t_0)}] +$$

$$\frac{f_1 f_4}{(k_1 - k_2)} \{ k_2 [1 - e^{-k_1(t-t_0)}] - k_1 [1 - e^{-k_2(t-t_0)}] \} \quad (3.10)$$

Braun et al.⁽²⁴⁾ used equation (3.9) to analyse the data of Hubbard and Robinson⁽²²⁾ for production of oil from a Colorado oil shale having a Fischer Assay of 26.7 gal/ton. The measured and calculated values of A/K_0 are found to be in agreement with each other.

Johnson et al⁽²⁵⁾ used thermogravimetric analysis (TGA) to study the pyrolysis of oil shale spheres. The sample weight was measured while the temperature was increased with heating time. They developed a complex kinetic model which incorporated both heat transfer and chemical kinetics, but the kinetic scheme required a series of ten coupled chemical reaction steps.

Campbell et al⁽²⁷⁾ obtained kinetic data on Colorado oil shale pyrolysis by both the isothermal and the non-isothermal technique. The non-isothermal results show that the oil evolution process can be quite accurately represented as a first order reaction.

Granoff and Nuttal⁽²⁸⁾ investigated the pyrolysis kinetics for large single particle (12.7mm diameter cylinder and sphere). The experiment was carried out at 384 to 520°C with nitrogen as pyrolyzing gas. The weight loss of the oil shale particle was continuously measured with a Cahn recording thermobalance. They also obtained the centreline temperature histories for the oil shale with a microthermocouple. The non-isothermal shrinking-core model and non-isothermal homogeneous model were developed in order to describe the pyrolysis process.

For the non-isothermal shrinking-core model, it is assumed that the reaction always occurs at the interface between the unreacted core and the surrounding spent shale layer. The model consists of the dynamic distributed energy balance, convective and radiant surface boundary condition,

and a first order kinetic controlled shrinking core material balance. The resulting equations must be solved simultaneously, since the rate of core shrinkage is strongly temperature dependent as indicated by the Arrhenius expression.

The partial differential equation describing the dynamic temperature profile within a sphere is,

$$\rho_s C_{ps} \frac{\partial T_s}{\partial t} = k_s \left[\frac{1}{r^2} \frac{\partial}{\partial r} r^2 \left(\frac{\partial T_s}{\partial r} \right) \right] + C \left(\frac{\partial a}{\partial t} \right) \Delta H_{rxn} \quad (3.11)$$

$$a = \frac{(w_0 - w_t)}{(w_0 - w_\infty)}$$

where the initial condition is,

$$T_s = T_{\text{initial}} \text{ at } t=0$$

$$T_g = \text{constant steady-state value at } t=0$$

and the boundary condition is,

$$Q_{rp} = hA_p(T_{rp} - T_g) + \delta \epsilon A_p(T_{rp}^a - T_w^a) \quad (3.12)$$

The shrinking-core material balance equations are,

$$\frac{\partial r_c}{\partial t} = -k_i \exp\left(-\frac{\Delta E}{RT_c}\right) \quad (3.13)$$

$$\frac{\partial a}{\partial t} = \frac{4\pi r_c^2 k_i \exp[(-\Delta E/RT_c)/C]}{0.75\pi r_p^3 C} \quad (3.14)$$

therefore the appearance rate of individual species is given as:

$$\frac{\partial a}{\partial t} = \frac{4\pi r_c^2 k_i \exp[(-\Delta E/RT_c)/C_i]}{0.75\pi r_p^3 C_i} \quad (3.15)$$

The model fits very well at high temperature (520°C), but is not so good at the lowest temperature.

The second model developed was the non-isothermal homogeneous model in which it is assumed that there are no temperature gradients within the particle. The particle temperature is given by:

$$\rho_s V_p C_{ps} \frac{\partial T_s}{\partial t} = h A_p (T_g - T_s) + \delta \epsilon_p A_p (T_w^4 - T_s^4) + k(1-a)V_p \quad (3.16)$$

The model was able to match both the high and low temperature conversion for small and moderate oil-sized spherical particles where the particle temperature is assumed to be uniform.

Wang and Noble⁽³¹⁾ carried out oil shale pyrolysis under non-isothermal conditions between 350 and 500°C. and at different pressures (78 and 765 kPa). They used a comprehensive analytical procedure to separate the oil shale into five individual components: polar, weak polar,

saturates, aromatics and olefins. They proposed a simplified kinetic scheme that include the distribution of products as follows:

$$\frac{\partial C_i}{\partial t} = \frac{k_i}{C} \exp\left[\frac{-E_i}{RT} - \left(\frac{fK_O}{C}\right)\left(\frac{RT^2}{E_O}\right) \exp\left(\frac{-E_O}{RT}\right)\right] \quad (3.17)$$

Yang and Sohn⁽³³⁾ studied a Chinese oil shale, and found that the mechanism of kerogen decomposition can be represented by an overall first-order kinetics.

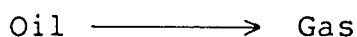
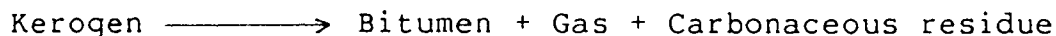
In view of the above survey, it appears that from an engineering standpoint, the rate of oil generation can be adequately described by an overall first order kinetics.

3.2 Development of the Kinetic Model

A model was derived to predict the change of kerogen, bitumen and oil content of the oil shale with time. The basic idea is that upon the application of heat, kerogen in the shale particles is first decomposed to bitumen and gas. The bitumen is defined as the benzene-soluble organic material that does not vaporize but remains in the shale sample. Then the bitumen is heated to decompose to form oil and gas, and carbonaceous product adheaved to the shale mineral matrix. Oil is defined as the condensable hydrocarbons and other compounds escaping from the shale sample, whereas gas is defined as the non-condensable vapours escaping from the shale sample. The carbonaceous residue is the benzene-insoluble portion of the kerogen

remaining in the spent shale. On further heating, oil is decomposed to gas and carbonaceous products.

The pyrolysis of kerogen is expressed as



The first two reactions take place in the solid phase and the time of reaction can be taken as the residence time of the solids. Whereas the oil decomposition occurs in the gas phase, and the time for reaction is very short i.e. the mean residence time of the gas (Vol of the gas phase/Flow rate of gas).

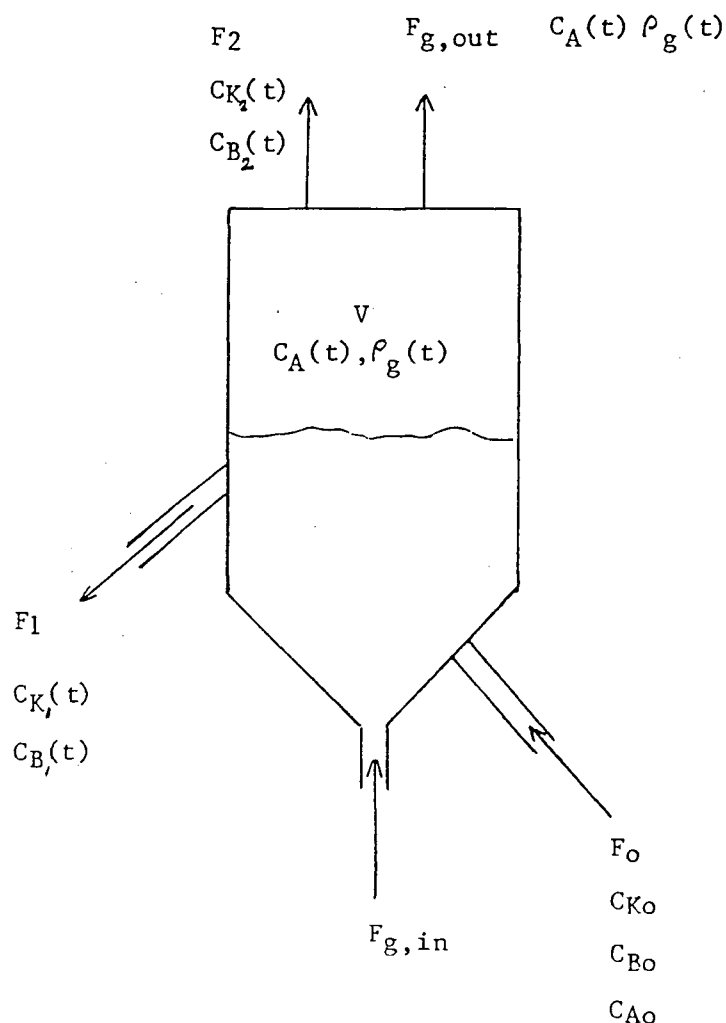
The kinetic equations used to describe the reactions are taken from Braun and Rothman⁽¹³⁾ and were presented in the beginning of Section 3.1. In the present research, the amount of oil produced is measured by sampling of the off-gas. Neither kerogen nor bitumen were measured.

The structure of the spouted bed is not taken into account. However, a few assumptions are made based on the characteristics of the spouted bed.

- 1) $F_0, C_{k0}, F_{g,in}, F_1, F_2, V$ are all constant.

- 2) Bed solids and gases within the reactor are well mixed.
- 3) The intraparticle temperature gradient of the oil shale is ignored because the time required to heat up the particles (in the range of 20 seconds, Section 2.6) is insignificant compared to the average holding time of the particle in the reactor (in the range of 30 minutes).

The configuration of the model is shown as below:



Unsteady State Material Balance

$$\begin{array}{ccccccccc} \text{weight} & & \text{weight} & & \text{weight} & & \text{weight} & & \text{weight} \\ \text{of solid} & + & \text{of gas} & - & \text{of solid} & - & \text{of gas} & = & \text{Accumulated} \\ \text{fed in} & & \text{inflow} & & \text{withdrawn} & & \text{outflow} & & \\ & & & & \text{\& entrained} & & & & \end{array}$$

$$F_0 + F(g,in)\rho(g,in) - (F_1 + F_2) - F(g,out)\rho(g,out) = \frac{dW}{dt} \quad (3.19)$$

Assuming $F_{g,in}\rho_{g,in} = F_{g,out}\rho_{g,out}$ (as spouting gas accounts for 97% of the total gas outflow), then (3.19) becomes,

$$F_0 - F_1 - F_2 = \frac{dW}{dt} \quad (3.20)$$

Kerogen Balance

$$\begin{array}{ccccccc} \text{Kerogen} & & \text{Kerogen} & & \text{Kerogen} & & \text{Kerogen} \\ \text{entering} & - & \text{withdrawn} & - & \text{decomposed} & = & \text{Accumulated} \\ \text{with shale} & & \text{\& entrained} & & & & \end{array}$$

$$F_0C_{K0} - F_2C_{K2} - F_1C_{K1} - r_K = \frac{dC_KW}{dt} \quad (3.21)$$

Bitumen Balance

$$\begin{array}{ccccccc} \text{Bitumen} & & \text{Bitumen} & & \text{Bitumen} & & \text{Bitumen} \\ \text{produced} & - & \text{decomposed} & - & \text{withdrawn} & = & \text{Accumulated} \\ \text{by kerogen} & & & & \text{\& entrained} & & \end{array}$$

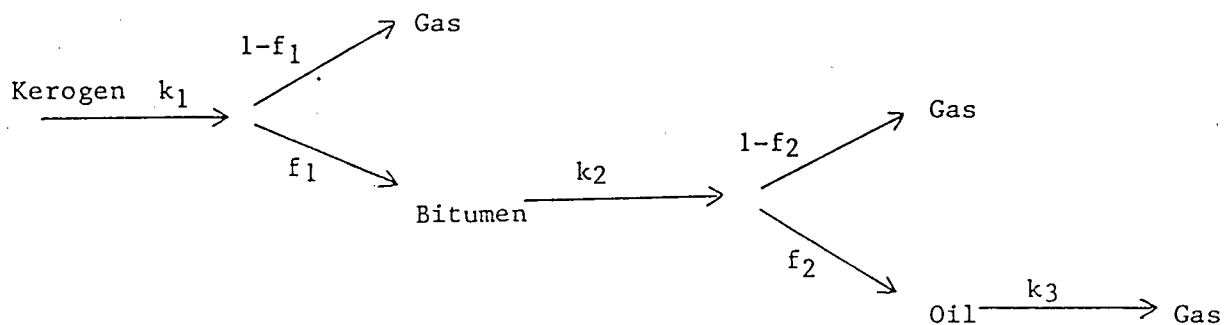
$$r_B - F_2 C_{B2} - F_1 C_{B1} = \frac{dC_B W}{dt} \quad (3.22)$$

Oil Balance

Oil produced by bitumen - Oil decomposed - Oil entrained = Oil Accumulated

$$r_A - F_g C_A = \frac{dC_A V}{dt} \quad (3.23)$$

Reaction Kinetics



$$r_K = -k_1 C_K W \quad (3.24)$$

$$r_B = f_1 k_1 C_K W - k_2 C_B W \quad (3.25)$$

$$r_A = f_2 k_2 C_B W - k_3 C_A V \quad (3.26)$$

From the experiment, F_0, F_1, F_2, V, C_{K0} are known, and from the literature, $k_1^0, k_2^0, E_1, E_2, f_1, f_2$ are known, then $W(t), C_K(t), C_B(t), C_A(t)$ can be solved from equations (3.20), (3.21), (3.22) and (3.23).

A simplified model with one less equation to solve was based on further assumption that W was constant at the average of the initial weight and final weight of the bed. This model can be used to work out k_3^0, E_3 and then solve for $C_K(t), C_B(t)$ and $C_A(t)$.

For Kerogen

Recall equation (3.21),

$$F_0 C_{K0} - F_2 C_{K2} - F_1 C_{K1} - r_K = \frac{dC_K W}{dt} \quad (3.21)$$

By assumption $C_{K1} = C_{K2} = C_K$ because of backmixing, and $W = \text{constant}$ then equation (3.21) becomes,

$$F_0 C_{K0} - F_2 C_K - F_1 C_K - r_K = W \frac{dC_K}{dt} \quad (3.27)$$

Substitute (3.24) into (3.27),

$$F_0 C_{K0} - F_2 C_K - F_1 C_K - k_1 C_K W = W \frac{dC_K}{dt} \quad (3.28)$$

Rearranging (3.28) gives,

$$\frac{F_0 C_{K0}}{W} - \left(k_1 + \frac{F_1}{W} + \frac{F_2}{W} \right) C_K = \frac{dC_K}{dt} \quad (3.29)$$

and

$$A = \frac{F_0 K_0}{W} \quad B = \left(k_1 + \frac{F_1}{W} + \frac{F_2}{W} \right)$$

$$\frac{dC_K}{dt} = A - BC_K \quad (3.30)$$

For Bitumen

Recall equation (3.22),

$$r_B - F_2 C_{B2} - F_1 C_{B1} = \frac{dC_B W}{dt} \quad (3.22)$$

For $C_{B1} = C_{B2} = C_B$, and taking W constant, and substituting (3.25) into (3.22), gives

$$f_1 k_1 C_K W - k_2 C_B W - (F_1 + F_2) C_B = W \frac{dC_B}{dt} \quad (3.31)$$

Rearranging (3.31) gives,

$$f_1 k_1 C_K - \left(\frac{F_1}{W} + \frac{F_2}{W} + k_2 \right) C_B = \frac{dC_B}{dt} \quad (3.32)$$

Let $C = f_1 k_1$

$$D = \frac{F_1}{W} + \frac{F_2}{W} + k_2$$

To solve for C_B , equation (3.30) and (3.32) have to be taken together. Using Laplace transformation, these become,

$$C_K = \frac{A}{B} (1 - e^{-Bt}) \quad (3.33)$$

$$C_B = CA (C_{11} + C_{12}e^{-Dt} + C_{13}e^{-Bt}) \quad (3.34)$$

where $C_{11} = \frac{1}{BD}$

$$C_{12} = \frac{1}{(D^2 - BD)}$$

$$C_{13} = \frac{1}{(B^2 - BD)}$$

Then

$$\text{Kerogen} = K_B W_{(\text{mass})} \quad (3.35)$$

$$\text{Bitumen} = C_B W_{(\text{mass})} \quad (3.36)$$

For Oil

Recall equation (3.23),

$$r_A - F_g C_A = \frac{dC_A V}{dt} \quad (3.23)$$

Substitute (3.26) into (3.23),

$$f_2 k_2 C_{BW} - k_3 C_A V - F_g C_A = \frac{dC_A V}{dt} \quad (3.37)$$

$$\frac{f_2 k_2 C_{BW}}{V} - C_A \left(\frac{F_g}{V} + k_3 \right) = \frac{dC_A}{dt} \quad (3.38)$$

Let

$$P = \frac{f_2 k_2 C_{BW}}{V} \quad Q = \frac{F_g}{V} + k_3$$

therefore,

$$C_A = \frac{P}{Q} (1 - e^{-Qt}) \quad (3.39)$$

Total oil accumulated over time, $t=0$ and $t=t$

$$\text{Oil Yield} = \int_0^t C_A F_g dt \quad (3.40)$$

Predictions of equation 3.40 will be compared with the accumulated oil yield determined by sampling the outlet vapour.

4. EXPERIMENTAL EQUIPMENT AND PROCEDURE*

4.1 Pyrolysis Apparatus

The apparatus used in this thesis was originally designed and built by A. Jarallah⁽²⁾ for coal pyrolysis. A number of modifications were made to improve the operation and reliability of the apparatus. The design characteristics of the major units are listed in Table 9. A schematic diagram of the experimental apparatus is shown in Figure 5.

A new feed system was installed to replace the original vibratory feeder which was difficult to control and was not designed to handle particles below 1mm diameter. The new system includes a plexi-glass hopper, a rotary feeder and a inclined glass section.

The feed hopper was 305mm high x 165mm diameter. It had a conical bottom which was fitted with a 12.5mm diameter ball valve. A plastic tube connected the feed hopper and the inclined inlet pipe section to balance the pressure in the feed hopper with that in the reactor in order to get a constant feed rate. A syntron magnetic vibrator (Model V-2-B) was mounted on the bottom of the hopper which aided the flow of the oil shale out of the rotary valve. The valve rotation speed was controlled by the G K Heller motor controller. Because of the low feed rate required, a 30:1 gear reductor was installed. The controller was always set

*

The author is indebted to Dr. G.K. Khoe who assisted with the modifications to the apparatus, and made many of the improvement in techniques and helped carry out some of the experimental runs.

TABLE 9: Design Characteristics of Spouted Bed Pyrolyzer System

Reactor:	Material - 317 Stainless Steel Inside diameter - 128mm Wall Thickness - 6.6mm Cone Angle - 70° Disengaging Section Diameter - 255mm Height (includes cone and disengagement section) - 1.22m
Spent Shale Receiver:	Material - Mild Steel Outside Diameter - 305mm Height - 0.91m
Oil Shale Hopper:	Material Steel - Plexi-glass Outside Diameter - 165mm Height - 305mm
Spouted Bed Furnace:	Electrical Rating - 6.9kW Maximum Temperature - 1200°C Heaters: 6 1/4-Round 304mm high x 178mm I.D. Heated Length - 0.69m
Spouted Gas Preheater:	Electrical Rating - 8.45kW Maximum Temperature - 1200°C Heaters: 4 semi-cylindrical 69.85mm x 44.45mm I.D. Flexible electrical heating tape Heated Length - 0.69m
Oil Shale Feeder:	Rotary Feeder

Gas-Solid Cyclone:	Material - Stainless Steel Diameter - 150mm Cylinder Height - 500mm Cone Height - 300mm
Condenser:	Shell - 316 Stainless Steel Inside Diameter - 128mm Wall Thickness - 6.6mm Tubes - 6 U-tubes 0.86m long Diameter - 12.7mm Area - 4130 cm ²
Oil Receiver:	Material - Glass and Stainless steel Inside Diameter - 229mm Height - 305mm
Oil Filter:	Material - Stainless steel Diameter of orifice - 19.1m
Piping:	Material - 316 Stainless steel

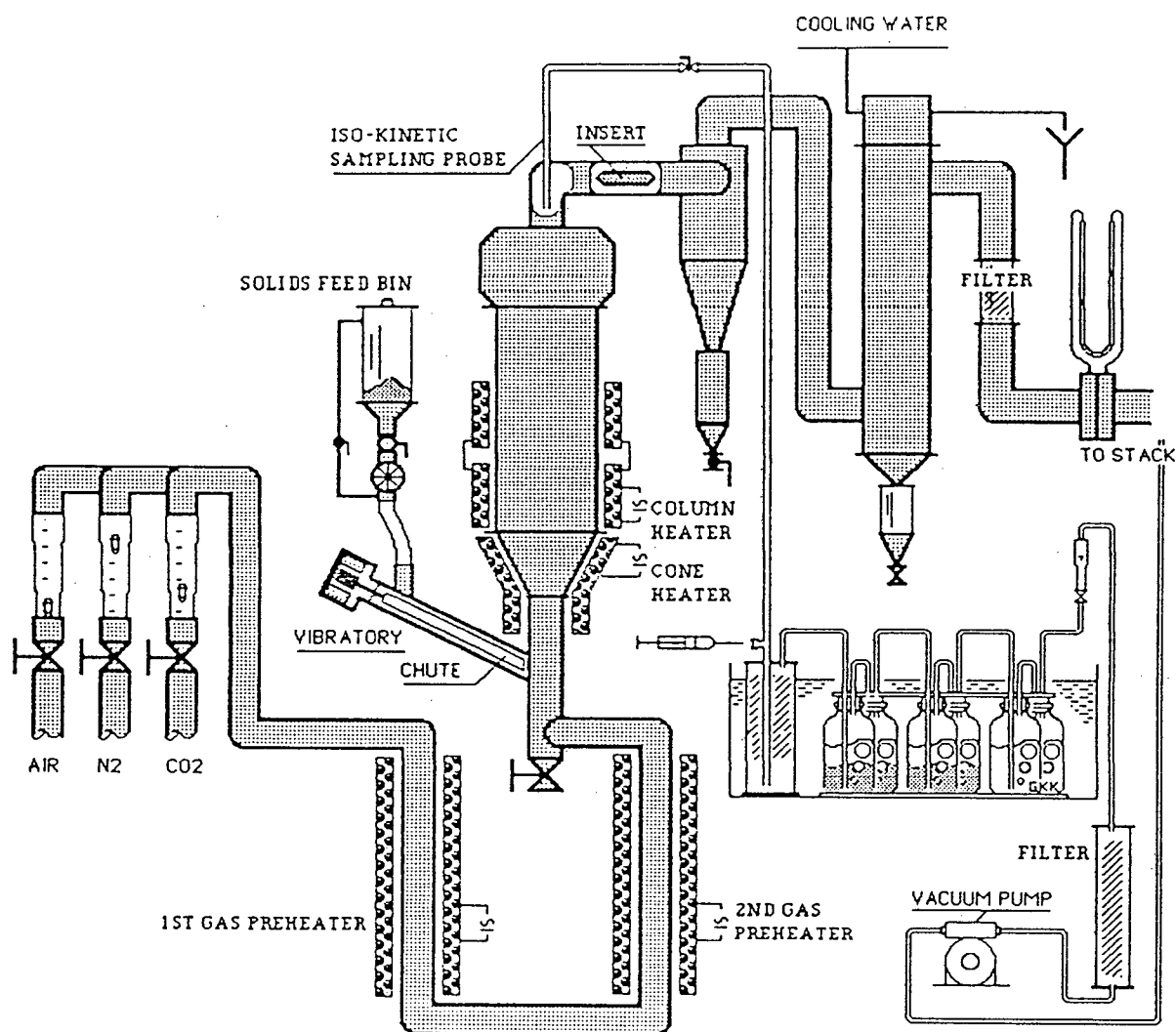


Fig 5: A Schematic Diagram for the Experimental Apparatus

below 10% of the maximum speed rate and slight fluctuations were recorded. For this reason, a higher gear ratio reducer is recommended.

The oil shale dropped from the rotary valve through the rubber tubing onto the copper pipe that was fitted inside a 25.4mm x 150mm QVF glass tube. A second syntron vibrator was attached to the end of the copper pipe to promote transfer of the oil shale directly to the inlet pipe of the reactor. Trials had been done in which the oil shale dropped directly onto the glass tubing itself, i.e. in the absence of the copper pipe, but accumulation of the solids and eventual blockage at the entrance of the inlet occurred.

The off-gas sampling train from which the oil yields were to be determined was completely rebuilt from Jarallah's design⁽²⁾. Instead of stainless steel impingers, glass impingers were used. These were easier to handle and provided a clear view during the experiment. The impinger train was immersed in a tank filled with cracked ice and water. The whole system rested on a trolley which could be carried to a fume hood for oil recovery. The position of the off-gas sampling point was also relocated. Previously, it was at the outlet pipe of the drying column that was placed after the last impinger. However, some of the methylene chloride solution had evaporated with the gas and therefore affected the gas chromatograph results. The off-gas sampling point was therefore located at the upstream of the first impinger (refer to Figure 5).

The heating system was also modified. The preheater had to be rebuilt because the original semi-cylindrical heaters were burnt out and as the heaters were touching the surface of the stainless steel pipe, a hole had been made in the pipe as well. An electric forced air duct heater element enclosed in a fluidized sand bed was then tried. The sand was used to improve the heat transfer and avoid hot spots in the heater box. This system failed as the electrical element overheated and melted. Finally, the Lindberg half circle heating unit was used. These consisted of 4 semicylindrical heaters of 44.5mm ID which were clamped around the 3.8cm diameter pipe to give a heated length of 698.5mm. The total electrical rating of these heaters was 7.2kW. To avoid a short circuiting of these heaters as occurred in the previous case, an air gap of 1.5mm was left between the heating element and the pipe section. To increase the rate of heat transfer, the pipe section was filled with ceramic Raschig rings. A thermocouple was inserted in the air gap, and the temperature was controlled by an Omega controller. As it was the temperature in the air gap that was measured, the control was a bit difficult.

In the original design, the main heater on the spouted bed reactor consisted of 16 quarter-cylindrical electrical elements each of 178mm ID and 152mm height. These were mounted around the main cylindrical section of the reactor to form a shell. An air gap of 18mm existed between inside of the heaters and the outside surface of the reactor. This

reduced the efficiency of heat transfer and the time for heating up was lengthy. After rearrangement, 6 quarter-cylindrical electrical elements were used. The heated section was 609.6mm high and the total electrical ratings for these heaters was 6.9kW. The air gap was reduced to 1.5mm, therefore the rate of heat transfer was improved and the heating up time was halved. The temperature was controlled by an Omega controller mounted on the control panel.

There was a serious heat loss between the preheaters and the main heater, therefore a flexible electrical heating tape (Heavily insulated Samox) was wrapped around the conical section of the reactor. The total electrical rating was 1.25 kW, and the power applied was adjusted by a variac.

Both the reactor and the downstream pipe were insulated by 5-7.5cm ceramic blanket to prevent heat loss to the surroundings.

Other modifications included provision of new gaskets in all joints; and the installation of an insert in the horizontal pipe upstream of the cyclone to reduce the cross-sectional area available for flow, so as to avoid the settling of solids in this region.

The temperature throughout the apparatus was measured by chromel-alumel thermocouples with 316 stainless steel sheath of 1.6mm diameter. In the reactor, and the preheaters, more rugged K-type thermocouples of 6.3 mm diameter were used.

4.2 Properties of the Oil Shale

The oil shales studied in this project were supplied by the Research Productivity Council of New Brunswick. The original coarse oil shale, as received was reduced in size using a jaw crusher. It was then screened to 3 different sizes: 2-4mm, 1-2mm and 0.5-1mm which were stored in separate plastic buckets. Representative samples of the oil shales were sent to the General Testing Laboratories of Vancouver for proximate and ultimate analyses. The results are listed in Table 10. Table 11 gives the analysis of oil shale ash and carbon. It can be seen that there is slight variation among the different sizes. Table 12 lists the modified Fischer Assay results for the different sizes of oil shale A and reports that larger size fractions have better oil yields. These analyses were carried out at the Research and Productivity Council of New Brunswick.

4.3 General Procedure

The basic mode of operation with this pyrolysis unit is to fill the reactor with inert solids (sand or spent shale), heat to the required temperature with air, then switch the gas to N_2/CO_2 or N_2 . The velocity of gas is set at 10% above the minimum spouting velocity. (The calculation for minimum spouting velocity is included in the computer program - Profile.) The oil shale is fed into the reactor over a period of 1 1/2 hour. In this case, the height of the bed will gradually rise with time. The oil is recovered from

TABLE 10: Proximate and Ultimate Analysis of Blend of Oil Shale A

Proximate Analysis

% Moisture	1.69
% Ash	72.53
% Volatiles	25.17
% Fixed Carbon	0.61
	100.00

Ultimate Analysis (Dry Basis)

% C	15.91
% H	2.05
% N	0.51
% S	0.92
% Cl	0.01
% Ash	73.78
% Oxygen (diff)	6.82
	100.00

TABLE 11: Analysis of Oil Shale Ash and Carbon

Size Fraction (mm)	0.5-1.0	1-2	2-4
Total Organic Carbon (%)	10.2	10.6	12.4
Total Carbon (%)	12.3	13.3	14.7
SiO ₂ (wt%)	43.4	41.9	41.6
Al ₂ O ₃	10.6	10.4	10.3
Fe ₂ O ₃	4.56	4.38	4.36
CaO	8.32	9.03	8.10
MgO	3.38	3.57	3.20
Na ₂ O	0.95	1.05	1.05
K ₂ O	1.63	1.60	1.57
SO ₃	1.70	1.87	2.22
Loss on Ignition	24.1	25.1	26.1
Ba (ppm)	310	306	283
Mn	602	568	508
Sr	309	333	302
Ti	2910	2560	2890

* Digested samples in mixture of acids, analyzed solution by inductively coupled Argon Plasma Spectrograph
Carbon and Sulphur by Leco Induction Furnace
Analyses by Can-Test Ltd.

TABLE 12: Modified Fischer Assay of Oil Shales

	<u>Shale Sample A</u>					<u>Shale Sample B</u>	
Size Fraction (mm)	0.5	0.5-1.0	1-2	2-4	4	0.5-1.0	1.0-2.0
Oil Yield (wt%)	5.2	5.5	7.8 8.1 7.95	8.1 7.6 7.85	7.6	2.9	4.5
Water Yield (wt%)	2.1	2.0	2.2 2.3 2.25	2.2 1.8 2.0	1.6	3.2	2.4
Gas Lost (wt%)	1.2	5.5	3.0 1.6 2.3	1.7 3.6 2.7	4.8	1.4	3.1
Char Yield (diff.)	91.5	87.0	87.0 88.0	87.0 88.0	86.0	92.5	90.0
Oil Yield (l.gal/ton)	12.1	12.7	18.0 18.6	18.9 17.4	17.4	6.7	10.4
Oil Density (g/ml at 15.5°C)	0.8562	0.8670	0.8670 0.8678	0.8563 0.8763	0.8752	0.8573	0.8634

Analysed at Research and Productivity Council, Fredericton

the off-gas sampling train which is activated 5 minutes after the oil shale feeding begins. The gas samples are obtained by syringe during the experiment.

Other sets of experiments were carried out in which the height of the bed material was kept constant. This was achieved by releasing part of the overflow material through a side pipe at the conical section of the spouted bed at specific time intervals (5 or 10 minutes). The overflow material dropped through a ball valve into a stainless steel pipe section with an end-cap. After closing the ball valve, the end-cap was unscrewed to release the overflow material. Then the end-cap was put on again, and the ball valve was opened to allow more material to be removed. In this way the reactor operated in a quasi-steady state, rather than having the solids holdup steadily increasing.

4.4 Detailed Operating Procedure

The screened oil shale (about 2 kg) was loaded into the feed hopper. The required amount of inerts (Ottawa sand -14 +20 mesh, 5.9kg) was charged into the reactor from the top. This gave a static bed height of 33cm. During charging, the air was turned on at a low rate to prevent the sand from dropping into the spouting gas inlet pipe and creating a blockage. To conserve nitrogen and carbon dioxide, air was first used for spouting to heat up the sand to the desired temperature. The tube section of the off-gas sampling line was installed and the ball valve closed. Then the air flow

was adjusted to the operating flow, and the main reactor heater, spouting gas preheater, tape heater and the cooling water for the condenser were all turned on.

During the heating up period, the assembly of the remaining parts including the impinger train was carried out. The impingers were prepared as explained in Section 4.5. Soon after the required temperature of about 500°C was reached, the air was replaced by a mixed gas stream of CO₂ and N₂ (volume ratio 15:85), and a period of 15 minutes was allowed to purge the air before oil shale feeding was started. It was recognised that when the temperature reached above 500°C. the air stream should be replaced with inert gas, as there was some oil which had been deposited in previous experiments along the pipe, which could be ignited if the temperature became too high. Before the oil shale feeding was begun, a zero feed rate gas sample was obtained. This was done by opening the ball valve of the impinger train, followed by extracting a blank gas sample using a syringe. The ball valve was then closed. The sample was injected into the gas chromatograph.

The oil shale feeder controller was set at the desired point and the feeder turned on. The time at which oil shale feeding started was recorded. After 5 minutes, the ball valve of the impinger train was opened and the gas sample pump was then turned on and oil collection started. The five minutes delay was designed to exclude the non-steady state effects during the initial minutes of feeding. Gas sample

flow rate was adjusted to the desired value and the gas sample rotameter reading was recorded. Gas samples were extracted at respectively 15, 30, 45, 60, 75 and 80 minutes. After the last extraction, the feeder, gas pump and heaters were turned off. Oil collection lasted for 75 minutes (5 to 80 minutes). All temperatures and pressures throughout the system were recorded, and the spouting gas rotameter reading was taken. The nitrogen inlet gas stream was used to cool the system. The feed hopper was emptied of unused oil shale to determine the oil shale feed rate.

4.5 Oil Collection

The oil vapour is collected by isokinetic sampling of the off-gas. The velocities of the gases in the main pipe and the sampling tube are set equal. The first impinger was a 9.5mm x 30mm QVF glass tube filled with glass wool to provide a large contacting surface for condensation and filtering effects. This also helped to retain heavier oil fraction.

The second to the fifth impingers were filled with a mixture of methylene chloride and water (2:1 volume ratio). The sixth impinger contained methanol to trap the remaining oil-mist and entrained methylene chloride. The last impinger contained water to trap any entrained methanol. The containers were interconnected in the last minute before the sampling line was activated in order to prevent a backspill of methylene chloride from the second impinger into the

first one. This could contaminate the gas samples that were extracted through a septum at the upstream of the first impinger. For this reason, a slight vacuum was always maintained during an interruption, and the ice was added to the water bath just before the start of the oil collection.

The day after the experiment, the impingers, interconnecting pipes and the tube sections of the sampling lines which connected to the main off-gas line were thoroughly rinsed with solvents (methylene chloride and methanol), and then cleansed and dried before the next experiment.

The solution in the impingers and the washing solution would then be filtered to remove all fine particles. The water was separated from the methyl chloride and methanol - oil solution by using separation funnel. Any remaining trace of water was removed by adding sodium sulphate to the solution. The solution was then filtered and evaporated in a rotary evaporator (at 55°C, 20mmHg) to recover the oil. The recovered oil was weighed and the weight was recorded.

4.6 Gas Analysis

The gas analysis was performed on a Hewett-packard 5710A gas chromatograph with a 3388A automatic integraton system. The column separates hydrogen, oxygen, nitrogen, methane, carbon dioxide and carbon monoxide. Because of the limitation of this gas chromatograph, the hydrocarbons with molecular weight higher than methane cannot be detected. For

a few experiments , the gas analysis was done by using a another chromatograph by K.C. Teo⁽³⁵⁾ which was able to resolve upto C₆ hydrocarbons. The gas sample was extracted by a syringe through a septum at the upstream of the first impinger. The gas samples were analyzed and the values reported for each run.

4.7 Spent Shale Determination and Analysis

After the experiment, the reactor and the cyclone receiver were emptied and the contents of each one were separatly weighed. The weight of the spent shale produced was obtained by subtracting the weight of original Ottawa sand from the total weight of above. Although some solids have passed through the cyclone and were not recovered, the weight of the material from the dust receiver was taken to represent the solid entrained.

5. RESULTS AND DISCUSSIONS

5.1 General considerations

There were 26 successful experiments done on the New Brunswick oil shale A. The experimental conditions for each run are listed in Table 13.

The oil yield is calculated from the weight of oil collected from the sampled gas, multiplied with the ratio of the mass flow rate of the sampled gas streams to the total gas output from the reactor, and then divided by the oil shale feed rate. Care was especially required in washing the impinger train and sampling lines to recover oil from the sampled gas because the final oil product weighed about 1-4 gm.

The gas yield by species is calculated from the individual gas analysis, the total gas output from the reactor and the oil shale feed rate. Because of the limitation of the gas chromatograph, hydrocarbon gases of molecular weight higher than methane and gaseous sulphur, and nitrogen compounds are not detected. However, it is expected that the quantities of these gases are very small.

The spent shale yield is calculated from the weight of shale remaining in the reactor and cyclone receiver vessel after the run and the oil shale feed rate. Data indicated that about $2/3$ of the oil shale feed remained in the reactor and cyclone receiver, and $1/3$ had passed through the cyclone as entrained fines. Because the cyclone is oversized, the collection efficiency is not high. Since a

TABLE 13: Experimental Conditions for Each Run

Expt. No	Particle Size mm	Temperature		Shale Feedrate (kg/hr)	Initial Bed Sand/Spent Shale (kg)	Pyrolyzing Gas N ₂ /CO ₂ (vol%)
		Bed	Inlet (°C)			
2	0.5-1	509	509	1.49	5.9/0.0	85/15
3	0.5-1	505	505	1.37	5.9/0.0	85/15
4	1-2	503	503	1.65	5.9/0.0	85/15
5	1-2	501	501	1.33	5.9/0.0	85/15
6A	2-4	507	518	1.25	5.9/0.0	85/15
6B	1-2	540	528	1.29	5.9/0.0	85/15
7	1-2	554	554	1.33	5.9/0.0	85/15
8	1-2	454	450	1.39	5.9/0.0	85/15
9	1-2	530	530	1.39	5.9/0.0	85/15
10	2-4	506	505	1.21	5.9/0.0	85/15
11	1-2	477	470	1.52	5.9/0.0	85/15
12	2-4	506	502	2.71	5.9/0.0	85/15
12A	2-4	506	502	1.94	5.9/0.0	85/15
14	1-2	500	491	1.35	5.9/0.0	100/0
15	1-2	480	470	1.37	0.0/5.0	85/15
16	1-2	470	470	1.26	0.0/5.0	85/15
17	1-2	500	500	1.27	5.9/0.0	100/0
18	0.5-1	501	498	1.27	5.9/0.0	85/15
19	1-2	470	480	3.39	0.0/5.0	85/15
20	1-2	472	476	4.45	0.0/5.0	85/15
21	2-4	518	518	1.3	5.9/0.0	85/15
22	1-2	470	480	1.63	2.4/3.0	85/15
23	1-2	474	474	1.13	4.1/1.5	85/15
24	1-2	500	500	1.89	5.9/0.0	85/15
25	1-2	505	506	3.32	5.9/0.0	85/15
26	2-4	471	476	1.35	5.9/0.0	85/15

significant amount of fines passed through the cyclone, therefore an overall mass balance could not be closed. It was found that a small fraction of the fines were stuck onto the wall of the cyclone, and mechanical brushing was employed in Runs 16 to 26 to recover as much of the fines as possible to obtain a more reliable spent shale yield.

5.2 Effect of Temperature on Oil Yield and Composition

The study of the temperature effect was done on two feed sizes: 1-2mm and 2-4mm, at a constant feed rate of 1.40 and 1.28kg/h respectively. All of these experiments were done in a bed of silica sand, with pyrolyzing gas of 15% CO₂ and 85% N₂. The height of the bed increased gradually as the feed shale accumulated in the reactor during the experiment. There are two temperatures of potential importance in the oil shale pyrolysis experiments; the inlet temperature and the bed temperature. The inlet temperature refers to the temperature of the preheated gas where it meets the shale at the bed inlet, and the bed temperature refers to the average temperature in the annulus of the spouted bed itself. If the heating rate in the inlet region is low, the particle will reach pyrolysis temperature only after passing into the bed. Then the bed temperature will govern the oil yield. If the heating rate in the inlet region is high and the particle begins to pyrolyze before reaching the bed, the inlet temperature will be important. In all experiments, the inlet temperature and the bed temperature were kept to the same

value within experimental error except for Run 6B. The calculated temperature history for the oil shale particles was presented in Section 2.5. It was shown that the particles are still near room temperature at the entrance of the spouted bed. In other words, pyrolysis of the shale particles does not start before the particles are in the bed, thus the inlet temperature is less important in this case.

Table 14 lists the results. Figure 6 and 7 are plots of oil yield versus temperature. It can be seen that a maximum oil yield exists at some optimum temperature. For particles of 1-2mm, the optimum temperature is around 470-490°C. The oil yield is 7.1% which represents 89.3% of the modified Fischer Assay yield. It can be seen that the result for Run 6B in Figure 6 is slightly above the smooth curve through the other results. If the oil yield is plotted against the inlet temperature the curve will seem to be smoother, so it was thought that the temperature difference of 12°C between the inlet temperature and the bed temperature has produced this result. However, the temperature history calculation suggested little effect of inlet temperature. Experiment 6B should be repeated to verify the reliability of this data point.

For the 2-4mm particle size, the small number of data points preclude the determination of an optimum temperature. The few results in Figure 6 suggest an optimum somewhere between 490 and 510°C. At 505°C the oil yield was 7.4% which

TABLE 14: Effect of Temperature on Oil Yield

Expt No.	Particle Size (mm)	Bed	Temperature Inlet (°C)	Shale Feedrate (kg/hr)	Oil wt%	Yield %Fischer Assay
8	1-2	454	450	1.39	4.3	54.1
11	1-2	477	470	1.52	7.1	89.3
5	1-2	501	501	1.33	6.3	79.2
4	1-2	503	503	1.65	5.8	73.0
9	1-2	530	530	1.39	3.3	41.5
6B	1-2	540	528	1.29	5.3	66.6
7	1-2	554	554	1.33	2.4	30.2
26	2-4	471	476	1.35	4.2	53.3
10	2-4	506	505	1.21	7.2	91.7
6A	2-4	507	518	1.25	7.4	94.3
21	2-4	518	518	1.30	3.3	42.0

Initial Bed Composition: Ottawa sand -14 +20 mesh

Initial Weight: 5.9 kg

Spouting Gas: 85% N₂ - 15% CO₂

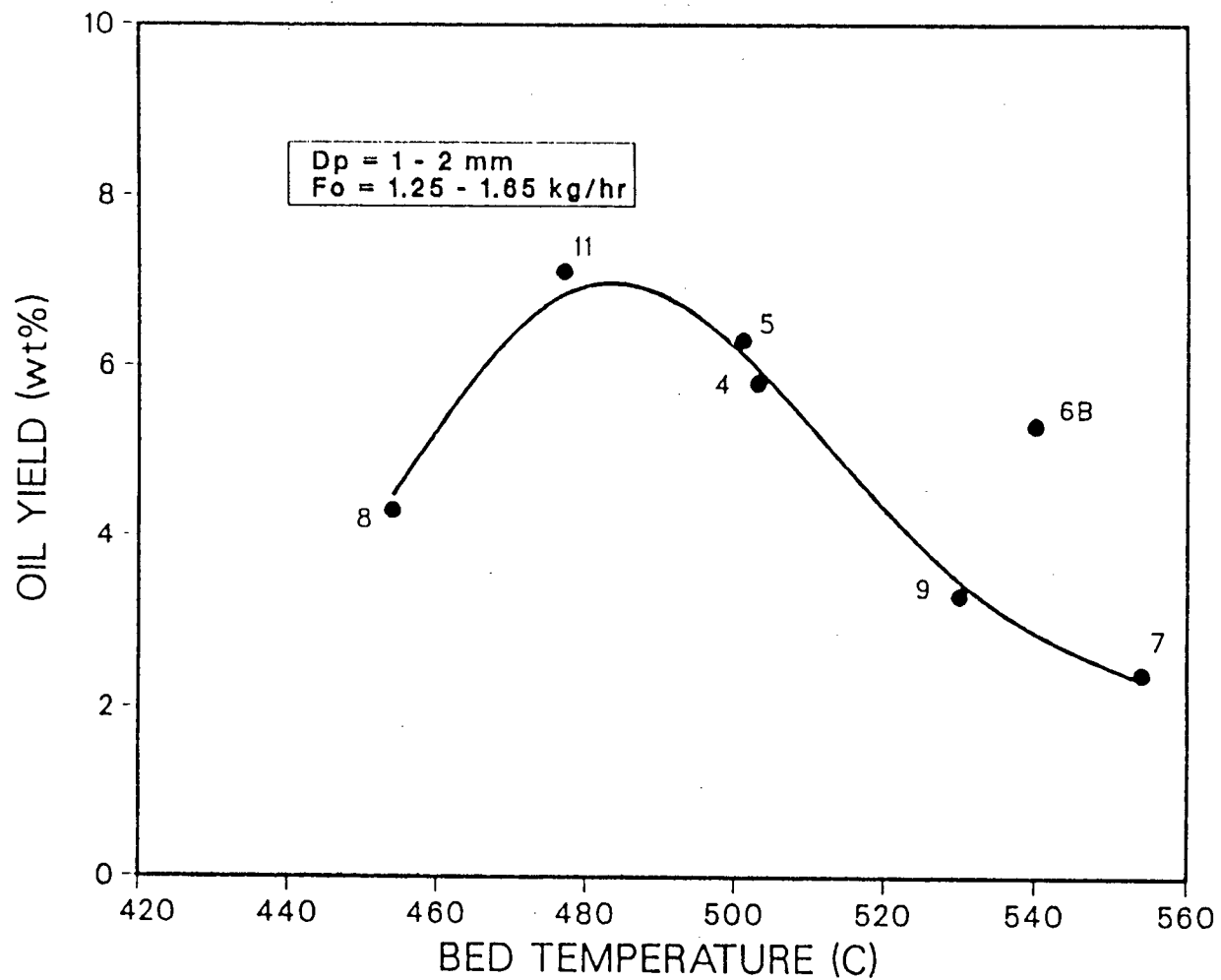


Fig 6: Oil Yield Versus Temperature Plot

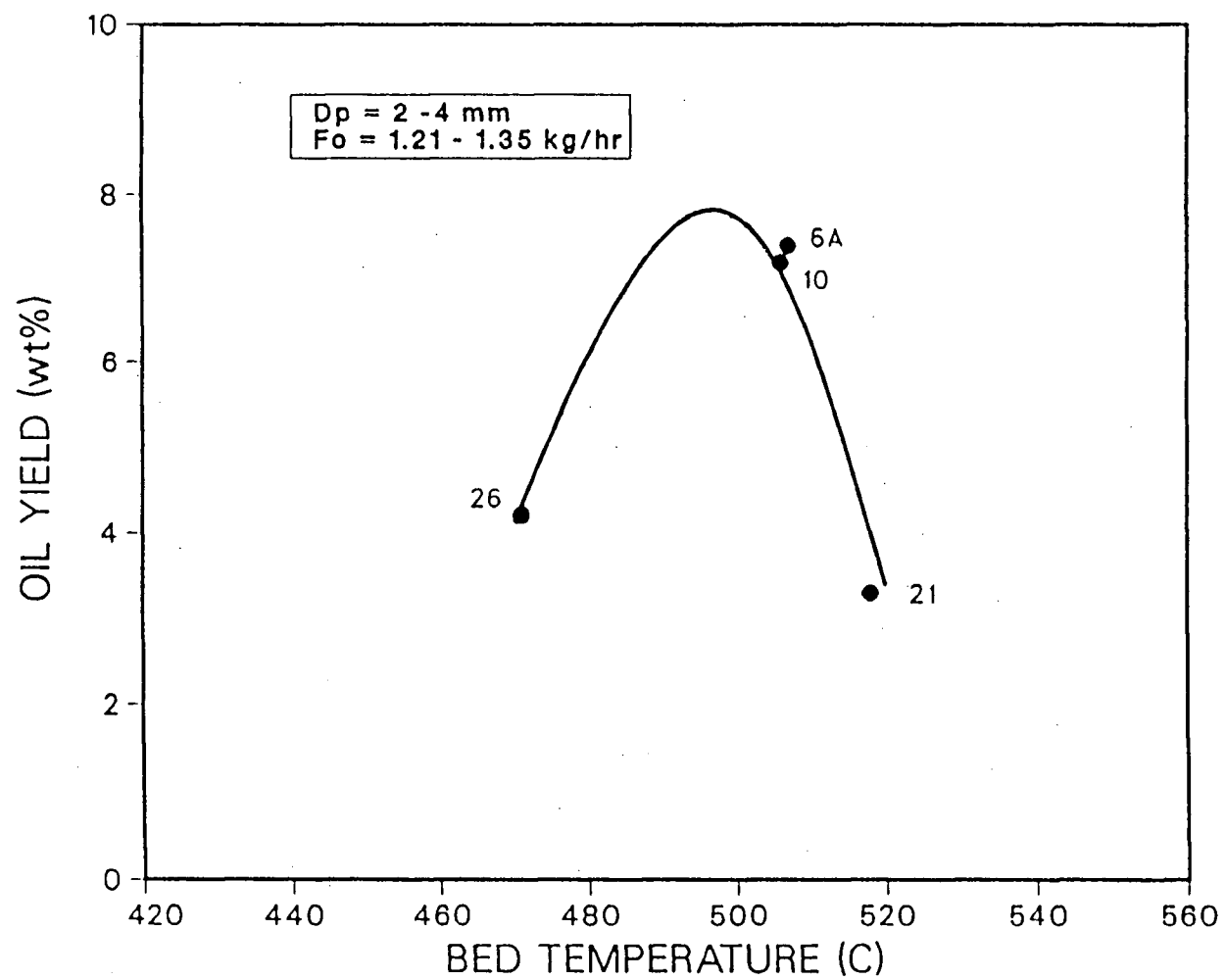


Fig 7: Oil Yield Versus Temperature Plot

represents 94.3% of the modified Fischer Assay yield. However, more experiments are required to quantify the temperature optimum.

Figure 8 shows a plot of the percentage of the Fischer Assay oil yield versus temperature plots for both 1-2mm and 2-4mm particle sizes. It can be seen that the curve for the 2-4mm is shifted slightly to the right, reflecting a higher optimum temperature for maximum oil yield compared to the 1-2mm size. This might arise because the 2-4mm particle is larger and will have larger internal temperature gradients, and will require a longer heating period or higher temperature to heat up the entire particle for complete pyrolysis. As mentioned earlier, more experiments are required to be done for 2-4mm sizes at 500-550°C. However, the trend of the Fischer Assay oil yield - Temperature curve in Figure 8 is in agreement with those observed by Liu et al.⁽²⁰⁾ (refer to Figure 2). They have also concluded that there is an optimum temperature corresponding to a maximum oil yield.

Table 15 lists the composition of the oils produced at different temperatures for particles of diameter 1-2mm. Typical oils contain 81.5-83.0% C, 10.6-10.9% H, 1% N and 5-6.8% is not accounted for. It was first thought that the unaccounted species present in the oils was either methanol or methylene chloride from the solvent train. An investigation was carried out by dissolving the oil in ethylbenzene and injecting into a 50m long DB5 capillary

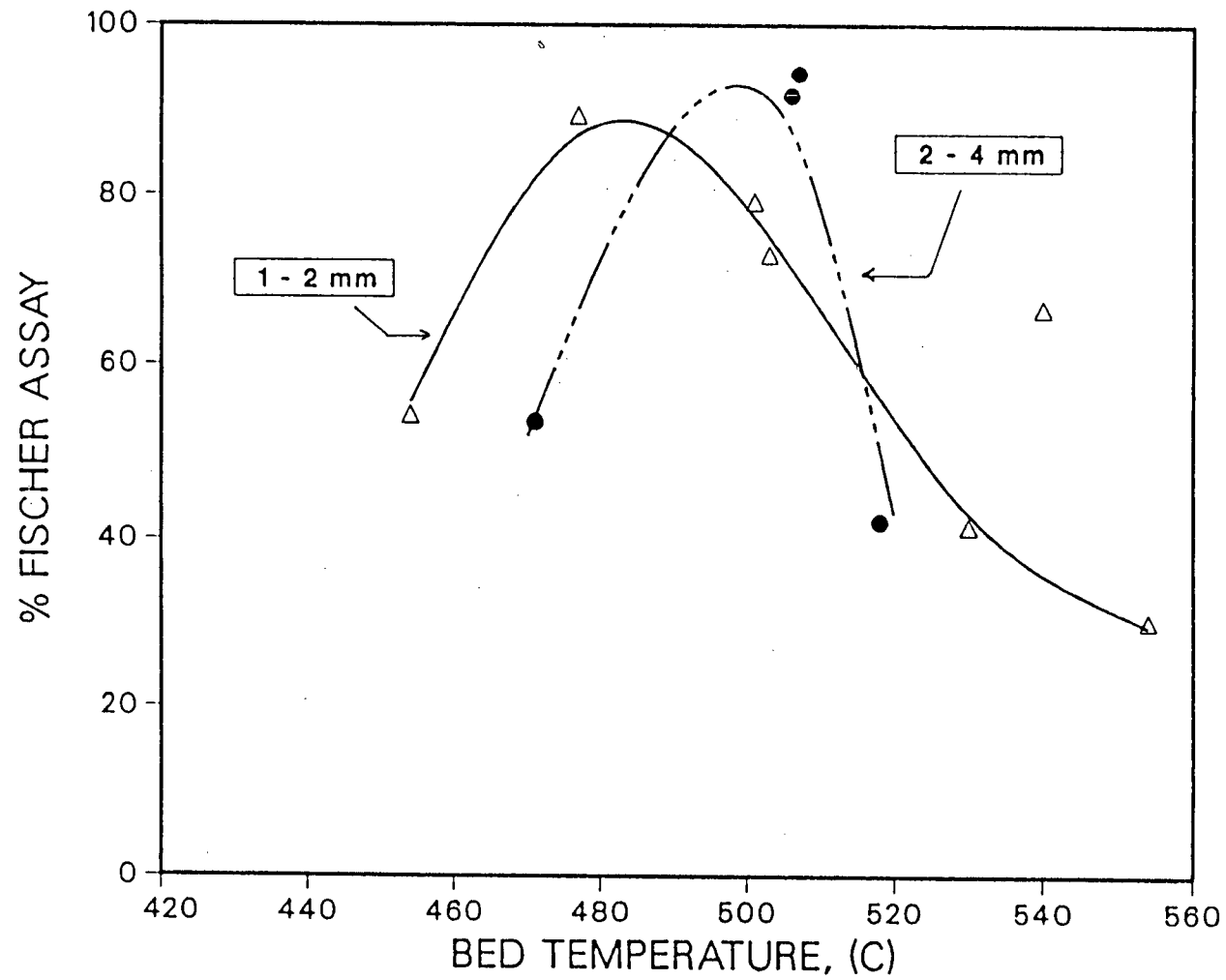


Fig 8: % Fischer Assay VS Temperature Plot

TABLE 15: Effect of Temperature on Oil Yield and Composition

Expt No.	Temperature		Shale Feedrate (kg/hr)	Oil wt%	Yield %Fischer Assay	C	Oil Analysis* (wt%)			**	Atomic Ratio H/C
	Bed	Inlet (°C)					H	N	S		
8	454	450	1.39	4.3	54.1	83.03	10.55	1.25		5.17	1.51
11	477	470	1.52	7.2	90.6						
5	501	501	1.33	6.3	79.2	82.46	10.66	1.13	0.63	5.12	1.54
4	503	503	1.65	5.8	73.0	81.47	10.70	1.02		6.81	1.57
6B	540	528	1.29	5.3	66.6	81.92	10.91	0.88		6.29	1.59
7	554	554	1.33	2.4	30.2	81.77	10.92	0.81		6.50	1.59

Oil Shale Particle Size: 1-2mm

Initial Bed Composition: Ottawa Sand -14 +20 mesh

Initial Weight: 5.9 kg

Spouting Gas: 85% N₂ - 15% CO₂

* Microanalytical Analysis

** Unaccounted

column in a chromatograph. Results indicated that neither methanol nor methylene chloride was present. The unaccounted species are as yet unidentified. As the pyrolysis temperature increases, the atomic H/C ratio increases. At the optimum temperature, H/C is 1.54, which seems to be in agreement with the expected values for shale oils produced by pyrolysis.

5.3 Effect of Oil Shale Particle Size on Oil Yield and Composition

The study of the particle size effect on oil yield and composition was carried out for 2-4, 1-2, and 0.5-1mm sizes. All of these experiments were done at about 506°C with 15% CO₂ and 85% N₂ as pyrolyzing gas. The bed was initially filled with silica sand, and the bed height increased gradually with time as the feed shale accumulated during the experiment.

Table 16 lists the results. Figure 9 shows the oil yield versus mean particle sizes. It can be seen that oil yield increases with increasing particle size. This is exactly opposite to the observation made by Jarallah⁽²⁾ on coal pyrolysis. He found that the tar yield decreases with increasing particle size, and his explanation is that there is an increased extent of secondary reactions which consume tar for larger particles. The extent of secondary reactions may be less significant in oil shale pyrolysis. If the experimental temperature is higher than the optimum

TABLE 16: Effect of Particle Size on Oil Yield

Expt No.	Particle Size (mm)	Bed	Temperature Inlet (°C)	Shale Feedrate (kg/hr)	Spent Shale In Bed (gm)	Oil wt%	Yield %Fischer Assay
18	0.5-1	501	498	1.26	681.0	2.4	43.6
3	0.5-1	505	505	1.37	454.0	4.2	76.4
2	0.5-1	509	509	1.49	510.8	2.4	43.6
5	1.0-2	501	501	1.33	681.0	6.3	79.2
4	1.0-2	503	503	1.65	539.1	5.8	73.0
10	2.0-4	506	505	1.21	652.6	7.2	91.7
6A	2.0-4	507	518	1.25	908.0	7.4	94.3

Initial Bed Composition: Ottawa Sand -14 +20 mesh

Initial Weight: 5.9 kg

Spouting Gas: 85% N₂ - 15% CO₂

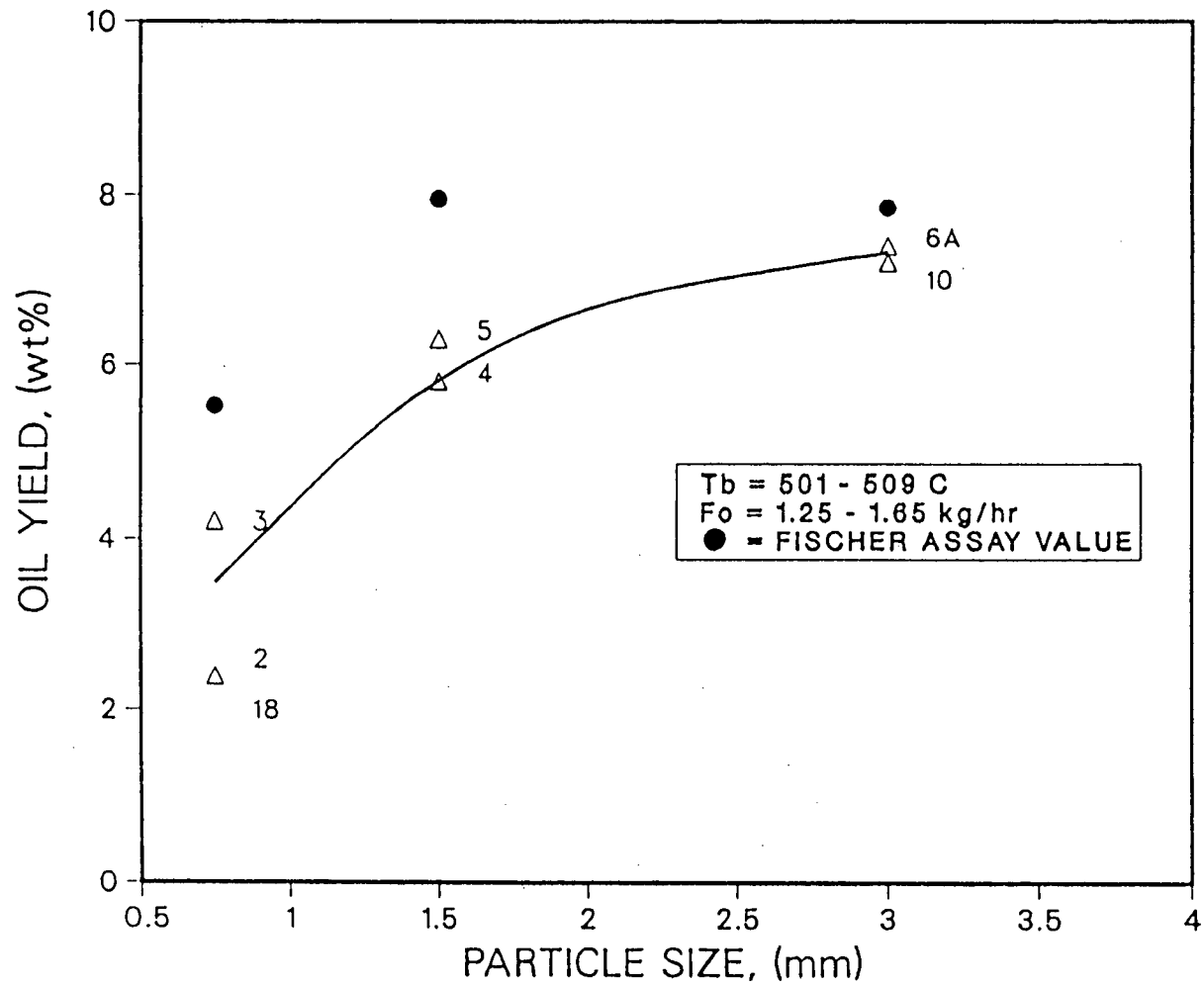


Fig 9: Oil Yield VS Particle Size Plot

temperature, the chance is greater that the oil is further decomposed to secondary volatiles. In the present case, the optimum temperature for 1-2mm particle size is around 475°C which is about 31°C lower than the experimental temperature in Figure 7. The extra temperature has enhanced secondary reaction, and therefore the oil yield obtained at 6.3% is lower than the maximum of 7.1%. Whereas for the 2-4mm size, the optimum temperature is around 505°C which is approximately the same as the temperature in Figure 6. For the 0.5-1mm particle size, although the optimum temperature was not studied, it is expected to be lower than 475°C. With the same argument, therefore the greater difference between the experimental and optimum temperature results in an even lower oil yield for the smallest particles.

Based on these observations, the dependance of oil yield on particle size will be different if the comparison is made at say 475°C. In this case, the 2-4mm particles will produce a lower oil yield as the optimum temperature has not been attained, whereas for the 0.5-1mm particle, the gap between the optimum and experimental temperature is reduced, so a higher oil yield is expected. Certainly, more tests at lower temperature should be carried out to provide a more complete picture.

Table 17 lists the elemental composition of the oils produced. There is no consistent trend among the three samples analyzed. The 2-4mm sized shale has the highest atomic H/C ratio and lowest unaccounted for species.

TABLE 17: Effect of Particle Size on Oil Yield and Composition

Expt No.	Particle Size (mm)	Temperature		Shale Feedrate (kg/hr)	Oil wt%	Yield %Fischer Assay	C	Oil Analysis* (wt%)			**	Atomic Ratio H/C
		Bed	Inlet					H	N	S		
2	0.5-1	509	509	1.49	2.4	43.6	81.58	11.02	0.7		6.70	1.61
3		505	505	1.37	4.2	76.4	82.18	10.73	1.05		6.04	1.56
4	1-2	503	503	1.65	5.8	73.0	81.47	10.70	1.02		6.81	1.57
5		501	501	1.33	6.3	79.3	82.46	10.66	1.13	0.63	5.12	1.54
6A	2-4	507	518	1.25	7.4	94.3	82.73	10.66	1.14		5.47	1.54
10		506	505	1.21	7.2	91.7	82.64	11.35	1.12		4.89	1.64

Initial Bed Composition: Ottawa Sand -14 +20 mesh

Initial Weight: 5.9 kg

Spouting Gas: 85% N₂ - 15% CO₂

* Microanalytical Analysis

** Unaccounted

5.4 Effect of Oil Shale Feed Rate on Oil Yield and Composition

The feed rate study was carried out for 2 sizes: 2-4mm and 1-2mm. All of these experiments were done at 500-506°C, using 15% CO₂ and 85% N₂ as pyrolyzing gas. The bed initially consisted of silica sand and the bed height increased gradually as the feed shale accumulated during the experiment.

Tables 18 and 19 list the results. Figures 10 and 11 show the plots of oil yield versus shale feed rate. Both curves indicate that there is a marked decrease of oil yield with increasing feed rate. For 1-2mm shale, the oil yield has dropped from 6.3% to 2.9% as the feed rate was increased from 1.33 to 3.32kg/h, which is a drop of 79.2 to 36.5% of modified Fischer Assay values. Similar results were observed for the 2-4mm sized shale where feed rate increases from 1.53 to 2.71kg/h resulted an oil drop from 7.4 to 2.0%, which is a drop of 94.3 to 25.5% of modified Fischer Assay values. It can be seen in Figure 10 that the first three points are in a straight line, indicating a linear decreasing effect and then the line approaches an asymptotic value. The reason for the decrease is presumably that the hot spent shale accumulated in the reactor has acted as a surface on which the secondary oil-consuming reactions occur, or perhaps as a catalyst for oil decomposition. This effect will be demonstrated further below. The trends in Figure 10 and 11 are in the same direction as those observed

TABLE 18: Effect of Feedrate on Oil Yield (Unsteady Height Expt.)

Expt No.	Temperature		Shale	Spent Shale	Oil Yield	% Fischer Assay
	Bed	Inlet (°C)	Feedrate (kg/hr)	In Bed (kg)	wt %	
5	501	501	1.33	0.68	6.3	79.2
4	503	503	1.65	0.54	5.8	73.0
24	506	506	1.90	1.31	3.4	42.8
25	505	506	3.32	1.46	2.9	36.5

Oil Shale Particle Size: 1-2mm

Initial Bed Composition: Ottawa Sand -14 +20 mesh

Initial Weight: 5.9 kg

Spouting Gas: 85% N₂ - 15% CO₂

TABLE 19: Effect of Feedrate on Oil Yield (Unsteady Height Expt.)

Expt No.	Bed	Temperature (°C)	Inlet	Shale Feedrate (kg/hr)	Spent Shale In Bed (kg)	Oil wt%	Yield % Fischer Assay
10	506		505	1.21	0.65	7.2	91.7
6A	507		518	1.25	0.91	7.4	94.3
12A	506		502	1.94	1.02	4.5	57.3
12	506		502	2.71	1.28	2.0	25.5

Oil Shale Particle Size: 2-4mm

Initial Bed Composition: Ottawa Sand -14 +20 mesh

Initial Weight: 5.9 kg

Spouting Gas: 85% N₂ - 15% CO₂

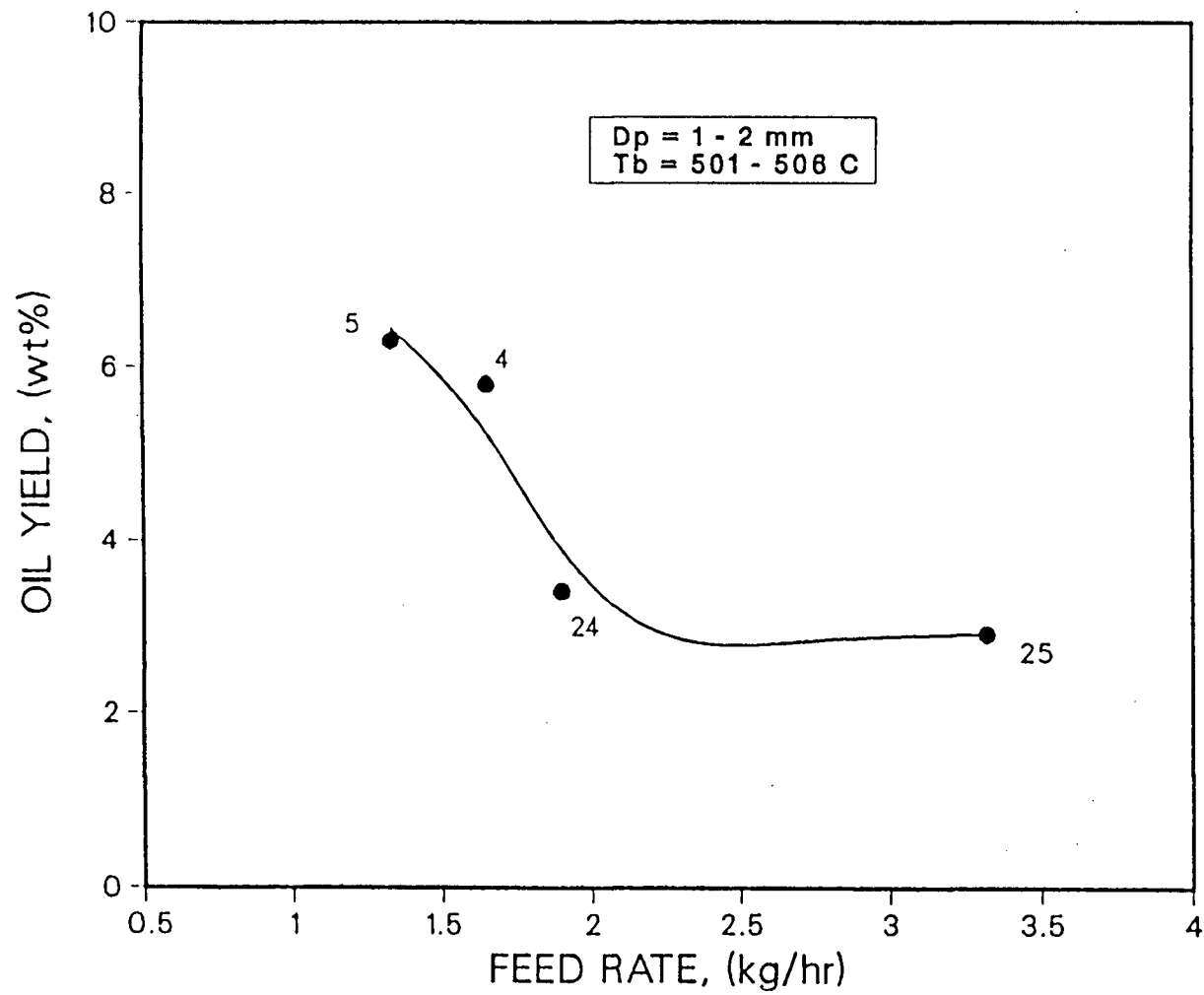


Fig 10: Oil Yield VS Feed Rate Plot

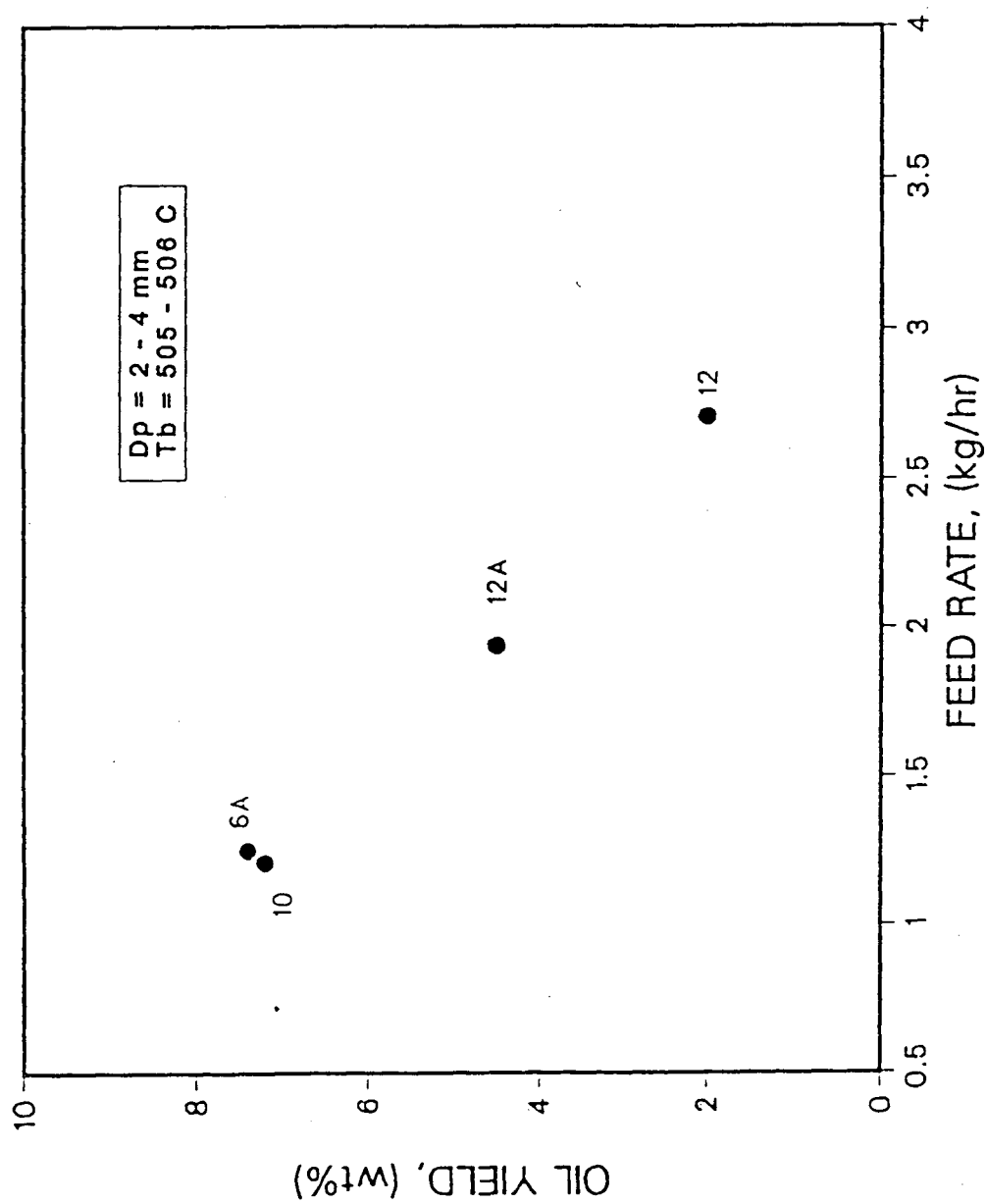


Fig 11: Oil Yield VS Feed Rate Plot

by Jarallah⁽²⁾ on coal pyrolysis.

Another series of feed rate experiments was carried out in a bed consisting initially of spent shale with the bed height kept constant by releasing the accumulated spent shale periodically through the bed overflow line. Table 20 lists the results. Figure 12 shows the oil yield versus feed rate plot. Results indicate that the oil yield has remained quite steady at 2.4-2.6% regardless of the feed rate. This value is very close to the lowest yield in previous Figure 10. This implies that the presence of spent shale has indeed enhanced secondary reactions of the oil (such as cracking), therefore dropping the oil yield significantly. A careful study of the two figures leads to the conclusion that with increasing feed rate in a sand bed, the oil yield will drop linearly in the beginning, and then gradually approach an asymptotic value of around 2.4%.

Table 21 lists the composition of the oil produced for the 2-4mm size. The hydrogen content decreases, but the hydrogen/carbon atomic ratio seems to increase from 1.46 to 1.56 as the oil yield falls off with increasing feed rate in the sand bed experiments.

5.5 Effect of Bed Material on Oil Yield

The study of the bed material effect on oil yield was carried out on shale of 1-2mm size at 470-477°C with 15% CO₂ and 85% N₂ as the pyrolyzing gas. For all experiments, the volume of the initial bed was kept the same (vol=3735cm³,

TABLE 20: Effect of Feedrate on Oil Yield (Steady Height Expt.)

Expt No.	Bed	Temperature (°C)	Inlet	Shale Feedrate (kg/hr)	Oil wt%	Yield % Fischer Assay
16	470		470	1.26	2.4	30.2
19	470		480	3.39	2.6	32.7
20	472		476	4.45	2.5	31.4

Oil Shale Particle Size: 1-2mm

Initial Bed Composition: Spent Shale

Initial Weight: 5.9 kg

Spouting Gas: 85% N₂ - 15% CO₂

* Periodic release of spent shale from the reactor to keep bed height steady

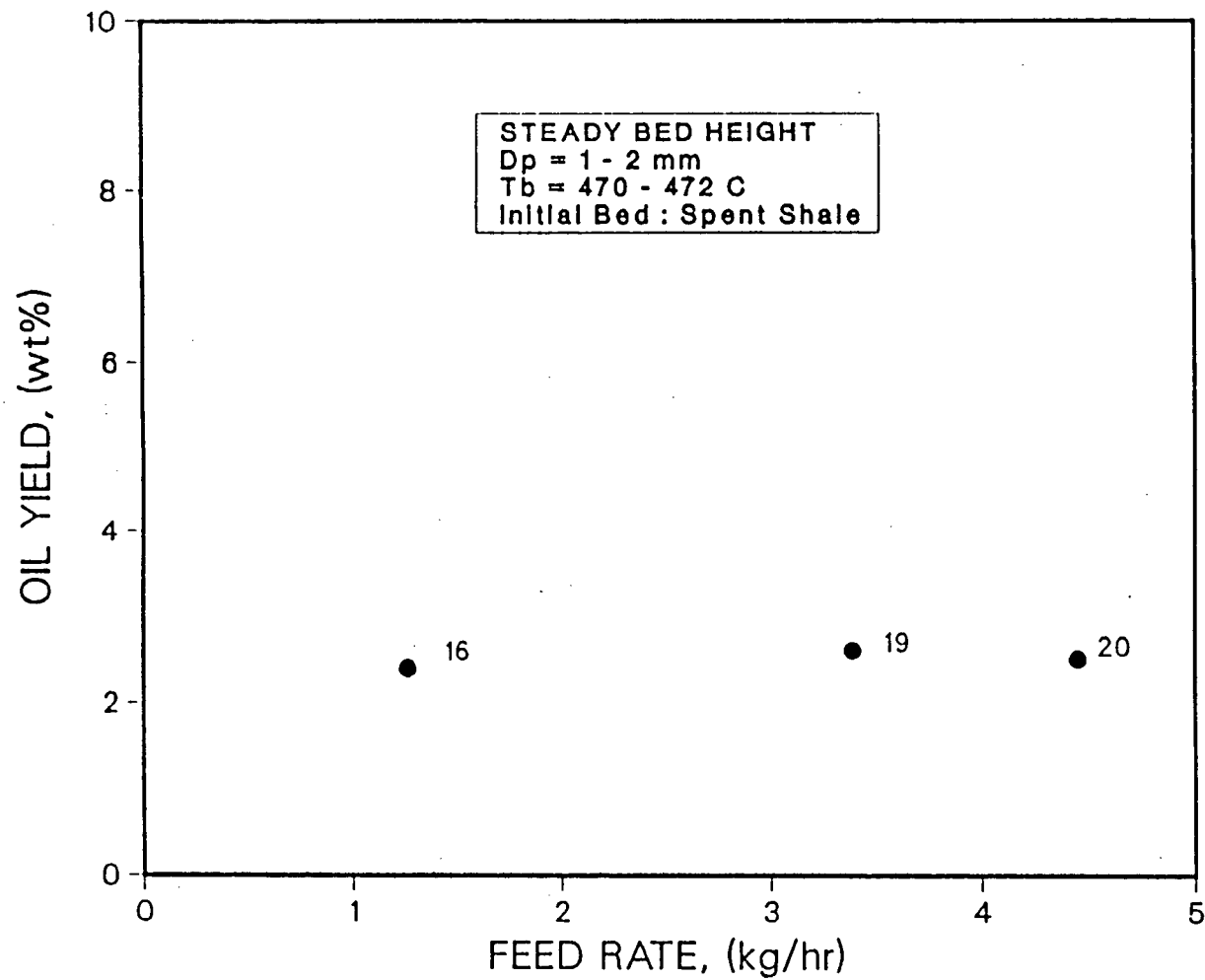


Fig 12: Oil Yield VS Feed Rate Plot

TABLE 21: Effect of Feedrate on Oil Yield and Composition

Expt No.	Temperature		Shale Feedrate (kg/hr)	oil wt%	Yield %Fischer Assay	C	Oil Analysis* (wt%)		**	Atomic Ratio H/C
	Bed	Inlet (°C)					H	N		
10	506	505	1.2	7.2	91.7	82.64	11.35	1.12	4.89	1.46
12A	506	502	1.94	4.5	57.3	83.65	10.77	1.23	4.35	1.53
12	506	502	2.71	2.0	25.5	83.42	10.89	1.29	4.40	1.56

Oil Shale Particle Size: 2-4mm

Initial Bed Composition: Ottawa Sand -14 +20 mesh

Initial Weight: 5.9 kg

Spouting Gas: 85% N₂ - 15% CO₂

* Microanalytical Analysis

** Unaccounted

initial bed depth=33cm), but the amount of spent shale in the bed ranges from 1 to 6.9kg. The remainder of the bed was silica sand. As the experiment proceeded, the bed height increased gradually as spent shale accumulated in the reactor.

Table 22 lists the results. Figure 13 shows the plot of the oil yield versus the final spent shale mass in the reactor after the run. The final mass represents the spent shale accumulated during the experiment. The results show that there is a marked decrease in oil yield with increasing spent shale mass in the bed. These experiments show essentially the same effect as the feed rate experiments. As more and more spent shale becomes available in the bed, the oil yield drops because the hot spent shale has acted as a sorbent for the oil or a catalyst for the secondary reactions. When the initial bed is comprised solely of spent shale, the oil yield drops to 2.4% which is equivalent to the asymptotic value for Figure 12. It can be concluded that the presence of spent shale has a negative effect on the oil yield. This is in agreement with the observation made by Levy et al⁽⁴³⁾. In their study, vaporized oil was passed through a packed bed of sand, or spent shale ash at temperatures between 500 and 600°C. In the case of sand bed, cracking was minimal at 500°C and gradually increased at higher temperatures. In the case for spent shale ash bed, coking was prevalent at all temperatures studied, and a major oil losses was resulted even at 500°C. The ash has

TABLE 22: Effect of Bed Material on Oil Yield

Expt. No	Temperature		Shale Feedrate (kg/hr)	Initial Bed		Final Spent Shale (kg)	Oil wt%	Yield %Fischer
	Bed	Inlet (°C)		Spent Shale (kg)	Sand			
11	470	477	1.52	0.0	5.9	1.0	7.1	89.3
23	474	474	1.13	1.5	4.1	2.25	3.9	49.0
22	470	470	1.63	3.0	2.4	3.73	2.7	34.0
16	470	470	1.26	5.0	0.0	6.84	2.4	30.2

Oil shale Particle Size: 1-2mm
Spouting Gas: 85% N₂ - 15% CO₂

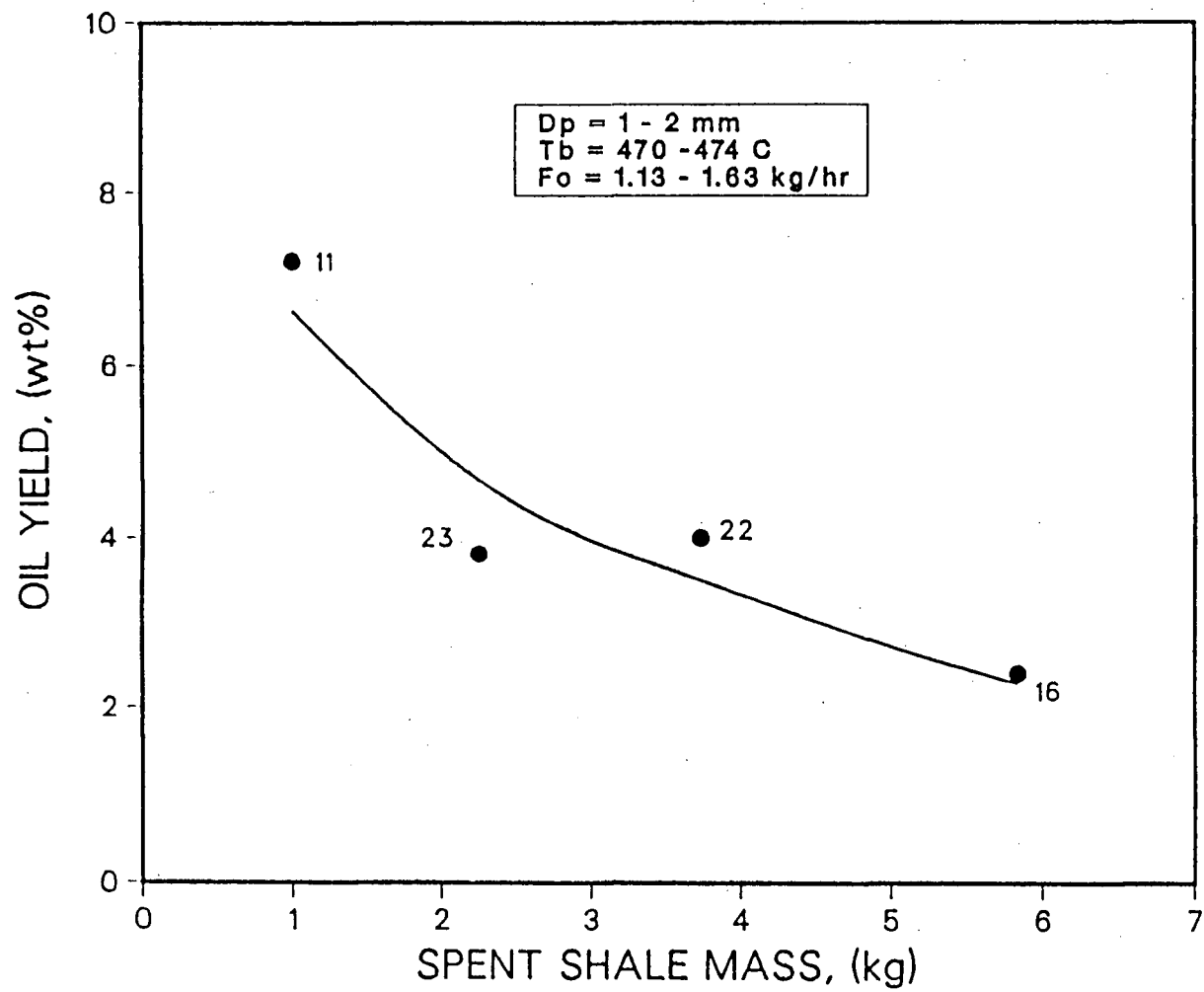


Fig 13: Oil Yield VS Spent Shale In Bed

catalysed the oil degradation greatly. On the other hand, this sorbent effect presumably is specific to the oil shale, as Floess et al.⁽³⁶⁾ found no difference in oil shale yields in fluidized beds of silica sand and calcined dolomite of surface area $6.3\text{m}^2/\text{g}$.

It should be noted that the feed rate actually fluctuated from 1.13 to 1.63kg/hr. This should not have affected the oil yield result because Figure 10 of Section 5.4 already shows that the oil yield remains around 6% in that feed range.

5.6 Effect of Pyrolyzing Gas on Oil Yield

Two experiments were done in the 1-2mm sized shale at 500°C using N_2 instead of the mixture of 15% CO_2 and 85% N_2 as pyrolyzing gas. Table 23 lists the results. The data are very reproducible, and both reflect a lower oil yield at 3.4% in nitrogen compared to 6.3% when using the N_2 / CO_2 mixture. An explanation of this unexpected result is not available yet. Bae⁽¹⁷⁾ observed that at atmospheric pressure, the oil yield is not affected by the nature of pyrolyzing gas (refer to Figure 1).

5.7 Gas Yields

The spouted bed retorting technique in which a large volume of gas is needed for spouting is not particularly well suited for measurement of gas yields, as concentration of produced gas in the off gas will tend to be very low.

TABLE 23: Effect of Pyrolyzing Gas Composition

Pyrolyzing Gas	85% N ₂ - 15% CO ₂		100% N ₂	
Expt. No	4	5	14	17
Temperature (Inlet/Bed) °C	503/503	501/501	491/500	500/500
Feed Rate (kg/hr)	1.65	1.33	1.35	1.27
Oil Yield (wt%)	5.8	6.3	3.4	3.4
Oil Yield (%Fischer Assay)	73.0	79.2	42.8	42.8
Oil Analysis (wt%)				
C	81.47	82.46	82.49	
H	10.70	10.66	10.89	
N	1.02	1.13	1.17	
S	-	0.63	0.75	
Unaccounted	6.81	5.12	4.70	
Atomic H/C Ratio	1.57	1.54	1.57	

Oil Shale Particle Size: 1-2mm

Initial Bed Composition: Ottawa Sand -14 +20 mesh

Initial Weight: 5.9 kg

Nevertheless some results were obtained.

As stated in Section 4.6, two chromatographs were used. For most of the runs, the GC used was set for concentration of H_2 , CO , CO_2 , and CH_4 in the percent range. A few analyses were also done on the second GC, which permitted determination of the above species and addition information on C_2H_2 , C_2H_4 , C_2H_6 , C_3H_8 and C_4H_{10} . Table 24 lists the results.

Hydrogen is produced during pyrolysis of oil shale. The yield ranges from 0.02 to 0.045%, and does not seem to be affected by particle sizes, feed rate and bed material. Figure 14 shows the plot of hydrogen yield versus temperature. The profile seems to be marked by two peaks although the data is scattered. According to Campbell et al⁽³⁷⁾, the peaks are associated with 'secondary' pyrolysis reaction of the carbon residue remaining after the primary bitumen decomposition.

Methane yields are recorded in a few experiments. Campbell et al⁽³⁷⁾ observed that methane is released during the oil generation, and higher temperature pyrolysis of the spent shale. The methane released during the secondary pyrolysis (above 500°C) may result primarily from the cleavage of methyl and methoxyl groups bonded to aromatic structures and possibly, from cleavage of methylene bridges between aromatic rings.

The evolution of C_2 and C_3 was determined by the second GC. Campbell et al⁽³⁷⁾ observed that these gases are evolved

TABLE 24: Gas Yields

Expt No	Particle Size (mm)	% Gas Yield (kg/kg shale)							Total
		H ₂	CH ₄	C ₂ H ₆	C ₃ H ₈	C ₄ H ₁₀	C ₅ H ₁₂	C ₆ H ₁₄	
2	0.5-1	0.028							0.028
3	0.5-1								
4	1-2	0.023	0.065	0.059	0.059	0.460			0.666
5	1-2	0.033	0.062	0.042	0.045	0.760			0.942
6A	2-4	0.037	0.098	0.049	0.060	0.820			1.064
6B	1-2	0.027	0.079	0.068	0.075	0.631			0.880
7	1-2	0.021	0.077	0.082	0.052	0.914			1.146
8	1-2	0.032	0.057	0.160	0.095	0.190	0.21		0.744
9	1-2	0.038	0.068	0.028	0.045	0.410	0.220	0.170	0.979
10	2-4	0.036	0.088	0.027	0.064		1.650	0.330	2.195
11	1-2	0.031	0.080	0.038	0.074	0.400	1.220	0.310	2.153
12	2-4	0.042							0.042
12A	2-4	0.024							0.024
14	1-2	0.037							0.037
15	1-2	0.022							0.022
16	1-2	0.034							0.034
17	1-2	0.018							0.018
18	1-2								
19	1-2	0.038							0.038
20	1-2	0.039	0.029						0.068
21	2-4	0.019							0.019
22	1-2	0.015							0.015
23	1-2	0.033							0.033
24	1-2	0.030							0.030
25	1-2	0.038	0.020						0.058
26	2-4	0.030							0.030

* The experimental conditions for each run are listed in Table 12

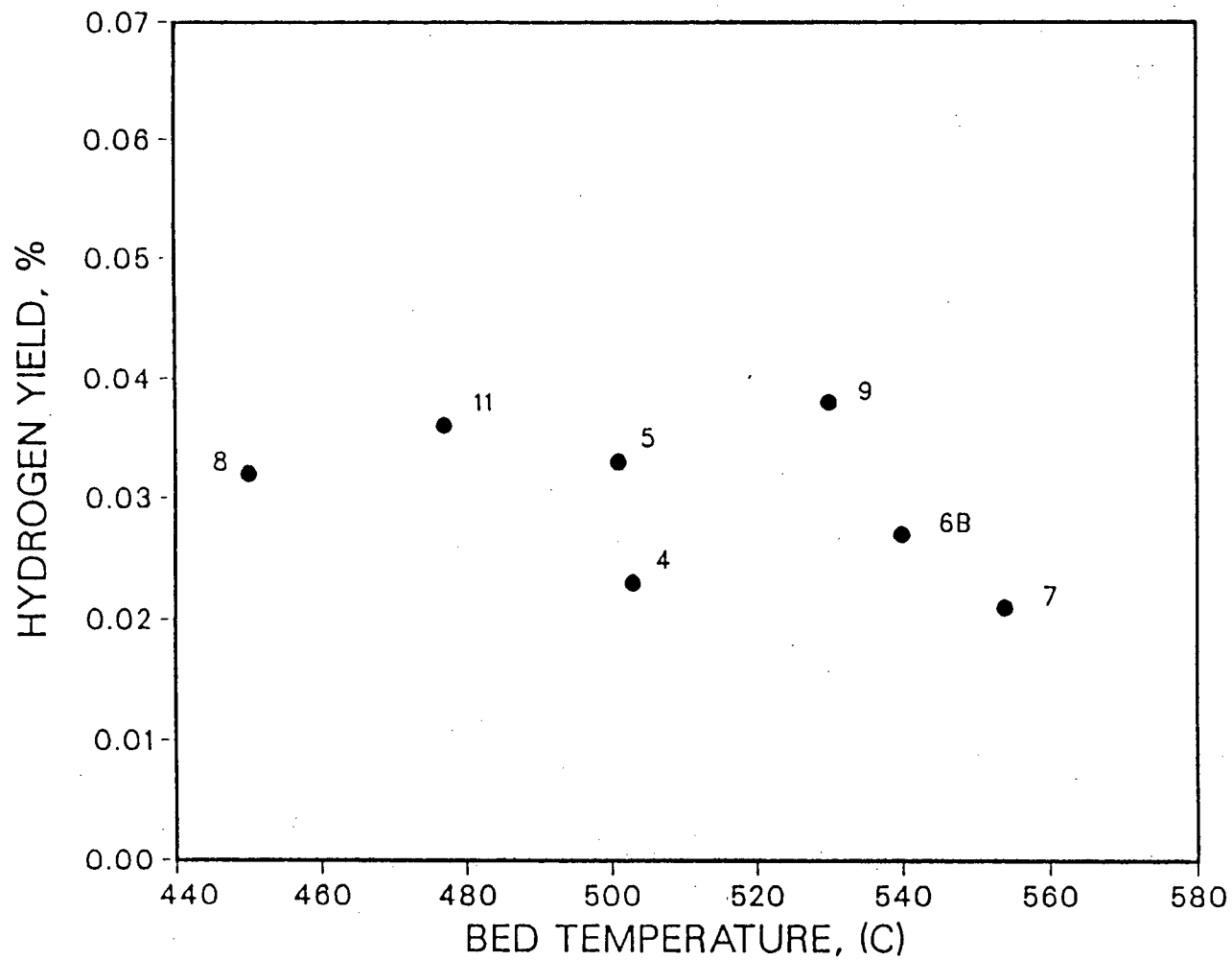


Fig 14: Hydrogen Gas Yield VS Temperature

during the oil generation, i.e. between 350-550°C. The evolution of C₄ and C₆ was determined in a few experiments only, therefore no conclusion can be drawn.

In most experiments, carbon dioxide was included in the pyrolyzing gas at a level of 15%. Because of the fluctuations of the gas inlet flowrate, it was difficult to determine its yield. However, it was noted that for the run done with nitrogen alone as pyrolyzing gas, there was no CO₂ nor CO produced. These results agreed with the findings of Campbell et al⁽³⁷⁾. They found that no CO₂ and CO were released during pyrolysis below the temperature of 550°C. The release of CO₂ and CO occurs primarily above 600°C. Carbon dioxide is produced during the decomposition and reaction of carbonate minerals present in the oil shale, and carbon monoxide is then produced by the subsequent reaction of CO₂ with carbon.

5.8 Spent Shale Yields

As mentioned in the beginning of the section, there was a substantial loss of entrained spent shales particles. Some had escaped to the atmosphere due to the inefficiency of the cyclone, and some had stuck onto the wall of the cyclone. From experiment 14 onwards, mechanical brushing had been used to recover the fines from the cyclone, and thus higher percentages of fines were recovered. Table 25 lists the compositions of spent shales found in the bed and recovered from the cyclone catch for three different particle sizes.

TABLE 25: Spent Shale Properties and Yield

Run	3		4		10	
Temperature(°C)	505/505		503/503		506/505	
Particle Size (mm)	0.5-1.0		1-2		2-4	
	Bed Shale	Cyclone Catch	Bed Shale	Cyclone Catch	Bed Shale	Cyclone Catch
Total Carbon (%wt)	4.91	6.84	4.64	6.87	5.33	5.89
Organic Carbon (%)	3.48	4.77	2.37	4.30	2.36	3.20
SiO ₂ (%wt)	56.7	61.2	51.6	52.4	50.3	59.8
Al ₂ O ₃	16.6	9.33	14.5	11.2	13.1	8.81
Fe ₂ O ₃	10.1	3.96	5.66	4.80	5.52	3.84
CaO	3.34	6.54	9.30	8.77	10.9	7.42
MgO	2.24	2.50	3.97	3.45	4.28	2.93
Na ₂ O	1.35	0.95	1.6	1.31	1.38	1.10
K ₂ O	2.64	1.58	2.23	1.83	2.17	1.55
Ba (ppm)	440	373	390	373	376	300
Mn	790	402	690	570	705	446
Sr	175	290	340	368	385	310
Ti	2960	2440	3430	2970	3180	2340

Mass balances using several species (Sr, Ba, Ti, Fe_2O_3) present in the shale, the bed material and the cyclone catch, all showed that the uncollected material which passed through the cyclone was about one-third of the oil shale feed. Also it can be observed that the cyclone catch contains higher carbon content than does the bed material which indicates that the entrained particles are generally incompletely reacted.

It was intended that the spent shale yield be calculated from the weight of the shale in the shale-sand mixture remaining in the reactor plus the weight of entrained fines in the cyclone after the run. In practice, the actual weight of shale remaining in the reactor cannot be obtained simply by weighing the total solids due to the fact that some of the sand was also entrained to the cyclone. Therefore, the method chosen to obtain the yield is by combining the weight of entrained particles in the cyclone receiver plus the weight of the bed after the run minus the weight of inert material originally present in the bed. Table 26 lists the results of the spent shale yield. Due to the incomplete recovery, the trends of the spent shale yield with process variable were not meaningful. Attrition is obviously a serious problem for processing these oil shales in a spouted bed.

TABLE 26: Spent Shale Yields

Expt No	Temperature		Particle	Shale	Spent Shale		Total	Spent
	Bed	Inlet	Size	Feedrate	Cyclone	Bed	Spent Shale	Shale Yield
	('C)		(mm)	(kg/hr)	(gm)		(gm)	(wt%)
2	509	509	0.5-1	1.49	681.0	510.8	1191.8	60.0
3	505	505	0.5-1	1.37	652.6	454.0	1106.6	60.4
4	503	503	1-2	1.65	681.0	539.1	1220.1	55.3
5	501	501	1-2	1.33	397.5	681.0	1078.5	60.8
6A	507	518	2-4	1.25	56.8	908.0	964.8	57.8
6B	540	528	1-2	1.29	397.5	681.0	1078.5	62.6
7	554	554	1-2	1.33	368.9	766.1	1135.0	62.8
8	450	450	1-2	1.38	539.1	595.9	1135.0	61.0
9	530	530	1-2	1.39	567.5	567.5	1135.0	61.0
10	506	505	2-4	1.21	454.0	652.6	1106.6	68.4
11	477	470	1-2	1.52	737.7	681.0	1418.7	70.0
12	506	502	2-4	2.71	1135.0	1276.8	2411.8	66.8
12A	506	502	2-4	1.94	567.5	1021.5	1589.0	61.4
14	500	491	1-2	1.35	835.2	500.0	1335.2	74.2
15	480	472	1-2	1.37	1779.1	(1135.0)*	664.1	66.0
16	470	470	1-2	1.26	948.6	0	948.6	56.5
17	500	500	1-2	1.27	621.0	510.7	1131.7	66.8
18	500	498	0.5-1	1.26	449.3	681.0	1130.3	67
19*	470	480	1-2	3.39	1602.7	1021.5	3298.0	82.1
20*	472	476	1-2	4.45	1906.8	(170.25)*	4823.7	84.3

21	518	518	2-4	1.30	514.0	1078.3	1592.3	91.8
22	470	480	1-2	1.63	803.7	1163.4	1967.1	90.0
23	474	474	1-2	1.13	736.4	595.8	1332.2	88.5
24	500	500	1-2	1.89	824.8	1305.3	2130.1	84.3
25	500	506	1-2	3.32	981.0	1459.2	2740.2	86.9
26	471	476	2-4	1.35	1161.8	170.3	1332.1	73.8

* Discharge for expt 19 is 673.8gm

* Discharge for expt 20 is 2746.6gm

* For experiments 15 and 24, the bed actually had a lost in weight of 1135.0 and 170.25gm respectively

6. Kinetic Model

6.1 General Discussion

From the simplified model developed in Section 3.2, equations (3.33), (3.34), (3.39) and (3.40) have been derived,

$$C_K = \frac{A}{B} (1 - e^{-Bt}) \quad (3.33)$$

$$C_B = CA (C_{11} + C_{12}e^{-Dt} + C_{13}e^{-Bt}) \quad (3.34)$$

$$C_A = \frac{P}{Q} (1 - e^{-Qt}) \quad (3.39)$$

$$\text{Oil Yield} = \int_0^t C_A F_g dt \quad (3.40)$$

with the Arrhenius relationships,

$$k_1 = k_1^{\circ} e^{-E_1/RT} \quad (6.1)$$

$$k_2 = k_2^{\circ} e^{-E_2/RT} \quad (6.2)$$

$$k_3 = k_3^{\circ} e^{-E_3/RT} \quad (6.3)$$

Taking k_1° , k_2° , E_1 and E_2 from the literature²⁴ and F_0 , F_1 , F_2 , V , C_{K0} and oil yield from the experiments, k_3° and E_3 can be solved for using UBC Library Program NL2SOL. The computer

program is included in Appendix C.

Table 27 lists the experimental data and literature values used for the generation of k_3° and E_3 . The predicted oil yield values and the experimental data are plotted in Figure 15. It can be seen that the model predicts a trend similar to the experimental data although the experimental oil yield drops more sharply at low temperatures. The predicted maximum oil yield occurs at a temperature of 440°C , which is some 37°C lower than that found by experiment. No measurements of kerogen and bitumen are available for checking the model.

The values of C_K , C_B , C_A and oil yield as functions of time can be calculated by UBC Library Program Jacobian using the following equations:

$$\frac{dC_K}{dt} = \frac{F_0 C_{K0}}{W} - \left(\frac{F_0}{W} + k_1 \right) C_K \quad (3.44)$$

$$\frac{dC_B}{dt} = f_1 k_1 C_K - \left(\frac{F_0}{W} + k_2 \right) C_B \quad (3.45)$$

$$\frac{dC_A}{dt} = \frac{f_2 k_2 C_B W}{V} - \left(\frac{F_g}{V} + k_3 \right) C_A \quad (3.46)$$

$$\text{Oil} = \int_0^t C_A F_g dt \quad (3.47)$$

TABLE 27: Effect of Temperature on Oil Yield (Predicted vs Experimental Values)

Expt No.	Particle Size (mm)	Bed	Temperature Inlet (°C)	Shale Feedrate (kg/hr)	Experimental Oil wt%	Predicted Oil wt%
(Unsteady Height Experiment)						
8	1-2	454	450	1.39	4.3	6.6
11	1-2	477	470	1.52	7.1	6.4
5	1-2	501	501	1.33	6.3	5.7
4	1-2	503	503	1.65	5.8	5.6
9	1-2	530	530	1.39	3.3	3.9
7	1-2	554	554	1.33	2.4	2.2

From Literature(23)

$$k_1^* = 14.4 \text{ s}^{-1}$$

$$E_1 = 44560 \text{ kJ/mol}$$

$$k_2^* = 2.025 \times 10^{-1} \text{ s}^{-1}$$

$$E_2 = 177580 \text{ kJ/mol}$$

From Calculation

$$k_3^* = 1.7 \times 10^{-14} \text{ s}^{-1}$$

$$E_3 = 244319.45 \text{ kJ/mol}$$

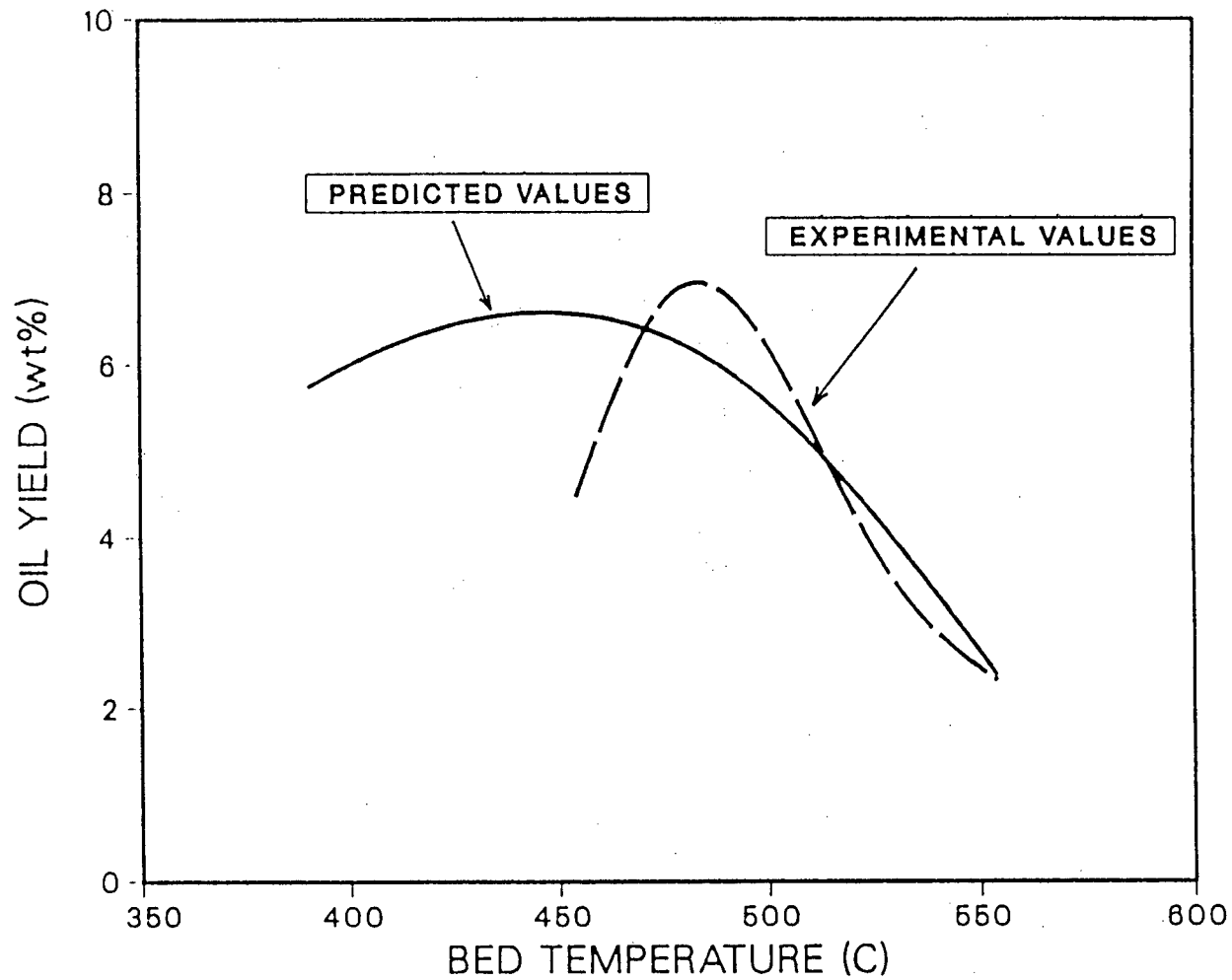


Fig 15: Oil Yield Versus Temperature Plot

Predicted Values VS Experimental Values

The results are plotted in Figure 16 for one experimental run. As expected, C_K , the concentration of kerogen, increases with time and then remains steady as a fraction of the kerogen is decomposed to form bitumen. C_B starts from zero and increases to some value, and then gradually remains constant as the bitumen is decomposed to oil. Oil concentration begins at zero, and gradually increases as it is produced by the decomposition of bitumen. At the same time, the oil degrades to form gas on further heating. The cumulative oil yield increases rapidly at the beginning, and then more slowly as time goes on and gradually approaches a constant value.

6.2 The effect of Rate Constant on Oil Yield

The effect of individual rate constants k_1 , k_2 and k_3 on oil yield was studied using the UBC library program Jacobian to solve the model. The k_1 , k_2 or k_3 of the Arrhenius relationship (eqn. 6.1-6.3) is multiplied by a factor while holding all other values constant. The computer printout for one experimental run is shown in Appendix C.6. The model gives the same final oil yield results even for different values of k_1 and k_2 . As k_1 increases, the time required for the kerogen to decompose to bitumen decreases. The time effect is also true for k_2 . As k_2 increases, the time for bitumen to decompose to oil is shorter. Changing k_3 , however, will affect the quantity and rate of oil degradation. For this reason, it can be seen that only k_3

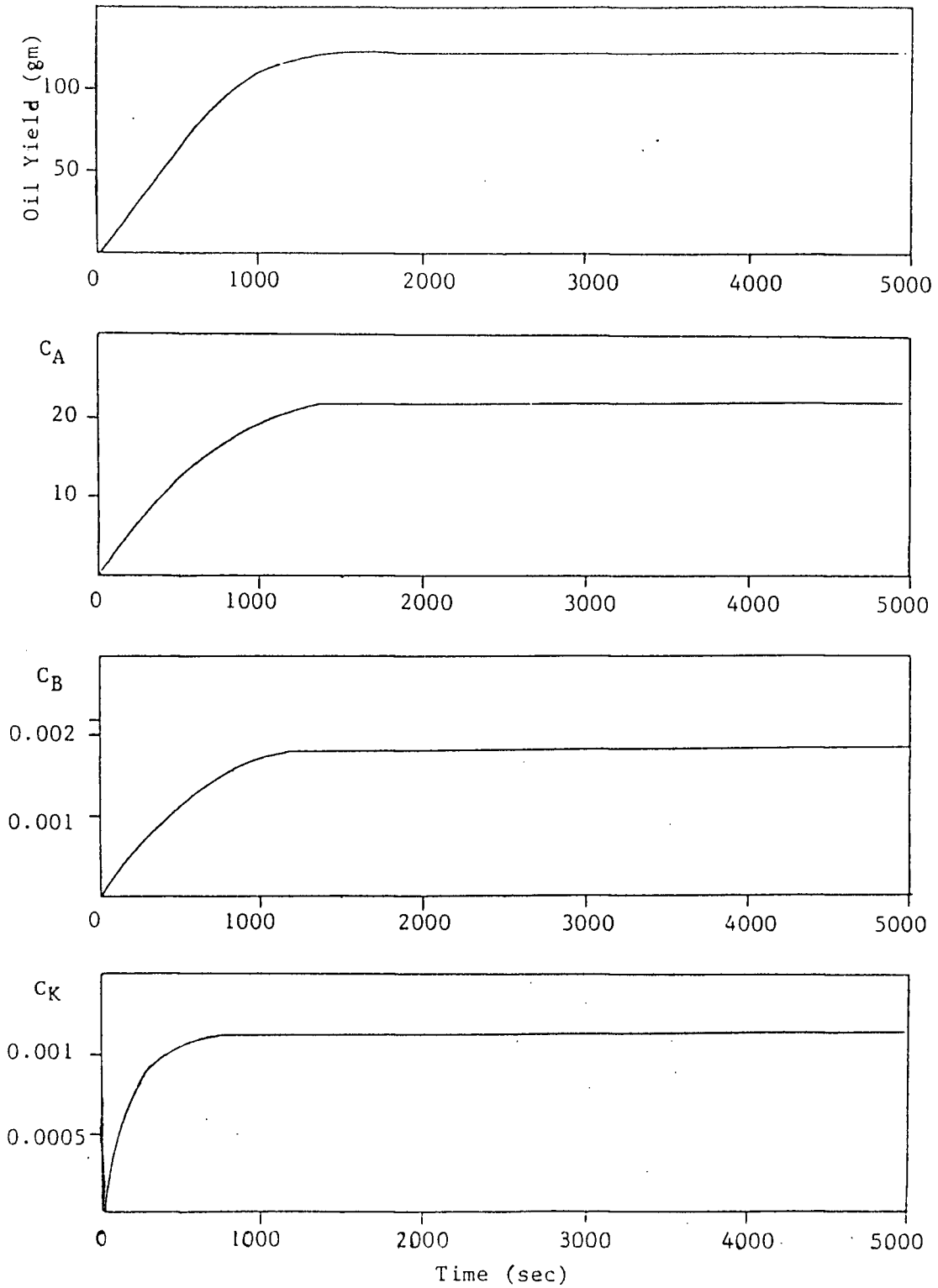


Fig. 16: C_K , C_B , C_A and Oil Yield vs Time Plot

and E_3 have an effect on the maximization of the oil yield. If some data of kerogen and bitumen were taken, a better model could be obtained.

6.3 The effect of Oil Shale Feed Rate on Oil Yield

Using the UBC Library Program Jacobian to solve the model, the effect of oil shale feed rate on oil yield was studied. Table 27 shows the comparison of the predicted oil yield results with the experimental values. Instead of a decreasing trend, the model predicted a constant oil yield value at 5.8 wt% for 2-4mm, and 5.5-6.0 for 1-2mm particle size. For the feed rate experiment carried under the steady height condition, again the model predicted a constant value at 6.6-6.7 wt % oil yield which is higher than the experimental value of 2.4-2.6 wt%. The predicted values indicate that the oil yield should be proportional to the feed rate. However the model does not take into consideration the effect of spent shale that acts as a catalyst for oil degradation. For future development of the model, the effect of spent shale should be included by putting the rate of oil decomposition proportional to the mass of spent shale.

TABLE 27: Effect of Feedrate on Oil Yield (Predicted vs Experimental Values)

Expt No.	Particle Size (mm)	Bed	Temperature (°C)	Inlet	Shale Feedrate (kg/hr)	Experimental Oil wt%	Predicted Oil wt%
(Unsteady Height Experiment)							
10	2-4	501		501	1.33	7.2	5.8
6A	2-4	503		503	1.65	7.4	5.8
12A	2-4	506		506	1.90	4.5	5.8
12	2-4	505		506	3.32	2.0	5.8
5	1-2	501		501	1.33	6.3	5.7
4	1-2	503		503	1.65	5.8	5.5
24	1-2	506		506	1.90	3.4	6.0
25	1-2	505		506	3.32	2.9	6.0
(Steady Height Experiment)							
16	1-2	470		470	1.26	2.4	6.8
19	1-2	470		480	3.39	2.6	6.7
20	1-2	472		476	4.45	2.5	6.6

7. CONCLUSION

The experimental studies have shown that New Brunswick oil shales can be pyrolyzed in a spouted bed reactor. At optimum pyrolysis temperature, shale particle sizes and feed rate, oil yields up to 94% of the Fischer Assay value were achieved.

The temperature effect was studied using two particle sizes: 1-2mm and 2-4mm. The optimum temperatures are around 457°C and 505°C respectively, and above this temperature the oil yields fall off.

Three particle size range were tested: 2-4mm, 1-2mm and 0.5-1mm. At a given feed rate and temperature, the oil yields increase with increasing mean particle size.

There is a marked decrease of oil yield with increasing shale feed rate in beds of sand. The hot spent shale which accumulates in the reactor appears to act as a sorbent for oil or a surface for the secondary oil-consuming reactions. Results of a series of experiments at fixed feed rate show that as the ratio of spent shale to sand in the initial bed increases, the oil yields decrease. For experiments in which the bed initially consisted only of spent shale, the oil yields remained at a constant low value regardless of the feed rate, over the range tested.

All the experiments were done using 15% CO₂ and 85%N₂ as pyrolyzing gas except for two experiments where N₂ was used alone. For the latter two runs, the oil yields decreased by 50%. No logical explanation for this result is

apparent, and some confirmation of this result is required.

Gas species produced in the pyrolysis are H_2 , CH_4 , C_2H_4 , C_2H_6 , C_3H_8 and C_4H_{10} . Carbon dioxide is not produced in the temperature range studied. The yields do not seem to be affected by shale particle sizes, feed rate and bed material. The reported gas yields were generally lower than the Fischer Assay values although for many runs the analytical equipment available did not detect hydrocarbons heavier than methane.

There is a substantial loss of shale which is entrained in the gases and passes through the cyclone. Due to the low percentage recovery, trends of the spent shale yield were not reliable.

A kinetic model which involves release of bitumen from the shale kerogen, and the subsequent decomposition of bitumen into oil accounts for the basic trends of the experimental results.

8. RECOMMENDATIONS FOR FUTURE WORK

As mentioned in the previous Sections 4 and 5, there are a few areas that need further studies. Modifications to the equipment and future work include:

- 1) An electrostatic precipitator should be installed downstream to enable better collection of oil from the pyrolysis of oil shale.
- 2) A more efficient cyclone should be used in order to collect all the entrained particles so as to do a better study on the spent shale trend.
- 3) A higher gear ratio reducer is recommended for the feed system to enable a more constant feeding rate during the experiment.
- 4) Modifications are recommended to the fountain section of the reactor in order to catch the spent shale ash to enable experiments to be carried out without interference of the spent shale which act as a catalyst for oil degradation.
- 5) More pyrolysis experiments should be carried out at the lower temperature range, specifically at 380-450°C in order to permit a better comparison with the model developed in Section 3.2.
- 6) Attempts should be made to collect some data on kerogen and bitumen content so as to obtain a better correlated model as discussed in Section 6.
- 7) The effect of the spent shale should be included in the future development of the model.

- 8) A set of oil yield vs temperature experiments should be carried out for the 0.5-1mm oil shale particle size so as to obtain the optimum temperature and compare the optimum oil yield with the Fischer Assay value.

NOMENCLATURE

A	Oil mass, kg
A_p	Surface area of particles, m^2
B	Bitumen mass, kg
Bi_H	Heat transfer Biot number, $h_p r_p / k_p$
C	Concentration of pyrolysable mass, kg/kg
C_i	Carbonaceous mass, kg
C_A	Concentration of oil, kg/kg
C_B	Concentration of bitumen, kg/kg
C_K	Concentration of kerogen, kg/kg
C_{p_f}	Heat capacity of fluid, KJ/kg·K
C_{p_p}	Heat capacity of particle, KJ/kg·K
C_{p_s}	Heat capacity of oil shale, KJ/kg·K
E	Activation energy, KJ/mol
f_1	Weight fraction of kerogen that yields bitumen
f_2	Weight fraction of bitumen that yields oil
f_3	Weight fraction of kerogen that yields gas
f_4	Weight fraction of bitumen that yields gas
F_0	Mass feed rate of oil shale, kg/s
F_1	Mass flow rate of entrained particles, kg/s
F_2	Mass flow rate of oil shale in the side line, kg/s
$F_{g,in}$	Spouting gas flow rate, m^3/s
Fo_H	Fourier number, at/r_p^2
G_i	Gas mass, kg

h_p	Heat transfer coefficient between fluid and particle, $J/m^2 \cdot s \cdot K$
ΔH_{rxn}	Heat of pyrolysis (assumed to be zero)
k_f	Thermal conductivity of fluid, $J/m \cdot s \cdot K$
k_p	Thermal conductivity of solid particle, $J/m \cdot s \cdot K$
K	Kerogen mass, kg
k_1	Frequency factor for kerogen, 1/s
k_2	Frequency factor for bitumen, 1/s
k_3	Frequency factor for oil, 1/s
k_1	Rate constant for kerogen, 1/s
k_2	Rate constant for bitumen, 1/s
k_3	Rate constant for oil, 1/s
M_p	Mass of a particle, kg
Nu	Nusselt number, $h_p d_p / k_f$
Pr	Prantl number, $Cp_f \mu / k_f$
Q_R	Heat transfer rate at particle surface, J/s
r	Radius, m
r_p	Radius of particle, m
r_K	Overall rate of Kerogen production, 1/s
r_B	Overall rate of Bitumen production, 1/s
r_A	Overall rate of Oil production, 1/s
R	Gas rate constant, $8.3143 J/mol \cdot K$
Re	Reynold number, $d_p u_p \rho_f / \mu$

t	Time, s
t_0	Initial time, s
T	Temperature, K
T_b	Bulk bed solid temperature, K
T_c	Temperature of shrinking core surface, K
T_g	Temperature of gas, K
T_p	Temperature of particle, K
T_R	Temperature of particle surface, K
T_s	Internal particle temperature, K
T_w	Wall or heater temperature, K
V	Volume of the vapor reaction zone, m^3
V_p	Particle volume, m^3
W	Weight of spent shale in bed, kg
w_0	Initial weight of particle, kg
w_t	Weight of particle at time t , kg
w_a	Final weight of particle, kg
a	Thermal diffusivity of particle, $k_p/(\rho_s \cdot C_{p_p})$, m^2/s
ϵ_v	Voidage
ϵ	Effective emissivity (0.9)
μ	Viscosity of fluid, $g/cm \cdot s$
ρ_s	Average density of oil shale, g/m^3
σ	Stefan-Boltzmann constant, $5.673 \times 10^{-12} J/cm^2 \cdot s \cdot K^4$

REFERENCE

1. Ranny, M.W., Oil Shale and Tar Sands Technology - Recent Developments , Noyes Data Corp., 1979.
2. Al-Jarallah, A.M., "Pyrolysis of Some Western Canadian Coals in a Spouted Bed Reactor," PhD thesis, University of British Columbia, 1983.
3. Stanfield, K.E., "Properties of Colorado Oil Shale," USBM Report of Investigations 4825, 1951.
4. Allred, V.D., "Kinetics of Oil Shale Pyrolysis," Quarterly of the Colorado School of Mines, Vol 62, No. 3, 657-669 (1967).
5. Henderick, T.A., Synthetic Fuels Data Handbook , Cameron Engineers Inc., 1975.
6. Pease, L.R., "Tosco Technology Applied to Eastern US Oil Shales," Eastern Oil Shale Symposium Proceedings (1981).
7. Margolis, M.J., "Fluidized Bed Oil Shale Retorting: A Bench Scale Evaluation for Eastern Oil Shale," Eastern Oil Shale Symposium Proceedings (1981).
8. Salib, P.F., Barua, S.K., and Furimsky, E., "Retorting of Oil Shale from New Brunswick, Canada," Energy Research Laboratories , Energy, Mines and Resources, CANMET, Ottawa (1986).
9. Mathur, K.B., and Epstein, N., Spouted Beds , Academic Press, 1974.
10. Kmiec, A., "Simultaneous Heat and Mass Transfer In Spouted Beds," Can. J. Chem. Eng., Vol 53, 18-24 (1975).
11. Grace, J.R., and Mathur, K.B., "Height and Structure of Fountain Region Above Spouted Bed," Can. J. Chem. Eng., Vol 58, 533-537 (1978).

12. Epstein, N., Lim, C.J., and Mathur, K.B., "Data and Models for Flow Distribution and Pressure Drop in Spouted Beds," Can. J. Chem. Eng., Vol 56, 436-447 (1978).
13. Foong, S.K., Lim, C.J., and Watkinson, A.P., "Coal Gasification in a Spouted Bed," Can. J. Chem. Eng., Vol 58, 84-91 (1980).
14. Smith, K.J., Arkun, Y., and Littman, H., "Studies on Modelling and Control of Spouted Bed Reactor - I," Chem. Eng. Sci., Vol 37, 567-579 (1982).
15. Vaid, R.P., and Sen Gupta, P., "Minimum Fluidised Velocities Beds of Mixed Solids," Can. J. Chem. Eng., Vol 56, 292 (1978).
16. Leite, A.C.B., Wodtke, R.M.P., Lisboa, A.C.L., and Restini, F., "Pyrolysis of Oil Shale Fines in a Spouted Bed Reactor," VI Congresso Brasileiro de Engenharia Quimica, Campinas, Julho (1984), XVI Congresso Latino Americano de Quimica, Rio de Janeiro, Outubro (1984).
17. Bae, J.H., "Some Effects of Pressure on Oil Shale Retorting," Annual Fall Meeting of the Society of Petroleum Engineers (AIME), 1968.
18. Furimsky, E., "Hydrogen Retorting of Oil Shales from Eastern Canada," Fuel Processing Technology, 8, 293-306 (1984).
19. Hill, G.R., "The Direct Production of a Low Pour Point High Gravity Shale Oil," ACS Symposium on Pyrolysis Reactions of Fossil Fuels, Pittsburgh (1966).
20. Lui, A.P., Mei, J.S., Shang, J.Y., and Zhang, G.Q., "Application of a Twin Fluidized-Bed Reactor for Retorting Combustion and Gasification /Combustion Processes," Proc. 7th International Conference on Fluidized Bed Combustion, 1270-1281 (1983)

21. Stanfield K.E., and Frost I.C., "Method of Assaying Oil Shale by Modification Fischer Retort," US Bureau of Mines Report of Investigation 4477 (1949).
22. Hubbard, A.B., and Robinson, W.E., US Bureau of Mines Report of Investigations 4744 (1950).
23. Cook, E.W., "Green River Shale-Oil Yields: Correlation with Elemental Analysis," Fuel, Vol 53, 16-20 (1974).
24. Braun, R.L., and Rothman, A.J., "Oil Shale Pyrolysis Kinetics and Mechanism of Oil Production," Fuel, Vol 54, 129-131 (1975).
25. Johnson, W.F., Walton, D.K., Keller, H.H., and Couch, E.J., Proceeding 8th Oil Shale Symposium, Colorado School Mines, 70(30), 237 (1975).
26. Finucane, D., George, J.H., and Harrist, H.G., "Perturbation Analysis of Second Order Effects in Kinetics of OilShale Pyrolysis," Fuel, Vol 56, 66-69 (1977).
27. Campbell, J.H., Keskinas, G.H., and Stout, N.D., "Kinetics of Oil Generation from Colorado Oil Shale," Fuel, Vol 57, 372-376 (1978).
28. Granoff, B., and Nuttall, H.E., "Pyrolysis Kinetics for Oil-Shale Particles," Fuel, Vol 56, 234-240 (1977).
29. Shih, S.M., and Sohn, H.Y., "Nonisothermal Determination of the Intrinsic Kinetics of Oil Generation from Oil Shale," Ind. Eng. Chem. Pro. Des. Dev., Vol 19, 420-426 (1980).
30. Wen, C.S., and Kobylinski, T.P., "Low Temperature Oil Shale Conversion," Fuel, Vol 62, 1269-1273 (1983).
31. Wang, C.C., and Noble, R.D., "Composition and Kinetics of Oil Generation from Non-isothermal Oil Shale Retorting," Fuel, Vol 62, 529-533 (1983).

32. Burnham, A.K., and Happe, J.A., "On the Mechanism of Kerogen Pyrolysis," *Fuel*, Vol 63, 1353-1356 (1984).
33. Yang, H.S., and Sohn, H.Y., "Kinetics of Oil Generation from Oil Shale from Liaoning Province of China," *Fuel*, Vol 63, 1511-1514 (1984).
34. Pan, Z., Feng, H.Y., and Smith, J.M., "Rates of Pyrolysis of Colorado Oil Shale," *AlChE Journal*, Vol 31, No. 5, 721-728 (1985).
35. Teo, K.C., Watkinson, A.P., and Jung, D.J., "Characterization and Storage Stability of Untreated and Hydrotreated Liquids from Spouted Bed Pyrolysis of Canadian Coals," Dept. of Chem. Eng., University of British Columbia, DSS File No. 20ST 23440-4-9074, DSS Contract Serial No. OST84-00151, Pg. 22-32 (1985).
36. Floess, J.K., Plawsky, J., Longwell, J.P., and Peters, W.A., "Effects of Calcined Dolomite on the Fluidised Bed Pyrolysis of a Colorado Oil Shale and a Texas Lignite," *Ind. Eng. Chem. Proc. Des. Dev.* Vol 24, 730-737 (1985)
37. Campbell, J.H., Koskinas, G.J., Gallegos, G., and Gregg, M., "Gas Evolution during Oil Shale Pyrolysis: Nonisothermal Rate Measurements," *Fuel*, Vol 59, 718-725 (1980).
38. Wu, Stanely W.M., "Hydrodynamic of Gas Spouting at High Temperature," MAsc. thesis, University of British Columbia, 1986.
39. Ekstrom, A., and Callaghan, G., "The Pyrolysis Kinetics of some Australian Oil Shales," *Fuel*, Vol 66, 331-337 (1987).
40. Parks, T.J., Lynch, L.J., and Webster, D.S., "Pyrolysis model of Rundle Oil Shale from in-situ ^1H n.m.r. data," *Fuel*, Vol 66, 338-344 (1987).

41. Wall, G.C., and Smith, S.J.C., "Kinetics of production of Individual Products from the Isothermal Pyrolysis of Seven Australian Oil Shales," Fuel, Vol 66, 345-349 (1987).
42. Gannon, A.J., and Henstridge, D.A., "Pyrolysis Stoichiometry for Three Kerogen Types," Fuel, Vol 66, 350-352 (1987).
43. Levy, J.H., Mallon, R.G., and Wall, G.C., "Vapour Phase Cracking and Coking of Three Australian Shale Oils: Kinetics in the Presence and Absence of Shale Ash," Fuel, Vol 66, 358-364 (1987).
44. Dung, N.V., Wall, G.C., and Kastl G., "Continuous Fluidized Bed Retorting of Condor and Stuart Oil Shales in a 150mm diameter Reactor," Fuel, Vol 66, 372-376 (1987).
45. Dung, N.V., "A New Concept for Retorting Oil Shales," Fuel, Vol 66, 377-383 (1987).
46. Charlton, Brian G., "Comparative Fluidized Bed Combustion Kinetics of some Australian Spent Oil Shales," Fuel, Vol 66, 384-387 (1987).

APPENDIX A

Temperature History Model

The heat transfer in a spouted bed has been discussed in Section 2.6. It is shown that the particle temperature profile is governed by the unsteady state diffusion equation,

$$\frac{\partial T}{\partial t} = \frac{a}{r^2} \frac{\partial(r^2 \partial T / \partial r)}{\partial r} \quad (2.4)$$

with the boundary condition for $r=R$,

$$K_p(\partial T / \partial r)_{r=r_p} = h_p(T_b - T_{r=r_p}) \quad (2.5)$$

From equation 2.4, the temperature profile of a particle as a function of time can be estimated along the longitude height of the 4 regions of a spouted bed: the spout, fountain (upward), fountain (downward) and annulus. The sketch of the different regions are shown in Figure 4. The equation can be written as a tridiagonal matrix. The radius of the particle is divided into 10 sections with $r(1)=r_c$, ie. the centre of the particle, and $r(10)=R$, ie. the surface of the particle, and the longitude height of the bed is also equally divided into 10 sections, thus forming a matrix of 10 x 10.

To put the equation in a matrix form, equation 2.4 has to be differentiated and put into finite series form,

$$\frac{a}{r^2} \left(2r \frac{\partial T}{\partial r} + r^2 \frac{\partial^2 T}{\partial r^2} \right) = \frac{\partial T}{\partial t} \quad (\text{A.1})$$

$$\frac{2a \partial T}{r \partial r} + a \frac{\partial^2 T}{\partial r^2} = \frac{\partial T}{\partial t} \quad (\text{A.2})$$

where

$$\frac{\partial T}{\partial r} = \frac{T_{n+1,t} - T_{n-1,t}}{2\Delta r} \quad (\text{A.3})$$

$$\frac{\partial^2 T}{\partial r^2} = \frac{T_{n+1,t} - 2T_{n,t} + T_{n-1,t}}{\Delta r^2} \quad (\text{A.4})$$

$$\frac{\partial T}{\partial t} = \frac{T_{n,t} - T_{n,t-1}}{\Delta t} \quad (\text{A.5})$$

therefore equation (A.2) becomes,

$$\begin{aligned} & \frac{2a}{r} \left(\frac{T_{n+1,t} - T_{n-1,t}}{2\Delta r} \right) + a \left(\frac{T_{n+1,t} - 2T_{n,t} + T_{n-1,t}}{\Delta r^2} \right) \\ & = \frac{T_{n,t} - T_{n,t-1}}{\Delta t} \end{aligned} \quad (\text{A.6})$$

Rearranging equation (A.6) gives,

$$\begin{aligned} & \left(-\frac{a}{r\Delta r} + \frac{a}{\Delta r^2}\right)T_{n-1,t} + \left(-\frac{2a}{\Delta r^2} - \frac{1}{\Delta t}\right)T_{n,t} + \left(\frac{a}{r\Delta r} + \frac{a}{\Delta r^2}\right)T_{n+1,t} \\ &= -\frac{T_{n,t-1}}{\Delta t} \end{aligned} \quad (\text{A.7})$$

At the boundary condition when $r=r_c=0$,
then (A.2) becomes,

$$3a\frac{\partial^2 T}{\partial r^2} = \frac{\partial T}{\partial r} \quad (\text{A.8})$$

$$3a\left(\frac{T_{n+1,t} - 2T_{n,t} + T_{n-1,t}}{\Delta r^2}\right) = \frac{T_{n,t} - T_{n,t-1}}{\Delta t} \quad (\text{A.9})$$

$$\begin{aligned} & \frac{3a}{\Delta r^2}T_{n-1,t} + \left(-\frac{6a}{\Delta r^2} - \frac{1}{\Delta t}\right)T_{n,t} + \frac{3a}{\Delta r^2}T_{n+1,t} \\ &= -\frac{T_{n,t-1}}{\Delta t} \end{aligned} \quad (\text{A.10})$$

The boundary condition at $r=0$ is $\frac{\partial T}{\partial r} = 0$ (A.11)

$$\left(\frac{T_{n+1,t} - T_{n-1,t}}{2\Delta r}\right) = 0 \quad (\text{A.12})$$

$$\text{or } T_{n+1,t} = T_{n-1,t} \quad (\text{A.13})$$

Therefore,

$$\left(-\frac{6a}{\Delta r^2} - \frac{1}{\Delta t}\right)T_{n,t} + \frac{6a}{\Delta r^2}T_{n+1,t} = -\frac{T_{n,t-1}}{\Delta t} \quad (\text{A.14})$$

The boundary condition at $r=R$ is

$$\frac{\partial T}{\partial r} = \frac{h_p}{k_p}(T_g - T) \quad (\text{A.15})$$

$$\text{or } \frac{T_{n+1,t} - T_{n-1,t}}{2\Delta r} = \frac{h_p}{k_p}(T_g - T_{n,t}) \quad (\text{A.16})$$

$$T_{n+1,t} = T_{n-1,t} + 2r \frac{h_p}{k_p}(T_g - T_{n,t}) \quad (\text{A.17})$$

Substituting the result into the general form of the (A.7) yields:

$$\begin{aligned} &\left(-\frac{a}{r\Delta r} + \frac{a}{\Delta r^2}\right)T_{n-1,t} + \left(-\frac{2a}{\Delta r^2} - \frac{1}{\Delta t}\right)T_{n,t} \\ &+ \left(\frac{a}{r\Delta r} + \frac{a}{\Delta r^2}\right)\left[T_{n-1,t} + \frac{2\Delta r h_p}{k_p}(T_g - T_{n,t})\right] = -\frac{T_{n,t-1}}{\Delta t} \end{aligned} \quad (\text{A.18})$$

$$\begin{aligned}
 \text{or } & \frac{2a}{\Delta r^2} T_{n-1,t} + \left[-\frac{2a}{\Delta r^2} - \frac{1}{\Delta t} - \frac{2\Delta r h_p}{k_p} \left(\frac{a}{r\Delta r} + \frac{a}{\Delta r^2} \right) \right] T_{n,t} \\
 & = -\frac{T_{n,t-1}}{\Delta t} - \frac{2\Delta r h_p}{k_p} \left(\frac{a}{r\Delta r} + \frac{a}{\Delta r^2} \right) T_g \quad (A.19)
 \end{aligned}$$

The coordinates of the matrix are listed in table 29.

A library program TRISLV is used to solve the tridiagonal equations. Table 30 lists the correlations used for estimation of the hydrodynamic properties for the spouted bed. There are a few assumptions made:

- 1) The velocity of the particle at the apex of the spouted bed is assumed to be zero.
- 2) The particle at the apex of the spouted bed is assumed to be at room temperature, 298°K, ie. the inlet temperature effect on the particle is ignored.
- 3) The calculation of the hydrodynamic properties of the spouted bed is based on sand as spouting media. The oil shale particle is assumed to follow the flow pattern of the sand.
- 4) The reactor temperature is assumed to be constant. There is assumed to be no heat loss to the surroundings.

Table 29: Coordinates of the Tridiagonal Matrix of spouted bed

$$b_1 = -\frac{2a}{\Delta r^2} - \frac{1}{\Delta t}$$

$$c_1 = \frac{2a}{\Delta r^2}$$

$$d_1 = -\frac{T_{n,t-1}}{\Delta t}$$

$$a_i = \frac{a}{\Delta r^2} - \frac{a}{r\Delta r}$$

$$b_i = -\frac{2a}{\Delta r^2} - \frac{1}{\Delta t}$$

$$c_i = \frac{a}{r\Delta r} + \frac{a}{\Delta r^2}$$

$$d_i = -\frac{T_{n,t-1}}{\Delta t}$$

$$a_n = \frac{2a}{\Delta r^2}$$

$$b_n = -\frac{2ah_p}{rk_p} - \frac{2ah_p\Delta r}{\Delta r^2 k_p} - \frac{2}{\Delta r^2} - \frac{1}{\Delta t}$$

$$d_n = -\frac{2ah_p T_g}{rk_p} - \frac{2ah_p T_g}{drk_p} - \frac{T_{n,t-1}}{\Delta t}$$

Table 30: Correlations used to estimate the hydrodynamic properties of spouted bed

		Reference
H_m	$0.105 \left(\frac{D_c}{D_p} \right)^{0.75} \left(\frac{D_c}{D_i} \right)^{0.4} \left(\frac{D_c}{\rho_p^{1/2}} \right)$	(9)
u_{ms}	$\left(\frac{D_p}{D_c} \right) \left(\frac{D_i}{D_c} \right)^{1/3} \left(\frac{2gHH(\rho_p - \rho_g)}{\rho_g} \right)^{0.5}$	(9)
D_s	$0.118(G)^{0.49}(D_c)^{0.68}$	(9)
u_{mf}	$0.5(\mu_{bf} + \mu_{tf})$	(10)
μ_{bf}	$\frac{nebf \cdot \mu}{D_p \rho_g}$	
$nebf$	$\frac{netf \cdot \mu}{D_p \rho_g}$	(10)
μ_{tf}	$[18.1^2 + 0.0192 \left(\frac{D_p^3 \rho_g (\rho_p - \rho_g) g}{\mu^2} \right)]^{1/2} - 18.1$	
$netf$	$[24.0^2 + 0.0546 \left(\frac{D_p^3 \rho_g (\rho_p - \rho_g) g}{\mu^2} \right)]^{1/2} - 24.0$	(10)
H_f	$\frac{(E_o^{1.46})(V_{pmax})^2(\rho_s)}{2g(\rho_s - \rho_g)}$	(12)
$v_{t(sput)}$	$\frac{(0.3)(0.2)(V_{max})DISJ}{(1-0.2)HH}$	
v_p (fountain)	$\left[\frac{V_{max}^2 - 2g(DISJ)(\rho_p - \rho_g)}{E_o^{1.46}\rho_p} \right]^{0.5}$	
v_p (falling)	$\left[\frac{2g(\rho_p - \rho_g)}{E_o^{1.46}\rho_p} \cdot (H - DISJ) \right]^{0.5}$	

- 5) The oil shale particle is assumed to be a perfect spherical particle.

The computer program consists of three sections. Section 1 specifies all the data and information of the spouted bed reactor, the properties of sand (spouting media), oil shale and spouting gas. It also calculates the hydrodynamic properties for the spouted bed. Section 2 of the program calls the subroutine Temp2 to Temp5 to calculate and print out the solutions. Section 3 of the program stores all the subroutines. The calculations were done on three average oil shale sizes: 3mm, 1.5mm and 0.75mm; and three reactor temperatures: 450, 500 and 550°C. Other profiles can be obtained by simply changing the data information in line 44, 45 and 46 of the program.

APPENDIX B

B.1 Calculations for Isokinetic Gas Sampling

Isokinetic sampling means that the velocities of the gases in the main pipe is the same as the velocities of gases in the sampling tube. To ensure this, the volumetric flow rate of the gas in the main pipe is first estimated, and the volumetric flow rate of the sample is then calculated and adjusted to the temperature of the sampling gas rotameter. A sample calculation for Run #2 is shown as below:

Oil shale particle size = 0.5-1.0mm

Temperature of the reactor = 501°C

Temperature of the sampling tube = 400°C

Mass flow rate of spouting gas = 4.95g/s

Mass flow rate of oil shale (as received) = 0.369g/s

Mass flow rate of oil shale (MAF) = 0.095g/s

Water vapor and gas expected to evolve from oil shale
= 0.019g/s

Total mass flow rate of gases = 4.969g/s

It can be seen that the spouting gas accounts for 99% of the gases, hence the mass flow rate and density of spouting gas are used for the purpose of this calculation.

Density of spouting gas at 501°C = 0.0004793g/cm³

Volumetric flow rate of gases = 10367.20cm³/s

Main pipe flow rate = 23.58cm²

Velocity of the spouting gas = 439.66cm/s

Sampling tube cross-sectional area = 0.7cm²

Volumetric flow rate of sample gas, 500°C = 307.76cm³/s

Volumetric flow rate of sample gas, 21°C = 117.0cm³/s

Hence the sample gas rotameter setting is adjusted accordingly.

B.2 Product Yield Calculation

The procedure used to calculate oil, gas and spent shale yields is outlined as below, and a simple computer program is written for this purpose.

$$\text{Oil Yield: } \frac{\text{oil}}{\text{Feed}} \times 100\%$$

$$\text{Spent Shale Yield: } \frac{\text{spent}}{\text{Feed}} \times 100\%$$

$$\text{Total Gas Yield: } \frac{\text{TG} - \text{SG}}{\text{Feed}} \times 100\%$$

TG = Total gas output, g/s

SG = Mass flow rate of spouting gas, g/s

APPENDIX C

Computer Programmes

C.1 Profile

Listing of PROFILE at 11:37:26 on MAY 28, 1987 for CCid=TITA

```

1      C *****
2      C
2.2    C      NAME OF THIS PROGRAM: PROFILE
2.4    C
2.8    C
3      C      THIS PROGRAM IS USED TO WORK OUT THE TEMPERATURE HISTORY OF
4      C      AN OIL SHALE PARTICLE IN THE 5 REGIONS OF A SPOUTED BED:
6      C      1) SPOUT REGION
7      C      2) FOUNTAIN REGION
8      C      3) FALLING REGION
9      C      4) ANNULUS REGION
10     C
11     C      THIS PROGRAM IS CONSISTED OF 3 SECTIONS:
12     C      SECTION 1) SPECIFIES ALL THE INFORMATION OF THE SPOUTED BED
13     C      BED REACTOR, PROPERTIES OF SAND (SPOUTING MEDIA)
14     C      AND PROPERTIES OF OIL SHALE. IT ALSO WORKS OUT
15     C      THE HYDRODYNAMIC PROPERTIES (HM, UMS, UMF ETC)
16     C      FOR THE SPOUTED BED
17     C
18     C      SECTION 2) CALLS THE SUBROUTINE TEMP2, TEMP3, TEMP4 AND
19     C      TEMP5 TO CALCULATE AND PRINT OUT THE TEMPERATURE
20     C      HISTORY FOR THE OIL SHALE AT A GIVEN SIZE AND
21     C      REACTOR TEMPERATURE
22     C
23     C      SECTION 3) STORES ALL THE SUBROUTINE TEMP2 TO TEMP5
24     C
25     C *****
26     C
27     C
28     C      IMPLICIT REAL*8 (A-H,O-Z)
29     C
30     C      DIMENSION DP(3),TEMPG(3),TERM(3)
31     C      DIMENSION BIOT2(20),BIOT3(20),BIOT4(20),BIOT5(20)
32     C      DIMENSION DIS1(20),DIS2(20),DIS3(20),DIS4(20),DIS5(20)
33     C      DIMENSION DTIME1(20),DTIME2(20),DTIME3(20),DTIME4(20)
34     C      DIMENSION DTIME5(20)
35     C      DIMENSION HP2(20),HP3(20),HP4(20),HP5(20)
36     C      DIMENSION R1(20),R2(20),R3(20),R4(20),R5(20)
37     C      DIMENSION T1(20,20),T2(20,20),T3(20,20),T4(20,20),T5(20,20)
38     C      DIMENSION UP2(20),UP3(20),UP4(20),UP5(20)
39     C
40     C      REAL KP,KPP,NU
41     C
42     C      READ DATA
43     C
44     C      DATA DP/0.3D0,O.15D0,O.075D0/
45     C      DATA TERM/567.96D0,784.35D0,355.2D0/
46     C      DATA TEMPG/723.D0,823.D0,773.D0/
47     C
48     C      USE DO-LOOP TO ESTIMATE THE TEMPERATURE PROFILE
49     C      FOR 3 DIFFERENT SIZES AT DIFFERENT TEMPERATURES
50     C
51     C      DO 9999 MM=1,3
52     C          TG=TEMPG(3)
53     C      DO 999 M=1,3
54     C          DIA=DP(3)
55     C          UT=TERM(3)
56

```

Listing of PROFILE at 11:37:26 on MAY 28, 1987 for CCId=TITA

```

57      C
58      C
59      C *****
60      C
61      C      SECTION 1) SPECIFY THE BASIC INFORMATIN OF THE SPOUTED BED
62      C      REACTOR, SAND PARTICLES, OIL SHALE AND SPOUTING GAS
63      C
64      C *****
65      C
66      C      INFORMATION OF THE SPOUTED BED REACTOR
67      C
68          DI=1.58DO
69          DC=12.8DO
70          DPIPE=1.58DO
71          HPIPE=17.8DO
72          APIPE=3.1416DO*(DPIPE**2.DO)/4.DO
73          HH=33.DO
74          ACOL=3.1416DO*(DC**2.DO)/4.DO
75          ES=0.95DO
76          EA=0.42DO
77          EO=0.7DO
78      C
79      C      PROPERTIES OF THE SAND PARTICLES
80      C
81          DPS=0.1121DO
82          RRS=DPS/2.DO
83          DENS=2.68DO
84      C
85      C      PROPERTIES OF THE OIL SHALE
86      C
87          RR=DIA/2.DO
88          DEN=2.DO
89          KPP=1.25D-2/4.186DO
89.5      CPP=1.13DO/4.186DO
90      C
91      C      PROPERTIES OF GAS
92      C
93          CP=(6.76DO+((0.606D-3)*TG)+((0.13D-6)*(TG**2.DO)))/28.DO
94          DENG=1.DO*((28.0DO*0.85DO)+(44.0DO*0.15DO))/82.05DO/TG
95          KP=0.0001257DO
96          VIS=0.00033DO
97      C
98      C      FURTHER INFORMATION
98.5      C      THE FOLLOWING DATA ARE TAKEN FROM STANELY WU'S THESIS
99      C
100          DIS5(1)=33.DO
100.5      DIS5(2)=32.DO
101          DIS5(3)=25.DO
102          DIS5(4)=20.DO
103          DIS5(5)=15.DO
104          DIS5(6)=10.DO
105          DIS5(7)=5.DO
106      C
106.5      UP5(2)=1.335DO
107          UP5(3)=1.289DO
108          UP5(4)=1.188DO
109          UP5(5)=1.059DO
110          UP5(6)=2.176DO

```

Listing of PROFILE at 11:37:26 on MAY 28, 1987 for CCid=TITA

```

111          UP5(7)=0.838DO
112      C
113      C    TO CALCULATE THE HYDRODYNAMIC PROPERTIES OF THE SPOUTED BED
114      C    BASED ON SAND AS SPOUTING MEDIA
115      C
116      C    TO CALCULATE MAXIMUM SPOUTABLE BED HEIGHT, HM
117      C
118          HM=0.105DO*((DC/DPS)**0.75DO)*((DC/DI)**0.4DO)*DC/(DENS**1.2DO)
119      C
120      C    TO CALCULATE MINIMUM SPOUTING VELOCITY, UMS
121      C
122          UMS=(DPS/DC)*((DI/DC)**(1.DO/3.DO))*((2.DO*980.DO*HH*
123      &      (DENS-DENG)/DENG)**(1.DO/2.DO))
124          U=1.1DO*UMS
125          Q=U*ACOL
126      C
127      C    TO CALCULATE THE DIAMETER OF SPOUT, DS
128      C
129          EMF=0.5DO
130          DENB=DENS*(1.DO-EMF)
131          G=DENG*U
132          DS=(0.118DO*((G*10.DO)**0.49DO)*((DC/100.DO)**0.68DO)/
133      &      (DENB**0.41DO))*100.DO
134          AS=3.1416DO*(DS**2.DO)/4.DO
135      C
136      C    TO CALCULATE MINIMUM FLUIDISATION VELOCITY, UMF
137      C
138          CONST=(DPS**3.DO)*(DENG*(DENS-DENG)*980.DO)/(VIS**2.DO)
139          NEBF=((18.1DO**2.DO)+(0.0192DO*CONST))**0.5DO)-18.1DO
140          UBF=NEBF*VIS/DPS/DENG
141          NETF=((24.DO**2.DO)+(0.0546DO*CONST))**0.5DO)-24.DO
142          UTF=NETF*VIS/DPS/DENG
143          UMF=0.5DO*(UBF+UTF)
144      C
145          WRITE(6,991)DIA
146      991  FORMAT(1H1,/, 'DIA OF OIL SHALE PARTICLE = ',F6.4, 'CM')
147          WRITE(6,992)UMS
148      992  FORMAT(/, 'MIN SPOUTING VELOCITY = ',F8.4, 'CM/SEC')
149          WRITE(6,993)U
150      993  FORMAT(/, 'SPOUTING VELOCITY = ',F8.4, 'CM/SEC')
151          WRITE(6,994)HM
152      994  FORMAT(/, 'MAX SPOUTABLE HEIGHT = ',F7.4, 'CM')
153          WRITE(6,995)DS
154      995  FORMAT(/, 'DIAMETER OF SPOUT = ',F6.4, 'CM')
154.3      WRITE(6,996)TG
154.6      996  FORMAT(/, 'REACTOR TEMPERATURE = ',F7.3, 'DEG K')
155      C
156      C
157      C *****
158      C
159      C    SECTION 2) CALL THE SUBROUTINES TO PERFORM THE CALCULATION AND
160      C    PRINT OUT THE RESULTS
161      C
162      C *****
163      C
164      C    INITIALISE ALL TEMPERATURES
165      C
166          DO 111 I=1,10

```

Listing of PROFILE at 11:37:26 on MAY 28: 1987 for CCId=TITA

```

167          T1(I,1)=771.9DO
167.011 C
168      111  CONTINUE
209      C
210      C
211      C *****
212      C *
213      C  CALL SUBROUTINE TEMP2 TO WORK OUT THE *
214      C  TEMPERATURE PROFILE IN THE SPOUT *
215      C *
216      C *****
217      C
217.2 C
217.4      WRITE(6,606)CP
217.6      606  FORMAT(//,F10.5)
217.8 C
218      CALL TEMP2(TG,DIA,CP,DENG,KP,VIS,RR,DEN,CPP,KPP,HH,ACOL,HM,O,
219      & AS,ES,EA,T1,UMF,T2,DTIME2,DIS2,R2,UP2,TT2,HP2,BIOT2)
220      C
221      C  WRITE TITLE
222      C
223      WRITE(6,200)DIA
224      200  FORMAT(1H1,'IN THE SPOUTING REGION FOR SIZE =',2X,F6.4,'CM')
225      C
226      C  WRITE OUT THE SOLUTIONS OF T2(I,J)
227      C
228      WRITE(6,201)
229      201  FORMAT(//2X,'VEL CM/SEC',20X,'TEMP DEG K',28X,'HEIGHT CM',
230      & 3X,'TIME',5X,'HP',4X,'BIOT NO')
231      C
232      DO 202 KK=1,10
233      J=11-KK
234      WRITE(6,203)UP2(J),(T2(I,J),I=1,10),DIS2(J),DTIME2(J),HP2(J),
235      & BIOT2(J)
236      203  FORMAT(//2X,F7.2,1X,10F6.1,2X,F6.3,2X,F7.5,2X,F7.4,2X,F5.2)
237      C
238      202  CONTINUE
239      C
240      C  WRITE OUT THE DELTA RADIUS FOR THE PARTICLE AT BOTTOM LINE
241      C
242      WRITE(6,204)(R2(I),I=1,10)
243      204  FORMAT(//10X,10F6.3)
244      C
245      C  TO WRITE OUT THE SUB-TIME FOR PARTICLE TO REACH TOP LINE
246      C  OF THE SPOUT
247      C
248      WRITE(6,205)TT2
249      205  FORMAT(///,'SUB-TIME=',F8.4,'SEC')
250      C
251      C
252      C *****
253      C *
254      C  CALL SUBROUTINE TEMP3 TO WORK OUT THE *
255      C  TEMPERATURE PROFILE IN THE FOUNTAIN REGION *
256      C *
257      C *****
258      C
259      CALL TEMP3(TG,DIA,DENG,KP,VIS,DENS,RR,DEN,CPP,KPP,U,UP2,T2,H,

```

Listing of PROFILE at 11:37:26 on MAY 28, 1987 for CCId=TITA

```

260      & T3,DTIME3,DIS3,R3,UP3,TT3,HP3,BIOT3)
261
262      C
263      C   WRITE TITLE
264      C
265      WRITE(6,300)DIA
266      300  FORMAT(1H1,'IN THE FOUNTAIN REGION FOR SIZE=''.2X,F6.4,'CM')
267      C
268      WRITE(6,301)H
269      301  FORMAT(/2X,'FOUNTAIN HEIGHT=''.F6.3,'CM')
270      C
271      C   WRITE OUT THE SOLUTIONS OF T3(I,J)
272      C
273      WRITE (6,302)
274      302  FORMAT(/2X,'VEL CM/SEC',20X,'TEMP DEG K',28X,'HEIGHT CM',
275      & 4X,'TIME',4X,'HP',4X,'BIOT NO')
276      C
277      DO 303 KK=1,10
278      J=11-KK
279      WRITE(6,304)UP3(J),(T3(I,J),I=1,10),DIS3(J),DTIME3(J),
280      & HP3(J),BIOT3(J)
281      304  FORMAT(/2X,F7.2,1X,10F6.1,2X,F6.3,2X,F6.4,2X,F7.5,2X,F5.2)
282      C
283      303  CONTINUE
284      C
285      C   WRITE OUT THE DELTA RADIUS FOR THE PARTICLE AT BOTTOM LINE
286      C
287      WRITE(6,305)(R3(I),I=1,10)
288      305  FORMAT(/10X,10F6.3)
289      C
290      C   TO WRITE OUT SUB-TIME FOR PARTICLE TO REACH THE FOUNTAIN
291      C
292      WRITE(6,306)TT3
293      306  FORMAT(///,'SUB-TIME=''.F6.4,'SEC')
294      C
295      C *****
296      C *
297      C   CALL SUBROUTINE TEMP4 TO WORK OUT THE
298      C   TEMPERATURE PROFILE IN THE FOUNTAIN FALLING REGION *
299      C *
300      C *****
301      C
302      CALL TEMP4(TG,DENG,KP,VIS,DIA,DEN,CPP,KPP,DENS,H,E0,U,UP3,
303      & T3,T4,DTIME4,DIS4,R4,UP4,TT4,HP4,BIOT4)
304      C
305      C   WRITE TITLE
306      C
307      WRITE(6,400)DIA
308      400  FORMAT(1H1,'IN THE FALLING REGION FOR SIZE = ''.2X,F6.4,'CM')
309      C
310      WRITE(6,401)
311      401  FORMAT(/2X,'VEL CM/SEC',20X,'TEMP DEG K',28X,'HEIGHT CM',
312      & 4X,'TIME',4X,'HP',4X,'BIOT NO')
313      C
314      C
315      C
316      C
317      C
318      C
319      C
320      DO 402 KK=1,10

```


Listing of PROFILE at 11:37:26 on MAY 28, 1987 for CCid=TITA

```

322          WRITE(6,403)UP4(KK),(T4(I,KK),I=1,10),DIS4(KK),DTIME4(KK),
323      &      HP4(KK),BIOT4(KK)
324      403      FORMAT(/2X,F7.2,1X,10F6.1,2X,F6.3,2X,F6.4,2X,F7.5,2X,
325      &      F5.2)
326      C
327      402      CONTINUE
328      C
329      C
330      C      WRITE OUT THE DELTA RADIUS FOR THE PARTICLE AT BOTTOM LINE
331      C
332          WRITE(6,404)(R4(I),I=1,10)
333      404      FORMAT(/10X,10F6.3)
334      C
335      C      WRITE OUT SUB-TIME FOR PARTICLE TO DROP FROM FOUNTAIN
336      C
337          WRITE(6,405)TT4
338      405      FORMAT(///,'SUB-TIME=',F6.4,'SEC')
339      C
340      C *****
341      C *
342      C      CALL SUBROUTINE TEMPS TO WORK OUT THE TEMPERATURE *
343      C      PROFILE IN THE ANNULUS REGION *
344      C *
345      C *****
346      C
347          CALL TEMP5(TG,DIA,DENG,KP,VIS,RR,DEN,CPP,KPP,HH,EA,ES,ACOL,AS,
348      &      UMF,HM,UP5,DIS5,T4,UP4,T5,DTIME5,R5,TT5,HP5,BIOT5)
349      C
350      C      WRITE TITLE
351      C
352          WRITE(6,500)DIA
353      500      FORMAT(1H1,2X,'IN THE ANNULUS REGION FOR SIZE=',F6.4,'CM')
354      C
355          WRITE(6,501)
356      501      FORMAT(/2X,'VEL CM/SEC',20X,'TEMP DEG K',28X,'HEIGHT CM',
357      &      4X,'TIME',4X,'HP',4X,'BIOT NO')
358      C
359          DO 502 KK=1,7
360          WRITE(6,503)UP5(KK),(T5(I,KK),I=1,10),DIS5(KK),DTIME5(KK),
361      &      HP5(KK),BIOT5(KK)
362      503      FORMAT(/2X,F7.2,1X,10F6.1,2X,F6.3,2X,F6.4,2X,F7.5,2X,
363      &      F5.2)
364      C
365      502      CONTINUE
366      C
367      C      WRITE OUT THE DELTA RADIUS FOR THE PARTICLE AT BOTTOM LINE
368      C
369          WRITE(6,504)(R5(I),I=1,10)
370      504      FORMAT(/10X,10F6.3)
371      C
372      C      WRITE OUT TOTAL TIME FOR PARTICLE TO GO DOWN TO ANNULUS
373      C
374          WRITE(6,505)TT5
375      505      FORMAT(///,'SUB-TIME=',F8.4,'SEC')
376      C
377      C      TO WORK OUT THE TOTAL TIME SPENT IN THE 5 REGIONS
378      C
379          TIME=TT1+TT2+TT3+TT4+TT5

```

Listing of PROFILE at 11:37:26 on MAY 28, 1987 for CCid=TITA

```

380          WRITE(6,600)TIME
381      600   FORMAT(///2X,'TOTAL TIME SPENT IN 5 REGIONS =',F8.4,'SEC')
382      C
383      999   CONTINUE
384      C
385      9999  CONTINUE
386          STOP
387          END
388      C
389      C *****
390      C
391      C      SECTION 3) STORE ALL THE SUBROUTINES
392      C
393      C *****
510      C
511      C
512      C *****
513      C
514      C      SUBROUTINE TEMP2
515      C
516      C *****
517      C
518      C
519      C      SUBROUTINE TEMP2(TG,DIA,CP,DENG,KP,VIS,RR,DEN,CPP,KPP,HH,ACOL,
520      &      HM,Q,AS,ES,EA,T1,UMF,T2,DTIME2,DIS2,R2,UP2,TT2,HP2,BIOT2)
521      C
522      C
523      C      IMPLICIT REAL*8 (A-H,O-Z)
524      C      DIMENSION A(100),B(100),C(100),D(100)
525      C      DIMENSION DTIME2(20),DIS2(20),R2(20),HP2(20),BIOT2(20)
526      C      DIMENSION T1(20,20),T2(20,20),UP2(20)
527      C      REAL KPP,NU,KP
528      C
529      C      SPECIFY CONDITIONS OF GRID
530      C
531      C      N=10
532      C      DR=RR/9.DO
533      C      DD=HH/9.DO
534      C      TT2=0.000
535      C      DTIME2(1)=0.000
536      C
537      C
538      C      INITIALISE ALL R(I)
539      C
540      C      DO 20 I=1,N
541      20      R2(I)=(I-1)*DR
542      C
543      C
544      C      INITIALISE ALL TEMPERATURES
545      C
546      C      DO 21 IK=1,10
547      C          T2(IK,1)=T1(IK,1)
548      21      CONTINUE
549      C
550      C
551      C      WORK OUT THE VERTICAL DISTANCE
552      C
553      C      DO 22 I=1,11

```

Listing of PROFILE at 11:37:26 on MAY 28, 1987 for CCid=TITA

```

554      22      DIS2(I)=DD*(I-1)
555      C
556      C   TO WORK OUT SPOUTING VELOCITY AT THE TOP OF THE SPOUT. USH
557      C
558      C
559      UA=UMF*(1.DO-((1.DO-(HH/HM))**3.DO))
560      QA=UA*(ACOL-AS)
561      QS=Q-QA
562      USH=QS/AS/ES
563      C
564      C
565      C   TO SET UP TRIDIAGONAL EQUATIONS TO SOLVE THE
566      C   TEMPERATURE HISTORY FOR A SINGLE PARTICLE
567      C
568      DO 23 J=2,11
569      C
570      C
571      C   TO WORK OUT THE UA AT EACH INTERVAL
572      C
573      IF (J.EQ.11) GOTO 24
574      UA=UMF*(1.DO-((1.DO-(DIS2(J)/HM))**3.DO))
575      QA=UA*(ACOL-AS)
576      QS=Q-QA
577      US=QS/AS/ES
578      UP2(J)=((0.3DO*0.2DO*USH)*(DIS2(J)/HH))/(1.DO-0.2DO)
579      GOTO 25
580      24      UA=UMF
581      QA=UA*(ACOL-AS)
582      US=QS/AS/ES
583      UP2(J)=((0.3DO*0.2DO*USH)*(DIS2(J)/HH))/(1.DO-0.2DO)
584      25      RV=DABS(US-UP2(J))
585      C
586      C   TO CALCULATE HP FOR THE OIL SHALE IN THE SPOUTING REGION
587      C
588      E=0.4DO
589      RE=DIA*RV*DENG/VIS
590      PR=CP*VIS/KP
591      AA=2.DO/(1.DO-((1.DO-E)**(1.DO/3.DO)))
592      BB=2.DO*E/3.DO
593      NU=AA+BB*(PR**(1.DO/3.DO))*(RE**0.55DO)
594      HP=NU*KP/2.DO/RR
595      JJ=J-1
596      HP2(JJ)=HP
597      BIOT2(JJ)=HP*RR/KPP
598      C
599      C
600      ALPHA=KPP/CP/DEN
601      C
602      C   TO WORK OUT THE DT
603      C
604      DTIME2(J)=DD/UP2(J)
605      TT2=TT2+DTIME2(J)
606      DT=DTIME2(J)
607      UP2(1)=0.0DO
608      C
609      C   SET COEFFICIENTS OF MATRICES
610      C
611      C   BOUNDARY CONDITION AT R=0

```

Listing of PROFILE at 11:37:26 on MAY 28, 1987 for CCid=TITA

```

612 C
613 B(1)=- (6.DO*ALPHA/(DR**2.DO))- (1.DO/DT)
614 C(1)=6.DO*ALPHA/(DR**2.DO)
615 C
616 C BOUNDARY CONDITION AT R=N
617 C
618 A(N)=2.DO*ALPHA/(DR**2.DO)
619 B(N)=(-1.DO/DT)- (2.DO*ALPHA*HP/R2(N)/KPP)-
620 > (2.DO*ALPHA/(DR**2.DO))- (2.DO*ALPHA*HP/DR/KPP)
621 C
622 C INITIALISE ALL VALUES OF A(I), B(I), AND C(I)
623 C
624 DO 26 IK=2,9
625 A(IK)=(ALPHA/(DR**2.DO))- (ALPHA/R2(IK)/DR)
626 B(IK)=(-2.DO*ALPHA/(DR**2.DO))- (1.DO/DT)
627 26 C(IK)=(ALPHA/R2(IK)/DR)+ (ALPHA/(DR**2.DO))
628 C
629 D(1)=-T2(1,J-1)/DT
630 DO 27 I=2,9
631 27 D(I)=-T2(I,J-1)/DT
632 D(N)=-(T2(N,J-1)/DT)- (2.DO*ALPHA*HP*TG/R2(N)/KPP)-
633 > (2.DO*ALPHA*HP*TG/DR/KPP)
634 C
635 C CALL LIBRARY PROGRAMM TO SOLVE THE TRI-DIA EQNS
636 C
637 CALL TRISLV(N,A,B,C,D,O,&99)
638 C
639 C STORE THE SOLUTIONS T2(I,J)
640 C
641 C
642 DO 28 II=1,N
643 T2(II,J)=D(II)
644 28 CONTINUE
645 C
646 23 CONTINUE
647 C
648 GOTO 299
649 99 WRITE(6,29)
650 29 FORMAT(///2X,'ERROR MESSAGE')
651 299 CONTINUE
652 C
653 RETURN
654 END
655 C
656 C
657 C *****
658 C *
659 C SUBROUTINE TEMP3 *
660 C *
661 C *****
662 C
663 C
664 SUBROUTINE TEMP3(TG,DIA,DENG,KP,VIS,DENS,RR,DEN,CPP,KPP,U,
665 & UP2,T2,H,T3,DTIME3,DIS3,R,UP3,TT3,HP3,BIOT3)
666 C
667 IMPLICIT REAL*8 (A-H,O-Z)
668 DIMENSION A(100),B(100),C(100),D(100)
669 DIMENSION BIOT3(20),DIS3(20),DTIME3(20),HP3(20),R(20)

```

Listing of PROFILE at 11:37:26 on MAY 28, 1987 for CCid=TITA

```

670      DIMENSION T2(20,20),T3(20,20),UP2(20),UP3(20)
671      REAL KP,NU,KPP
672      C
673      C      TO CALCULATE THE HEIGHT OF FOUNTAIN REGION, H.
674      C
675      UP3(1)=UP2(10)
676      UP3(11)=0.0DO
677      EO=0.7DO
678      H=(EO**1.46DO)*(UP3(1)**2.DO)*DENS/((DENS-DENG)/2.DO/980.DO)
679      C
680      C      TO WORK OUT THE TEMPERATURE OF DIFFERENT PARTICLE SIZE
681      C
682      C
683      C      SPECIFY CONDITIONS OF GRID
684      C
685      N=10
686      DR=RR/9.DO
687      DD=H/9.DO
688      TT3=0.0DO
689      DTIME3(1)=0.0DO
690      C
691      C
692      C      INITIALISE ALL R(I)
693      C
694      DO 30 I=1,N
695      30      R(I)=(I-1)*DR
696      C
697      C
698      C      INITIALISE ALL TEMPERATURES
699      C
700      DO 31 II=1,10
701      T3(II,1)=T2(II,10)
702      31      CONTINUE
703      C
704      C
705      C      WORK OUT THE VERTICL DISTANCE
706      C
707      DO 32 I=1,11
708      32      DIS3(I)=DD*(I-1)
709      C
710      C
711      C      TO SET UP TRIDIAGONAL EQUATIONS TO SOLVE THE TEMPERATURE
712      C      HISTORY FOR A SINGLE PARTICLE
713      C
714      DO 33 J=2,11
715      C
716      C
717      IF (J.EQ.11) GOTO 34
718      C
719      C      TO WORK OUT THE VELOCITY OF PARTICLE AT EACH INTERVAL IN
720      C      THE FOUNTAIN REGION
721      C
722      UP3(J)=((UP3(1)**2.DO)-(2.DO*980.DO*DIS3(J)*(DENS-DENG)/DENS/
723      >      (EO**1.46DO)))*0.5DO
724      C
725      C      TO WORK OUT THE DELTA TIME
726      C
727      DTIME3(J)=DD/UP3(J-1)

```

Listing of PROFILE at 11:37:26 on MAY 28, 1987 for CCid=TITA

```

728          TT3=TT3+DTIME3(J)
729          DT=DTIME3(J)
730      C
731      34      CONTINUE
732      C
733          RV=DABS(U-UP3(J))
734      C
735      C      TO CALCULATE HP FOR THE COAL PARTICLE IN FOUNTAIN REGION
736      C
737          RE=DIA*RV*DENG/VIS
738          NU=0.42DO+0.35DO*(RE**0.8DO)
739          HP=NU*KP/2.DO/RR
740          ALPHA=KPP/PPP/DEN
741          JJ=J-1
742          HP3(JJ)=HP
743          BIOT3(JJ)=HP*RR/KPP
744      C
745      C      SET COEFFICIENTS OF MATRICS
746      C
747      C      BOUNDARY CONDITION AT R=0
748      C
749          B(1)=-((6.DO*ALPHA/(DR**2.DO))-((1.DO/DT)
750          C(1)=6.DO*ALPHA/(DR**2.DO)
751      C
752      C
753      C      BOUNDARY CONDITION AT R=N
754      C
755          A(N)=2.DO*ALPHA/(DR**2.DO)
756          B(N)=((-1.DO/DT)-(2.DO*ALPHA*HP/R(N)/KPP)-
757          > (2.DO*ALPHA/(DR**2.DO))-((2.DO*ALPHA*HP/DR/KPP)
758      C
759      C      INITIALISE ALL VALUES OF A(I), B(I), C(I)
760      C
761          DO 35 IK=2,9
762              A(IK)=(ALPHA/(DR**2.DO))-((ALPHA/R(IK)/DR)
763              B(IK)=((-2.DO*ALPHA/(DR**2.DO))-((1.DO/DT)
764              C(IK)=(ALPHA/R(IK)/DR)+(ALPHA/(DR**2.DO))
765      35      CONTINUE
766      C
767          D(1)=-T3(1,J-1)/DT
768      C
769          DO 36 I=2,9
770              D(I)=-T3(I,J-1)/DT
771      36      CONTINUE
772      C
773      C
774          D(N)=-((T3(N,J-1)/DT)-(2.DO*ALPHA*HP*TG/R(N)/KPP)-
775          > (2.DO*ALPHA*HP*TG/DR/KPP)
776      C
777      C
778      C      CALL LIBRARY PROGRAM TO SOLVE THE TRI-DIA EQUATIONS
779      C
780          CALL TRISLV(N,A,B,C,D,O,&99)
781      C
782      C
783      C      STORE THE SOLUTIONS T3(I,J)
784      C
785          DO 37 II=1,N

```

Listing of PROFILE at 11:37:26 on MAY 28, 1987 for CCid=TITA

```

786          T3(II,J)=D(II)
787      37      CONTINUE
788      C
789      33      CONTINUE
790      C
791      C
792          GOTO 39
793      99      WRITE(6,38)
794      38      FORMAT(///2X,'ERROR MESSAGE')
795      C
796      39      RETURN
797          END
798      C
799      C
800      C
801      C *****
802      C *
803      C      SUBROUTINE TEMP4 *
804      C *
805      C *****
806      C
807      C
808          SUBROUTINE TEMP4(TG,DENG,KP,VIS,DIA,DEN,CPP,KPP,DENS,H,EO,U,
809      &  UP3,T3,T4,DTIME4,DIS4,R,UP4,TT4,HP4,BIOT4)
810      C
811          IMPLICIT REAL*8 (A-H,O-Z)
812          DIMENSION A(100),B(100),C(100),D(100)
813          DIMENSION BIOT4(20),DIS4(20),DTIME4(20),HP4(20),R(20)
814          DIMENSION T3(20,20),T4(20,20),UP3(20),UP4(20)
815          REAL NU,KP,KPP
816      C
817      C      SPECIFY CONDITIONS OF OIL SHALE
818      C
819          RR=DIA/2.DO
820          DEN=2.ODO
821          KPP=1.25D-2/4.186DO
822      C
823      C      SPECIFY CONDITION OF GRID
824      C
825          N=10
826          DR=RR/9.DO
827          DD=H/9.DO
828          TT4=0.ODO
829          DTIME4(1)=0.ODO
830          UP4(1)=0.ODO
831      C
832      C      INITIALISE ALL R(I)
833      C
834          DO 40 I=1,N
835      40      R(I)=(I-1)*DR
836      C
837      C
838      C      INITIALISE ALL TEMPERATURES
839      C
840          DO 41 II=1,10
841      41      T4(II,1)=T3(II,10)
842      C
843      C

```

Listing of PROFILE at 11:37:26 on MAY 28, 1987 for CCId=TITA

```

844      C      WORK OUT THE VERTICAL DISTANCE
845      C
846      DO 42 I=1,11
847      42      DIS4(I)=DD*(I-1)
848      C
849      C
850      C      TO SET UP TRIDIAGONAL EQUATIONS TO SOLVE THE TEMPERATURE
851      C      HISTORY FOR A SINGLE PARTICLE
852      C
853      DO 43 J=2,11
854      C
855      C      TO WORK OUT THE VELOCITY OF PARTICLE AT EACH INTERVAL
856      C      OF THE FALLING REGION
857      C
857.3      IF (J .EQ. 11) GOTO 44
857.6      C
858      UP4(J)=((2.DO*980.DO*(DENS-DENG)/DENS/(EO**1.46DO))*
859      &      (H-DIS4(11-J)))*O.5DO
859.5      C
859.7      44      UP4(11)=UP3(1)
860      C
861      C
862      C      TO WORK OUT THE DELTA TIME
863      C
864      DTIME4(J)=DD/UP4(J)
865      TT4=TT4+DTIME4(J)
866      DT=DTIME4(J)
867      C
868      C
869      C      TO CALCULATE HP FOR THE OIL SHALE IN THE FALLING REGION
870      C
871      RV=DABS(U-UP4(J))
872      RE=DIA*RV*DENG/VIS
873      NU=O.42DO+O.35DO*(RE**O.8DO)
874      HP=NU*KP/2.DO/RR
875      ALPHA=KPP/PPP/DEN
876      JJ=J-1
877      HP4(JJ)=HP
878      BIOT4(JJ)=HP*RR/KPP
879      C
880      C      SET COEFFICIENTS OF MATRICS
881      C
882      C      BOUNDARY CONDITION AT R=0
883      C
884      B(1)=-((6.DO*ALPHA/(DR**2.DO))-((1.DO/DT)
885      C(1)=6.DO*ALPHA/(DR**2.DO)
886      C
887      C
888      C      BOUNDARY CONDITION AT R=N
889      C
890      A(N)=2.DO*ALPHA/(DR**2.DO)
891      B(N)=((-1.DO/DT)-(2.DO*ALPHA*HP/R(N)/KPP)-
892      &      (2.DO*ALPHA/(DR**2.DO)))-(2.DO*ALPHA*HP/DR/KPP)
893      C
894      C      INITIALISE ALL VALUES OF A(I),B(I),C(I)
895      C
896      DO 45 IK=2,9
897      A(IK)=(ALPHA/(DR**2.DO))-(ALPHA/R(IK)/DR)

```


Listing of PROFILE at 11:37:26 on MAY 28, 1987 for CCid=TITA

```

898          B(IK)=(-2.DO*ALPHA/(DR**2.DO))- (1.DO/DT)
899          C(IK)=(ALPHA/R(IK)/DR)+(ALPHA/(DR**2.DO))
900      45      CONTINUE
901      C
902          D(1)=-T4(1,J-1)/DT
903          DO 46 I=2,9
904              D(I)=-T4(I,J-1)/DT
905      46      CONTINUE
906      C
907      C
908          D(N)=- (T4(N,J-1)/DT)- (2.DO*ALPHA*HP*TG/R(N)/KPP)-
909      &  (2.DO*ALPHA*HP*TG/DR/KPP)
910      C
911      C      CALL LIBRARY PROGRAM TO SOLVE THE TRI-DIA EQUATIONS
912      C
913          CALL TRISLV(N,A,B,C,D,O,&99)
914      C
915      C      STORE THE SOLUTIONS T4(I,J)
916      C
917          DO 47 II=1,N
918              T4(II,J)=D(II)
919      47      CONTINUE
920      C
921      43      CONTINUE
922      C
923      C
924          GOTO 49
925      99      WRITE(6,48)
926      48      FORMAT(///2X,'ERROR MESSAGE')
927      C
928      49      RETURN
929      END
930      C
931      C
932      C
933      C *****
934      C *
935      C      SUBROUTINE TEMP5 *
936      C *
937      C *****
938      C
939      C
940          SUBROUTINE TEMP5(TG,DIA,DENG,KP,VIS,RR,DEN,CPP,KPP,HH,EA,ES,
941      &  ACOL,AS,UMF,HM,UP5,DIS5,T4,UP4,T5,DTIME5,R,TT5,HP5,BIOT5)
942      C
943          IMPLICIT REAL*8 (A-H,O-Z)
944          DIMENSION A(100), B(100), C(100), D(100)
945          DIMENSION BIOT5(20),DIS5(20),DTIME5(20),HP5(20),R(20)
946          DIMENSION T4(20,20),T5(20,20),UP4(20),UP5(20)
947          REAL NU, KP, KPP
948      C
949      C
950      C      SPECIFY CONDITIONS OF GRID
951      C
952          N=10
953          DR=RR/9.DO
954          TT5=0.000
955          DTIME5(1)=0.000

```

Listing of PROFILE at 11:37:26 on MAY 28, 1987 for CCid=TITA

```

956      C
957      C
958      C      INITIALISE ALL R(I)
959      C
960      DO 50 I=1,N
961      R(I)=(I-1)*DR
962      50    CONTINUE
963      C
964      C
965      C      INITIALISE ALL TEMPERATURE
966      C
967      DO 51 IK=1,10
968      T5(IK,1)=T4(IK,10)
969      51    CONTINUE
970      C
971      C      WORK OUT THE VERTICAL DISTANCE
972      C
973      C
974      C      TO SET UP TRIDIAGONAL EQUATIONS TO SOLVE THE TEMPERATURE
975      C      HISTORY FOR A SINGLE PARTICLE
976      C
977      DO 52 J=2,8
978      C
979      C      TO WORK OUT THE UA AT EACH INTERVAL
980      C
981      UP5(1)=UP4(10)
982      UA=UMF*(1.DO-((1.DO-(DIS5(J-1)/HM)**3.DO)))
983      QA=UA*(ACOL-AS)
984      RV=DABS(UA-UP5(J-1))
985      C
986      C
987      C      TO CALCULATE HP FOR THE OIL SHALE PARTICLE IN THE ANNULUS
988      C
989      RE=DIA*RV*DENG/VIS
990      NU=0.42DO+0.35DO*(RE**0.8DO)
991      HP=NU*KP/2.DO/RR
992      JJ=J-1
993      HP5(JJ)=HP
994      BIOT5(JJ)=HP*RR/KPP
995      C
996      ALPHA=KPP/CPP/DEN
997      C
998      C      TO WORK OUT DT
999      C
1000     IF (J.EQ. 8)GOTO 53
1001     DTIME5(J)=(DIS5(J-1)-DIS5(J))/UP5(J-1)
1002     TT5=TT5+DTIME5(J)
1003     DT=DTIME5(J)
1004     53    CONTINUE
1005     C
1006     C      TO SET COEFFICIENTS OF MATRICES
1007     C
1008     C      BOUNDARY CONDITION AT R=0
1009     C
1010     B(1)=- (6.DO*ALPHA/(DR**2.DO))- (1.DO/DT)
1011     C(1)=6.DO*ALPHA/(DR**2.DO)
1012     C
1013     C      BOUNDARY CONDION AT R=N

```

Listing of PROFILE at 11:37:26 on MAY 28, 1987 for CCId=TITA

```

1014      C
1015          A(N)=2.DO*ALPHA/(DR**2.DO)
1016          B(N)=(-1.DO/DT)-(2.DO*ALPHA*HP/R(N)/KPP)-
1017          & (2.DO*ALPHA/(DR**2.DO))-(2.DO*ALPHA*HP/DR/KPP)
1018      C
1019      C      INITIALISE ALL VALUES OF A(I), B(I), AND C(I)
1020      C
1021          DO 54 IK=2,9
1022              A(IK)=(ALPHA/(DR**2.DO))-(ALPHA/R(IK)/DR)
1023              B(IK)=(-2.DO*ALPHA/(DR**2.DO))-(1.DO/DT)
1024          54      C(IK)=(ALPHA/R(IK)/DR)+(ALPHA/(DR**2.DO))
1025      C
1026          D(1)=-T5(1,J-1)/DT
1027          DO 55 I=2,9
1028          55      D(I)=-T5(I,J-1)/DT
1029          D(N)=- (T5(N,J-1)/DT)-(2.DO*ALPHA*HP*TG/R(N)/KPP)-
1030          &      (2.DO*ALPHA*HP*TG/DR/KPP)
1031      C
1032      C
1033      C
1034      C      CALL LIBRARY PROGRAMM TO SOLVE THE TRI-DIA EQNS
1035      C
1036          CALL TRISLV(N,A,B,C,D,O,&99)
1037      C
1038          DO 56 II=1,N
1039          56      T5(II,J)=D(II)
1040          CONTINUE
1041      C
1042          52      CONTINUE
1043      C
1044          GOTO 58
1045          99      WRITE(6,57)
1046          57      FORMAT(///2X,'ERROR MESSAGE')
1047      C
1048          58      RETURN
1049      END

```

C.2 Entrance

Listing of ENTRANCE at 13:07:28 on JUN 11, 1987 for CCid=TITA

```

1      C *****
2      C
3      C      NAME: ENTRANCE
4      C
5      C      THIS PROGRAM IS USED TO ESTIMATE THE TEMPERATURE PROFILE
6      C      FOR A PARTICLE IN THE ENTRANCE SECTION OF THE SPOUTED BED
7      C
8      C *****
9
10     IMPLICIT REAL*8 (A-H,O-Z)
11     DIMENSION A(100),B(100),C(100)
12     DIMENSION D(100), DTIME(100), DIS(100)
13     DIMENSION R(100),T(100,100)
14     DIMENSION DP(3),VELT(3),TEMPG(3)
15     REAL KP,NU
16     C
17     C
18     C      READ DATA
19     C
20     DATA DP/0.3000,0.1500,0.0750/
21     DATA VELT/567.966600, 784.35800,355.0200/
22     DATA TEMPG/723.000,773.000,823.000/
23     C
24     C      TO WORK OUT THE TEMP PROFILE FOR TWO DIFFERENT GAS TEMPERATURE
25     C
26     DO 777 JJ=1,3
27
28     C
29     C
30     C      SPECIFY CONDITIONS OF SPOUTING GAS
31     C
32     TG=TEMPG(JJ)
33     KP=0.000150800
34     DENG=1.00*(28.00*0.8500 +44.00*0.1500)/82.0500/TG
35     VIS=0.0003300
36     CP=(6.7600+((0.6060-3)*TG)+((0.130-6)*(TG**2.00)))/28.00
37     C
38     C
39     C      CONDITION OF SAND PARTICLE
40     C
41     DPS=0.1121100
42     RRS=DPS/2.00
43     DENS=2.6800
44     C
45     C
46     C      DATA ON THE REACTOR
47     C
48     DI=1.5800
49     DC=12.800
50     HC=76.200
51     ACOL=3.141600*(DC**2.00)/4.00
52     HH=33.000
53     C
54     C
55     C      DATA ON THE ENTRANCE REGION
56     C
57     DPIPE=1.5800
58     HPIPE=17.800

```

Listing of ENTRANCE at 13:07:28 on JUN 11, 1987 for CCid=TITA

```

59      APIPE=3.1416DO*(DPIPE**2.DO)/4.DO
60      C
61      C      USE DO-LOOP TO ESTIMATE THE TEMPERATURE PROFILE
62      C      FOR 3 DIFFERENT SIZES
63      C
64      DO 999 M=1,3
65      DIA=DP(M)
66      UT=VELT(M)
67      C
68      C
69      C      WRITE TITLE
70      C
71      WRITE(6,101)DP(M)
72      101  FORMAT(1H1,'IN THE ENTRANCE REGION FOR SIZE =',2X,F6.4,'CM')
73      WRITE(6,111)TG
74      111  FORMAT(//,1X,'THE TEMPERATURE OF THE GAS IS ',F6.1,' DEG K')
75      C
76      C
77      C      SPECIFY CONDITIONS OF OIL SHALE PARTICLE
78      C
79      RR=DIA/2.DO
80      DEN=2.0DO
81      E=0.4DO
82      KPP=1.25D-2/4.186DO
83      CPP=1.13DO/4.186DO
84      C
85      C
86      C      TO WORK OUT HM BASED ON SAND PROPERTIES
87      C
88      GEMA=1.
89      HM=0.105DO*((DC/DPS)**0.75DO)*((DC/DI)**0.4DO)*DC/(DENS**1.2DO)
90      WRITE(6,41)HM
91      41  FORMAT(//,'HM=',F8.4,'CM')
92      C
93      C      TO CALCULATE THE MINIMUM SPOUTING VELOCITY USING
94      C      MARTHER GISHLER MODEL
95      C
96      UMS=(DPS/DC)*((DI/DC)**(1.DO/3.DO))*((2.DO*980.DO*HH*
97      &      (DENS-DENG)/DENG)**(1.DO/2.DO))
98      U=1.1DO*UMS
99      Q=U*ACOL
100     VEL=Q/APIPE
101     V=VEL-UT
102     RV=VEL-V
103     C
104     C
105     C      TO CALCULATE HP FOR OIL SHALE PARTICLE
106     C
107     RE=DIA*RV*DENG/VIS
108     PR=CP*VIS/KP
109     AA=2.DO/((1.DO-E)**(1.DO/3.DO))
110     BB=2.DO*E/3.DO
111     C
112     C      IN THE ENTRANCE REGION
113     C
114     NU=2.DO+0.6DO*(RE**0.5DO)*(PR**(1.DO/3.DO))
115     HP=NU*KP/2.DO/RR
116     ALPHA=KPP/CP/DEN

```

Listing of ENTRANCE at 13:07:28 on JUN 11, 1987 for CCid=TITA

```

117 C
118 C
119 C SPECIFY CONDITIONS OF GRID
120 C
121 C N=10
122 C DR=RR/9.DO
123 C DT=HPIPE/9.DO/V
124 C
125 C
126 C SET ALL DELTA TIME
127 C
128 C DO 4 I=1,N
129 4 DTIME(I)=DT*(I-1)
130 C
131 C
132 C INITIALISE ALL R(I)
133 C
134 C DO 5 I=1,N
135 5 R(I)=(I-1)*DR
136 C
137 C
138 C INITIALISE ALL TEMPERATURES
139 C
140 C DO 10 I=1,N
141 10 T(I,1)=298.DO
142 C
143 C
144 C WORK OUT THE VERTICAL DISTANCE
145 C
146 C DO 6 I=1,N
147 6 DIS(I)=V*DTIME(I)
148 C
149 C
150 C TO SET UP TRIDIAGONAL EQUATIONS TO SOLVE THE
151 C TEMPERATURE HISTORY FOR A SINGLE PARTICLE
152 C
153 C DO 30 J=2,11
154 C
155 C
156 C SET COEFFICIENTS OF MATRICS
157 C
158 C BOUNDARY CONDITION AT R=0
159 C
160 C B(1)=- (6.DO*ALPHA/(DR**2.DO))-(1.DO/DT)
161 C C(1)=6.DO*ALPHA/(DR**2.DO)
162 C
163 C BOUNDARY CONDITION AT R=N
164 C
165 C A(N)=2.DO*ALPHA/(DR**2.DO)
166 C B(N)=(-1.DO/DT)-(2.DO*ALPHA*HP/R(N)/KP)-
167 > (2.DO*ALPHA/(DR**2.DO))-(2.DO*ALPHA*HP/DR/KP)
168 C
169 C
170 C INITIALISE ALL VALUES OF A(I), B(I) AND C(I)
171 C
172 C DO 20 IK=2,9
173 C A(IK)=(ALPHA/(DR**2.DO))-(ALPHA/R(IK)/DR)
174 C B(IK)=(-2.DO*ALPHA/(DR**2.DO))-(1.DO/DT)

```

Listing of ENTRANCE at 13:07:28 on JUN 11, 1987 for CCid=TITA

```

175      20      C(IK)=(ALPHA/R(IK)/DR)+(ALPHA/(DR**2.DO))
176      C
177          D(1)=-T(1,J-1)/DT
178          DO 40 I=2,9
179      40      D(I)=-T(I,J-1)/DT
180          D(N)=-T(N,J-1)/DT-(2.DO*ALPHA*HP*TG/R(N)/KP)-
181      >      (2.DO*ALPHA*HP*TG/DR/KP)
182      C
183      C
184      C      CALL LIBRARY PROGRAM TO SOLVE THE TRI-DIA EQNS
185      C
186          CALL TRISLV(N,A,B,C,D,O,899)
187      C
188      C
189      C      STORE THE SOLUTIONS T(I,J)
190      C
191          DO 50 II=1,N
192          T(II,J)=D(II)
193      50      CONTINUE
194      C
195      30      CONTINUE
196      C      GO TO 500
197      C
198      99      WRITE(6,103)
199      103      FORMAT(//,'SOLUTIONS ARE')
200      500      CONTINUE
201      C
202      C
203      C      WRITE OUT THE SOLUTIONS OF T(I,J)
204      C
205          WRITE(6,301)
206      301      FORMAT(//'SEC',20X,'TEMPERATURE DEG K',28X,' CM ')
207      C
208          DO 200 KK=1,10
209          J=11-KK
210          WRITE(6,300)DTIME(J),(T(I,J),I=1,10),DIS(J)
211      300      FORMAT(//1X,F5.4,2X,10F6.1,2X,F6.3)
212      C
213      200      CONTINUE
214      C
215      C
216      C      WRITE OUT THE DELTA RADIUS FOR THE PARTICLE AT BOTTOM LINE
217      C
218          WRITE(6,400)(R(I),I=1,10)
219      400      FORMAT(//8X,10F6.3)
220      C
221      C
222      999      CONTINUE
223      C
224      777      CONTINUE
225          STOP
226          END

```


C.3 Calculate

Listing of CALCULATE at 14:22:12 on MAY 28, 1987 for CCid=TITA

```

1  C *****
2  C
3  C   NAME OF THIS PROGRAM: CALCULATE
4  C
5  C   THIS PROGRAM IS USED TO CALCULATE THE DATA FOR ANALYSIS
6  C   SECTION 1: TO CALCULATE OIL YIELD
7  C   SECTION 2: TO CALCULATE SPENT SHALE YIELD
8  C   SECTION 3: TO CALCULATE TOTAL GAS AND INDIVIDUAL GAS YIELDS
9  C *****
10 C
11 C
12 C   REAL NF
13 C
14 C   READ DATA
15 C
16 C   SN=5.37!
17 C   CF=1801.5/80./60.
18 C   FEED=
19 C   WRITE(6,8)CF
20 C   8   FORMAT(2X,'CF=',F7.4)
21 C   CFMA=CF
22 C   SG=0.158
23 C   WRITE(6,333)CF
24 C   333  FORMAT(2X,'CF',F7.4)
25 C
26 C *****
27 C
28 C   SECTION 1: TO CALCULATE OIL YIELD
29 C
30 C *****
31 C
32 C
33 C   OYIELD=(OIL/FEED)*100.0
34 C   WRITE(6,11)OYIELD
35 C   11   FORMAT(/,'OIL YIELD=',F10.5)
36 C
37 C
38 C *****
39 C
40 C   SECTION 2: TO CALCULATE SPENT SHALE YIELD
41 C
42 C *****
43 C
44 C   SYIELD=(SPENT/FEED)*100.0
45 C   WRITE(6,22)SYIELD
46 C   22   FORMAT(/,'SPENT SHALE YIELD=',F10.5)
47 C
48 C
49 C *****
50 C
51 C   SECTION 3: TO CALCULATE TOTAL GAS AND INDIVIDUAL GAS YIELDS
52 C
53 C *****
54 C
55 C   READ VOLUME PERCENTAGE OF INDIVIDUAL FROM GAS CHROMOTOGRAPH
56 C
57 C   VH2=0.03324
58 C   VCO2=15.2390

```

Listing of CALCULATE at 14:22:12 on MAY 28, 1987 for CCId=TITA

```

59      V02=0.0000
60      VN2=84.727
61      VCH4=0.00
62      VCO=0.0
63      C
64      C
65      WRITE(6,1)
66      1  FORMAT(1H1,21X,'H2',7X,'CO2',7X,'O2',8X,'N2',8X,'CH4',
67      & 8X,'CO')
68      WRITE(6,2)VH2,VCO2,V02,VN2,VCH4,VCO
69      2  FORMAT(/,2X,'VOL %',12X,6(F7.4,3X))
70      C
71      C  TO CORRECT FOR AIR LEAKED INTO THE SYSTEM
72      C
73      AIR=V02+(V02*(0.79/0.21))
74      COR=100./(100.-AIR)
75      C
76      CVH=VH2*COR
77      CVC02=VCO2*COR
78      CVN2=(VN2-(V02*(0.79/0.21)))*COR
79      CVCH4=VCH4*COR
80      CVCO=VCO*COR
81      C
82      C  TO WRITE THE CORRECTED VOLUME PERCENTAGE OF INDIVIDUAL GAS
83      C
84      WRITE(6,10)CVH,CVC02,CVN2,CVCH4,CVCO
85      10  FORMAT(/,2X,'CORRECTED VOL %',2X,2(F7.4,3X),10X,3(F7.4,3X))
86      C
87      C  TO CALCULATE WEIGHT PERCENTAGE FOR INDIVIDUAL GAS
88      C
89      WH2=(2./82.07/293.)*CVH
90      WCO2=(44./82.07/293.)*CVC02
91      WN2=(28./82.07/293.)*CVN2
92      WCH4=(16./82.07/293.)*CVCH4
93      WCO=(28./82.07/293.)*CVCO
94      TW=WH2+WCO2+WN2+WCH4+WCO
95      C
96      C
97      HF=100.*WH2/TW
98      CO2F=100.*WCO2/TW
99      NF=100.*WN2/TW
100     CH4F=100.*WCH4/TW
101     COF=100.*WCO/TW
102     C
103     C  TO WRITE THE WEIGHT PERCENTAGE OF INDIVIDUAL GAS
104     C
105     WRITE(6,20)HF,CO2F,NF,CH4F,COF
106     20  FORMAT(/,2X,'WEIGHT %',9X,2(F7.4,3X),10X,3(F7.4,3X))
107     WRITE(6,30)TW
108     30  FORMAT(/,2X,'TW=',F10.4)
109     C
110     C  WEIGHT FRACTION OF NITROGEN
111     C
112     NF=(WN2+WCO2)/TW
113     WRITE(6,7)NF
114     7  FORMAT(2X,F10.5)
115     TG=SN/NF
116     C

```

Listing of CALCULATE at 14:22:12 on MAY 28, 1987 for CCid=TITA

```

117 C
118 C   GAS PRODUCED DUE TO PYROLYSIS
119 C
120     PGAS=TG-SN
121     WRITE (6,11)TG,PGAS
122 11   FORMAT(2X,F10.5,5X,F10.5)
123 C
124 C   GAS YIELD
125 C
126     YIELD=100.*(TG-SN)/CFMA
127 C
128     WRITE(6,21)YIELD
129 21   FORMAT(2X,'TOTAL YIELD OF GAS=',F7.4)
130 C
131 C   INDIVIDUAL GAS YIELD
132 C
133     YH=(TG/FEED)*(WH2/TW)*100.
134     YCH4=(TG/FEED)*(WCH4/TW)*100.
135     YCO=(TG/FEED)*(WCO/TW)*100.
136 C
137 C
138 C   WRITE THE YIELD OF INDIVIDUAL GAS
139 C
140     WRITE(6,31)YH,YCH4,YCO
141 31   FORMAT(/,2X,'YIELD %',11X,F7.4,32X,2(F7.4))
142 C
143 C
144     RETURN
145     END

```

C.4 Model

Listing of MODEL at 12:26:52 on MAY 28, 1987 for CCid=TITA

```

1      C *****
2      C
3      C   NAME OF THIS PROGRAM: MODEL
4      C
5      C   THIS PROGRAM USES UBC LIBRARY PROGRAM NL2SNO TO SOLVE FOR
6      C   THE PARAMETERS K3 & E3, INORDER TO OBTAIN THE RATE CONSTANT
7      C   FOR THE OIL TO GASES REACTION.
8      C   THE OTHER PARAMETERS K1, K2, E1, E2, FRACT1, FRACT2, AND
9      C   KO ARE TAKEN FROM THE LITERATURES.
10     C *****
11     C
12     C
13     C
14     C   IMPLICIT REAL*8 (A-H,K,O-Z)
15     C   INTEGER I,L,N,KK
16     C   COMMON/BLKA/FO(10),F1(10),F2(10),W(10),TEMP(10),SIZE(10),
17     C   & FEED(10),AEXPT(10),ACAL(10),MUM(10)
18     C   DIMENSION P(6), IV(66),V(5000), R(10)
19     C   EXTERNAL CALCR
20     C
21     C   READ IN DATA
22     C
23     C   DO 1100 MM=1,6
24     C     READ(5,551)MUM(MM),FO(MM),F1(MM),F2(MM),W(MM),TEMP(MM),
25     C   & SIZE(MM),FEED(MM),AEXPT(MM)
26     C   551  FORMAT(I4,1X,F6.4,1X,F6.4,1X,F5.3,1X,F6.1,1X,F5.1,1X,F4.2,
27     C   & 1X,F6.1,1X,F6.2)
28     C     WRITE(6,66)TEMP(MM),AEXPT(MM),FO(MM),F1(MM)
29     C   66   FORMAT(1X,F10.4,2X,F10.4,2X,F10.4,2X,F10.4)
30     C   1100 CONTINUE
31     C
32     C   TO DEFINE THE N, M, P, IV AND V
33     C
34     C     N=6
35     C     M=2
36     C     P(1)=1.7D14
37     C     P(2)=2.D5
38     C     CALL DFALT (IV,V)
39     C     V(42)=1.0D-25
40     C     IV(17)=1000
41     C     IV(18)=1000
42     C
43     C   WRITE INITIAL GUESS VALUES
44     C
45     C     WRITE(6,666) (P(I), I=1,2)
46     C   666  FORMAT('INITIAL GUESS=',1P2G16.8)
47     C
48     C   TO CALL FOR LIBRARY PROGRAM NL2SNO
49     C
50     C     CALL NL2SNO(N,M,P,CALCR,IV,V,IPARM,RPARM,FPARM)
51     C
52     C     WRITE(6,120) IV(1)
53     C   120  FORMAT('RETURN CODE =', I10)
54     C     WRITE(6,140) (P(I), I=1,2)
55     C   140  FORMAT('SOLUTION:', 1P2G16.8)
56     C
57     C     EE=2.718281728DO
58     C     RR=8.314DO

```

Listing of MODEL at 12:26:52 on MAY 28, 1987 for CCid=TITA

```

59      K1=14.4DO
60      K2=2.025D10
61      E1=44560.DO
62      E2=177580.DO
63      T=4800.DO
64
65      C
66      C      TO CALCULATE THE PREDICTED OIL YIELD VALUE BASED ON
67      C      K3 AND E3 VALUES OBTAINED FROM THE NL2SNO PROGRAM
68      C
69      DO 22 I=1,N
70          TEMPA=TEMP(I)+273.DO
71          T=4800.DO
72          KC1=K1*EE**(-(E1/(RR*TEMPA)))
73          KC2=K2*EE**(-(E2/(RR*TEMPA)))
74          KC3=P(1)*EE**(-(P(2)/(RR*TEMPA)))
75          WF=(13.DO*454.DO)+(W(I)/2.DO)
76          FRACT2=0.62DO/0.9DO
77          A=F0(I)*0.11DO/WF
78          B=KC1+(F1(I)/WF)+(F2(I)/WF)
79          C=0.9DO*KC1
80          D=(F1(I)/WF)+(F2(I)/WF)+KC2
81          C11=1.DO/B/D
82          C12=1.DO/((D**2)-(B*D))
83          C13=1.DO/((B**2)-(B*D))
84          CB=C*A*(C11+(C12*(EE**(-D*T)))+(C13*(EE**(-B*T))))
85          VOL=0.0322DO*1.3DO
86          FN=0.000472DO*TEMPA/293.DO
87          TT=VOL/FN
88          PP=KC2*FRACT2*CB*WF/VOL
89          Q=(FN/VOL)+KC3
90          CA=(PP/Q)*(1.DO-(DEXP(-Q*TT)))
91          OIL=(FN*PP/Q)*((T+((DEXP(-Q*T))/Q))-(1.DO/Q))
92          ACAL(I)=OIL
93      22  CONTINUE
94      C
95      C      WRITE THE FINAL RESULTS
96      C
97          WRITE(6,1111)
98      1111  FORMAT(10X,'TEMP',9X,'TIME',5X,'OIL CALCULATED',8X,'OIL EXPT')
99      C
100      DO 40 KK=1,N
101          WRITE(6,515)TEMP(KK),T,ACAL(KK),AEXPT(KK)
102      515  FORMAT(5X,F10.4,4X,F10.4,4X,F10.4,8X,F10.4)
103      40  CONTINUE
104      C
105          STOP
106          END
107
108
109      C *****
110      C      *
111      C      SUBROUTINE: CALCR  *
112      C      *
113      C      *****
114      C
115      C
116      SUBROUTINE CALCR(N,M,P,NF,R,IPARM,RPARM,FPARM)

```

Listing of MODEL at 12:26:52 on MAY 28, 1987 for CCid=TITA

```

117      C
118          IMPLICIT REAL*8 (A-H,K,O-Z)
119          DIMENSION P(M), R(N)
120          COMMON /BLKA/ FO(10),F1(10),F2(10),W(10),TEMP(10),SIZE(10),
121      &          FEED(10),AEXPT(10),ACAL(10),MUM(10)
122      C
123      C
124          EE=2.718281728DO
125          RR=8.314DO
126          K1=14.4DO
127          K2=2.025D10
128          E1=44560.DO
129          E2=177580.DO
130          T=4800.DO
131
132      C
133      C      TO CALCULATE PREDICTED CK,CB AND CA VALUES BASED ON GUESSED
134      C      K3 AND E3
135      C
136          DO 20 I=1,N
137              TEMPA=TEMP(I)+273.DO
138              T=4800.DO
139              KC1=K1*EE**(-(E1/(RR*TEMPA)))
140              KC2=K2*EE**(-(E2/(RR*TEMPA)))
141              KC3=P(1)*EE**(-(P(2)/(RR*TEMPA)))
142              WF=(13.DO*454.DO)+(W(I)/2.DO)
143              FRACT2=0.62DO/0.9DO
144              A=FO(I)*0.11DO/WF
145              B=KC1+(F1(I)/WF)+(F2(I)/WF)
146              C=0.9DO*KC1
147              D=(F1(I)/WF)+(F2(I)/WF)+KC2
148              C11=1.DO/B/D
149              C12=1.DO/((D**2)-(B*D))
150              C13=1.DO/((B**2)-(B*D))
151              CB=C*A*(C11+(C12*(EE**(-D*T)))+(C13*(EE**(-B*T))))
152              VOL=0.0322DO*1.3DO
153              FN=0.000472DO*TEMPA/293.DO
154              TT=VOL/FN
155              PP=KC2*FRACT2*CB*WF/VOL
156              Q=(FN/VOL)+KC3
157              CA=(PP/Q)*(1.DO-(DEXP(-Q*TT)))
158              OIL=(FN*PP/Q)*((T+((DEXP(-Q*T))/Q))-(1.DO/Q))
159              ACAL(I)=OIL
160      C
161      C      TO CALCULATE THE DIFFERENCE BETWEEN EXPERIMENTAL AND PREDICTED
162      C      OIL YIELD VALUE
163      C
164          R(I)=ACAL(I)-AEXPT(I)
165      C
166      20  CONTINUE
167          RETURN
168      C
169          END
170

```


C.5 Jac

Listing of JAC at 12:27:06 on MAY 28, 1987 for CCId=TITA

```

1      C *****
2      C
3      C   NAME OF THIS PROGRAM: JAC
4      C
5      C   THIS PROGRAM USES UBC LIBRARY PROGRAM JACOBIAN TO SOLVE
6      C   FOR THE SET OF DIFFERENTIAL EQUATIONS TO CALCULATE KEROGEN,
7      C   BITUMEN, AND OIL AS A FUNCTION OF TIME AT A GIVEN SET OF
8      C   OPERATING CONDITIONS.
9      C
10     C   dW/dt = YDOT(1)
11     C   dCK/dt = YDOT(2)
12     C   dCB/dt = YDOT(3)
13     C   dCA/dt = YDOT(4)
14     C
15     C *****
16     C
17
18     IMPLICIT REAL*8 (A-H,K,O-Z)
19     EXTERNAL FUNC,PD
20     COMMON/BLKA/FO(10),F1(10),F2(10),WW(10),TEMP(10),SIZE(10),
21     & FEED(10),AEXPT(10),ACAL(10),MUM(10),WF(10),WT
22     COMMON/BLKB/KC1,KC2,KC3,FRACT1,FRACT2,FN,V,I
23     COMMON/GEAR9/HUSED,NQUSED,NSTEP,NFE,NJE
24     DIMENSION YO(112),A(10)
25
26     C
27     C   READ IN DATA, MM=NO OF DATA READ IN
28     C
29     MM=3
30     DO 110 M=1,MM
31     READ(5,55)MUM(M),FO(M),F1(M),F2(M),WW(M),TEMP(M),SIZE(M),
32     & FEED(M),AEXPT(M)
33     55   FORMAT(I4,1X,F6.4,1X,F6.4,1X,F5.3,1X,F6.1,1X,F5.1,1X,F4.2,
34     & 1X,F6.1,1X,F6.2)
35     WRITE(6,11)AEXPT(M),TEMP(M),F1(M),WW(M)
36     11   FORMAT(2X,4(F10.4,2X))
37     110  CONTINUE
38     C
39     C   DEFINE ALL PARAMETERS AND BASIC INFORMATION
40     C
41     DO 1001 I=1,MM
42     EE=2.718281728DO
43     K1=10.4DO
44     K2=2.285D10
45     K3=1.7D14
46     E1=44560.DO
47     E2=177580.DO
48     E3=244319.45
49     FRACT1=0.9
50     FRACT2=0.62DO/FRACT1
51     WF(I)=(13.DO*454.DO)+(WW(I)/2.DO)
52     WT=WF(I)
53     V=0.0322DO*1.3DO
54     RR=8.314DO
55     C
56     C
57     TEMPA=TEMP(I)+273.DO
58     KC1=K1*DEXP(-(E1/(RR*TEMPA)))

```

Listing of JAC at 12:27:06 on MAY 28, 1987 for CCid=TITA

```

59      KC2=K2*DEXP(-(E2/(RR*TEMPA)))
60      KC3=K3*DEXP(-(E3/(RR*TEMPA)))
61      FN=0.000472DO*TEMPA/293.DO
62
63      C
64      WRITE(6,66)KC1,KC2,KC3
65      66      FORMAT(//,'KC1=',F10.8,3X,'KC2=',F10.8,3X,'KC3=',F10.8)
66
67      C
68      C      SET VALUES FOR THE LIBRARY PROGRAM GEAR
69      C
70      N=4
71      HO=1.D-7
72      EPS=1.D-4
73      METH=2
74      MITER=2
75      MF=10*METH+MITER
76      ML=3
77      MU=3
78      TOUT=100.DO
79      INDEX=1
80      C
81      TO=0.DO
82      YO(1)=13.DO
83      C
84      C      INITIALISE THE VALUES OF YO AT TIME=0
85      C
86      DO 5 J=2,4
87      5      YO(J)=0.000
88      C
89      C      WRITE TITLE
90      C
91      WRITE(6,41)
92      41      FORMAT(5X,'TIME',8X,'W',12X,'CK',12X,'CB',12X,'CA')
93      C
94      C      CALL GEARB TO SOLVE PROBLEM
95      C
96
97      10      CALL GEARB(N,TO,HO,YO,TOUT,EPS,MF,INDEX,ML,MU,FUNC,PD,6)
98      C
99      WRITE(6,20)TOUT,WT,YO(2),YO(3),YO(4)
100     20      FORMAT(2X,F8.2,4(3X,F10.5))
101
102     IF(INDEX .EQ. 0)GOTO 40
103     WRITE(6,30)INDEX
104     30      FORMAT(//26X,'ERROR RETURN WITH INDEX =',I3)
105     GOTO 50
106     40      TOUT=TOUT+400.DO
107     IF(TOUT .GE. 4900.DO)GOTO 50
108     GOTO 10
109     50      WRITE(6,60)NSTEP
110     60      FORMAT(//21X,'PROBLEM COMPLETED IN',I5,'STEPS')
111     C
112     C      CALCULATE OIL AT THE FINAL TIME
113     C
114     WRITE(6,69)YO(3),YO(1)
115     69      FORMAT(2(F10.5,2X))
116     C

```

Listing of JAC at 12:27:06 on MAY 28, 1987 for CCid=TITA

```

117      X=4800.DO
118      P=FRACT2*KC2*YO(3)*WT/V
119      Q=(FN/V)+KC3
120      OIL=(FN*P/Q)*((X+((DEXP(-Q*X))/Q))-(1.DO/Q))
121      ACAL(I)=OIL
122      WRITE(6,44)OIL
123      44  FORMAT('OIL =', F10.4)
124      C
125      1001 CONTINUE
126      DO 1 II=1,MM
127      WRITE(6,1111)TEMP(II),ACAL(II)
128      1111 FORMAT(//,F6.2,2X,F7.2)
129      1  CONTINUE
130      STOP
131      END
132
133
134      C *****
135      C *
136      C   SUBROUTINE FUNC *
137      C *
138      C *****
139
140      SUBROUTINE FUNC(N,T,Y,YDOT)
141      IMPLICIT REAL*8 (A-H,K,O-Z)
142      DIMENSION Y(4),YDOT(4)
143      COMMON/BLKA/FO(10),F1(10),F2(10),W(10),TEMP(10),SIZE(10),
144      & FEED(10),AEXPT(10),ACAL(10),MUM(10),WF(10),WT
145      COMMON/BLKB/KC1,KC2,KC3,FRACT1,FRACT2,FN,V,I
146      C
147      C
148      YDOT(1)=FO(I)-F1(I)-F2(I)
149      YDOT(2)=(FO(I)*O.11DO/WT)-(((FO(I)/WT)+KC1)*Y(2))
150      YDOT(3)=(FRACT1*KC1*Y(2))-(((FO(I)/WT)+KC2)*Y(3))
151      YDOT(4)=(FRACT2*KC2*Y(3)*WT/V)-(((FN/V)+KC3)*Y(4))
152      RETURN
153      END
154
155
156      C *****
157      C *
158      C   DUMMY SUBROUTINE PD *
159      C *
160      C *****
161
162      SUBROUTINE PD(N,T,Y,P,NDIMPD,ML,MU)
163      IMPLICIT REAL*8 (A-H,K,O-Z)
164      DIMENSION Y(N),P(NDIMPD,N)
165      RETURN
166      END

```

C.6 Jac (Printout)

Increasing KC1

KC1= 5 x KC1 KC2=0.00337898 KC3=0.00037883

TIME	W	CK	CB	CA
100.00	6051.00000	0.00021	0.00038	2.77130
500.00	6051.00000	0.00022	0.00145	16.72927
900.00	6051.00000	0.00022	0.00173	20.44090
1300.00	6051.00000	0.00022	0.00179	21.37767
1700.00	6051.00000	0.00022	0.00181	21.61381
2100.00	6051.00000	0.00022	0.00182	21.67278
2500.00	6051.00000	0.00022	0.00182	21.68747
2900.00	6051.00000	0.00022	0.00182	21.69148
3300.00	6051.00000	0.00022	0.00182	21.69184
3700.00	6051.00000	0.00022	0.00182	21.69180
4100.00	6051.00000	0.00022	0.00182	21.69219
4500.00	6051.00000	0.00022	0.00182	21.69247

KC1=10 x KC1 KC2=0.00337898 KC3=0.00037883

TIME	W	CK	CB	CA
100.00	6051.00000	0.00011	0.00046	3.49169
500.00	6051.00000	0.00011	0.00148	17.03408
900.00	6051.00000	0.00011	0.00173	20.53415
1300.00	6051.00000	0.00011	0.00180	21.41725
1700.00	6051.00000	0.00011	0.00181	21.63994
2100.00	6051.00000	0.00011	0.00182	21.69574
2500.00	6051.00000	0.00011	0.00182	21.70991
2900.00	6051.00000	0.00011	0.00182	21.71281
3300.00	6051.00000	0.00011	0.00182	21.71394
3700.00	6051.00000	0.00011	0.00182	21.71461
4100.00	6051.00000	0.00011	0.00182	21.71447
4500.00	6051.00000	0.00011	0.00182	21.71394

KC1= 50 x KC1 KC2=0.00337898 KC3=0.00037883

TIME	W	CK	CB	CA
100.00	6051.00000	0.00002	0.00052	4.19059
500.00	6051.00000	0.00002	0.00149	17.25547
900.00	6051.00000	0.00002	0.00174	20.60514
1300.00	6051.00000	0.00002	0.00180	21.44784
1700.00	6051.00000	0.00002	0.00182	21.66002
2100.00	6051.00000	0.00002	0.00182	21.71425
2500.00	6051.00000	0.00002	0.00182	21.72718
2900.00	6051.00000	0.00002	0.00182	21.73055
3300.00	6051.00000	0.00002	0.00182	21.73167
3700.00	6051.00000	0.00002	0.00182	21.73151
4100.00	6051.00000	0.00002	0.00182	21.73124
4500.00	6051.00000	0.00002	0.00182	21.73124

KC1= 100 x KC1 KC2=0.00337898 KC3=0.00037883

TIME	W	CK	CB	CA
100.00	6051.00000	0.00001	0.00052	4.27888
500.00	6051.00000	0.00001	0.00149	17.28228
900.00	6051.00000	0.00001	0.00174	20.61495
1300.00	6051.00000	0.00001	0.00180	21.45220
1700.00	6051.00000	0.00001	0.00182	21.66309
2100.00	6051.00000	0.00001	0.00182	21.71656
2500.00	6051.00000	0.00001	0.00182	21.72962
2900.00	6051.00000	0.00001	0.00182	21.73265
3300.00	6051.00000	0.00001	0.00182	21.73393
3700.00	6051.00000	0.00001	0.00182	21.73416
4100.00	6051.00000	0.00001	0.00182	21.73372
4500.00	6051.00000	0.00001	0.00182	21.73339

Increasing KC2

KC1=0.01689492 KC2= 5 X KC2 KC3=0.00037883

TIME	W	CK	CB	CA
100.00	6051.00000	0.00052	0.00010	3.40206
500.00	6051.00000	0.00105	0.00034	19.95759
900.00	6051.00000	0.00110	0.00036	21.69000
1300.00	6051.00000	0.00110	0.00037	21.82659
1700.00	6051.00000	0.00110	0.00037	21.83867
2100.00	6051.00000	0.00110	0.00037	21.83761
2500.00	6051.00000	0.00110	0.00037	21.83987
2900.00	6051.00000	0.00110	0.00037	21.83983
3300.00	6051.00000	0.00110	0.00037	21.84067
3700.00	6051.00000	0.00110	0.00037	21.84042
4100.00	6051.00000	0.00110	0.00037	21.83975
4500.00	6051.00000	0.00110	0.00037	21.83986

KC1=0.03378984 KC2= 10 X KC2 KC3=0.00037883

TIME	W	CK	CB	CA
100.00	6051.00000	0.00052	0.00007	4.87035
500.00	6051.00000	0.00105	0.00017	20.42427
900.00	6051.00000	0.00110	0.00018	21.76849
1300.00	6051.00000	0.00110	0.00018	21.87208
1700.00	6051.00000	0.00110	0.00018	21.88049
2100.00	6051.00000	0.00110	0.00018	21.88077
2500.00	6051.00000	0.00110	0.00018	21.88094
2900.00	6051.00000	0.00110	0.00018	21.88112
3300.00	6051.00000	0.00110	0.00018	21.88088
3700.00	6051.00000	0.00110	0.00018	21.88068
4100.00	6051.00000	0.00110	0.00018	21.88069
4500.00	6051.00000	0.00110	0.00018	21.88081

KC1=0.16894918 KC2= 50 X KC2 KC3=0.00037883

TIME	W	CK	CB	CA
100.00	6051.00000	0.00052	0.00002	6.78531
500.00	6051.00000	0.00105	0.00004	20.68129
900.00	6051.00000	0.00110	0.00004	21.81870
1300.00	6051.00000	0.00110	0.00004	21.90688
1700.00	6051.00000	0.00110	0.00004	21.91321
2100.00	6051.00000	0.00110	0.00004	21.91394
2500.00	6051.00000	0.00110	0.00004	21.91418
2900.00	6051.00000	0.00110	0.00004	21.91357
3300.00	6051.00000	0.00110	0.00004	21.91348
3700.00	6051.00000	0.00110	0.00004	21.91379
4100.00	6051.00000	0.00110	0.00004	21.91378
4500.00	6051.00000	0.00110	0.00004	21.91366

KC1=0.33789836 KC2= 100 X KC2 KC3=0.00037883

TIME	W	CK	CB	CA
100.00	6051.00000	0.00052	0.00001	7.04378
500.00	6051.00000	0.00105	0.00002	20.70764
900.00	6051.00000	0.00110	0.00002	21.82087
1300.00	6051.00000	0.00110	0.00002	21.90879
1700.00	6051.00000	0.00110	0.00002	21.91601
2100.00	6051.00000	0.00110	0.00002	21.91758
2500.00	6051.00000	0.00110	0.00002	21.91746
2900.00	6051.00000	0.00110	0.00002	21.91720
3300.00	6051.00000	0.00110	0.00002	21.91753
3700.00	6051.00000	0.00110	0.00002	21.91772
4100.00	6051.00000	0.00110	0.00002	21.91764
4500.00	6051.00000	0.00110	0.00002	21.91760

Increasing KC3

KC1=0.00337898		KC2=0.00189415		KC3= 5 X KC3	
TIME	W	CK	CB	CA	
100.00	6051.00000	0.00052	0.00014	0.92593	
500.00	6051.00000	0.00105	0.00119	12.67593	
900.00	6051.00000	0.00110	0.00163	18.23956	
1300.00	6051.00000	0.00110	0.00176	19.84550	
1700.00	6051.00000	0.00110	0.00179	20.28006	
2100.00	6051.00000	0.00110	0.00180	20.38640	
2500.00	6051.00000	0.00110	0.00180	20.41554	
2900.00	6051.00000	0.00110	0.00180	20.42144	
3300.00	6051.00000	0.00110	0.00180	20.42108	
3700.00	6051.00000	0.00110	0.00180	20.42134	
4100.00	6051.00000	0.00110	0.00180	20.42187	
4500.00	6051.00000	0.00110	0.00180	20.42171	

KC1=0.00337898		KC2=0.00378831		KC3= <u>10</u> X KC3	
TIME	W	CK	CB	CA	
100.00	6051.00000	0.00052	0.00014	0.89680	
500.00	6051.00000	0.00105	0.00119	11.96279	
900.00	6051.00000	0.00110	0.00163	17.16337	
1300.00	6051.00000	0.00110	0.00176	18.66119	
1700.00	6051.00000	0.00110	0.00179	19.06403	
2100.00	6051.00000	0.00110	0.00180	19.16432	
2500.00	6051.00000	0.00110	0.00180	19.19162	
2900.00	6051.00000	0.00110	0.00180	19.19713	
3300.00	6051.00000	0.00110	0.00180	19.19735	
3700.00	6051.00000	0.00110	0.00180	19.19782	
4100.00	6051.00000	0.00110	0.00180	19.19849	
4500.00	6051.00000	0.00110	0.00180	19.19836	

KC1=0.00337898		KC2=0.01894153		KC3= <u>50</u> X KC3	
TIME	W	CK	CB	CA	
100.00	6051.00000	0.00052	0.00014	0.71225	
500.00	6051.00000	0.00105	0.00119	8.24347	
900.00	6051.00000	0.00110	0.00163	11.65281	
1300.00	6051.00000	0.00110	0.00176	12.63242	
1700.00	6051.00000	0.00110	0.00179	12.88867	
2100.00	6051.00000	0.00110	0.00180	12.95430	
2500.00	6051.00000	0.00110	0.00180	12.97087	
2900.00	6051.00000	0.00110	0.00180	12.97498	
3300.00	6051.00000	0.00110	0.00180	12.97647	
3700.00	6051.00000	0.00110	0.00180	12.97676	
4100.00	6051.00000	0.00110	0.00180	12.97664	
4500.00	6051.00000	0.00110	0.00180	12.97668	

KC1=0.00337898		KC2=0.03788306		KC3= 100 X KC3	
TIME	W	CK	CB	CA	
100.00	6051.00000	0.00052	0.00014	0.56242	
500.00	6051.00000	0.00105	0.00119	5.93075	
900.00	6051.00000	0.00110	0.00163	8.31349	
1300.00	6051.00000	0.00110	0.00176	8.99782	
1700.00	6051.00000	0.00110	0.00179	9.17796	
2100.00	6051.00000	0.00110	0.00180	9.22189	
2500.00	6051.00000	0.00110	0.00180	9.23268	
2900.00	6051.00000	0.00110	0.00180	9.23522	
3300.00	6051.00000	0.00110	0.00180	9.23585	
3700.00	6051.00000	0.00110	0.00180	9.23601	
4100.00	6051.00000	0.00110	0.00180	9.23602	
4500.00	6051.00000	0.00110	0.00180	9.23601	